



Preliminary reliability analysis on the Thames Estuary: Dartford Creek to Gravesend

Date July 2006

Report Number T07-06-07

Revision Number 1_0

Task Leader: TU Delft

Partner Name: HR Wallingford

FLOODsite is co-funded by the European Community
Sixth Framework Programme for European Research and Technological Development (2002-2006)
FLOODsite is an Integrated Project in the Global Change and Eco-systems Sub-Priority
Start date March 2004, duration 5 Years

Document Dissemination Level

PU Public
PP Restricted to other programme participants (including the Commission Services)
RE Restricted to a group specified by the consortium (including the Commission Services)
CO Confidential, only for members of the consortium (including the Commission Services)

DOCUMENT INFORMATION

Title	Preliminary Reliability Analysis on the Thames Estuary
Lead Author	Foekje Buijs
Contributors	Ben Gouldby, Paul Sayers
Distribution	
Document Reference	

DOCUMENT HISTORY

Date	Revision	Prepared by	Organisation	Approved by	Notes
03/07/2006	1_0	Foekje Buijs	HR Wallingford	Ben Gouldby	Draft for discussion at Task 4/5/6/7/8 Workshop in Delft (20.07.06)

ACKNOWLEDGEMENT

The work described in this publication was supported by the European Community's Sixth Framework Programme through the grant to the budget of the Integrated Project FLOODsite, Contract GOCE-CT-2004-505420.

DISCLAIMER

This document reflects only the authors' views and not those of the European Community. This work may rely on data from sources external to the FLOODsite project Consortium. Members of the Consortium do not accept liability for loss or damage suffered by any third party as a result of errors or inaccuracies in such data. The information in this document is provided "as is" and no guarantee or warranty is given that the information is fit for any particular purpose. The user thereof uses the information at its sole risk and neither the European Community nor any member of the FLOODsite Consortium is liable for any use that may be made of the information.

© **FLOODsite Consortium**

SUMMARY

This report describes reliability analysis undertaken on flood defences along the Dartford Creek to Gravesend Stretch of the Thames Estuary. This stretch comprises flood defences of varying types that are can potentially fail through different mechanisms. Fault trees have been constructed that identify the primary, historically observed, failure mechanisms associated with defence types. These fault trees have been used within the context of a reliability analysis. Some of the primary outputs from this analysis comprise annual probability of failure for each defence length and fragility curves for each defence length.

CONTENTS

Document Information	ii
Document History	ii
Acknowledgement	ii
Disclaimer	ii
Summary	iii
Contents	v
1. Introduction	1
1.1 Introduction to Task 7	1
1.2 Background to the Preliminary Reliability analysis on the Thames	1
2. Overview of defence reliability analysis	3
3. Description of the Dartford Creek to Gravesend flood defence system	4
3.1 Introduction to the Site	4
3.2 Historical failure events	6
3.3 Description of structure types and failure mechanisms	7
3.3.1 Earth embankments	7
3.3.2 Concrete walls	9
3.3.3 Sheet pile walls	11
3.3.4 Floodgates	13
3.4 Data sources	14
3.4.1 Geometry	14
3.4.2 Soil conditions	15
3.4.3 Hydraulic boundary conditions	16
4. Main flood defence types and their failure mechanisms	19
4.1 Fault trees, failure mechanisms and limit state equations	19
4.2 Earth embankments	19
4.2.1 Representation of the structure	19
4.2.2 Fault tree	20
4.2.3 Discussion failure mechanisms	20
4.3 Concrete walls	24
4.3.1 Representation of the structure	24
4.3.2 Fault tree	25
4.3.3 Discussion failure mechanisms	25
4.4 Anchored sheet pile walls	27
4.4.1 Representation of structure	27
4.4.2 Fault tree	28
4.4.3 Discussion failure mechanisms	28
5. Single cross section and system reliability methods	32
5.1 Single cross section reliability method	32
5.1.1 Method to establish fragility and the annual probability of failure	32
5.1.2 Method to establish sensitivity indices	33
5.2 Evaluation of defence length reliability methods	35
5.2.1 Introduction to length effect	35
5.2.2 Influence of variations in length effect approach to flood defence reliability	38
6. Discussion of the results	43
6.1 Description of the products of the reliability analysis	43

6.2	Reliability analysis of the earth embankments	44
6.2.1	Fragility	44
6.2.2	Annual probability of failure.....	46
6.2.3	Sensitivity of the reliability to the random variables	48
6.2.4	Comparison of Dartford Creek to Gravesend fragility to broad scale fragility.....	50
6.3	Reliability analysis of the concrete walls.....	54
6.3.1	Fragility	55
6.3.2	Annual probability of failure.....	57
6.3.3	Sensitivity of the reliability to the random variables	57
6.3.4	Comparison of Dartford Creek to Gravesend fragility to broad scale fragility.....	63
6.4	Sheet pile walls	64
6.4.1	Fragility	65
6.4.2	Annual probability of failure.....	67
6.4.3	Sensitivity of the reliability to the random variables	67
6.4.4	Comparison of Dartford Creek to Gravesend fragility to broad scale fragility.....	69
7.	Conclusions and further steps.....	73
7.1	Conclusions.....	73
6.2	Further steps.....	75
8.	References	76
 Appendices		
	Appendix A: Inventory Dartford Creek to Gravesend borehole data archive	81
	Appendix B: Limit state equations of the failure mechanisms	83

1. Introduction

1.1 Introduction to Task 7

The complex relationship between individual elements of a flood defence system and its overall performance is poorly understood and difficult to predict routinely (i.e. the combination of failure modes and their interaction and changes in time and space). Task 7 focuses on developing reliability analysis techniques and incorporating present process knowledge on individual failure modes as well as interactions between failure modes (collated through Tasks 4, 5 and 6). Figure 1 shows the structure of Task 7.

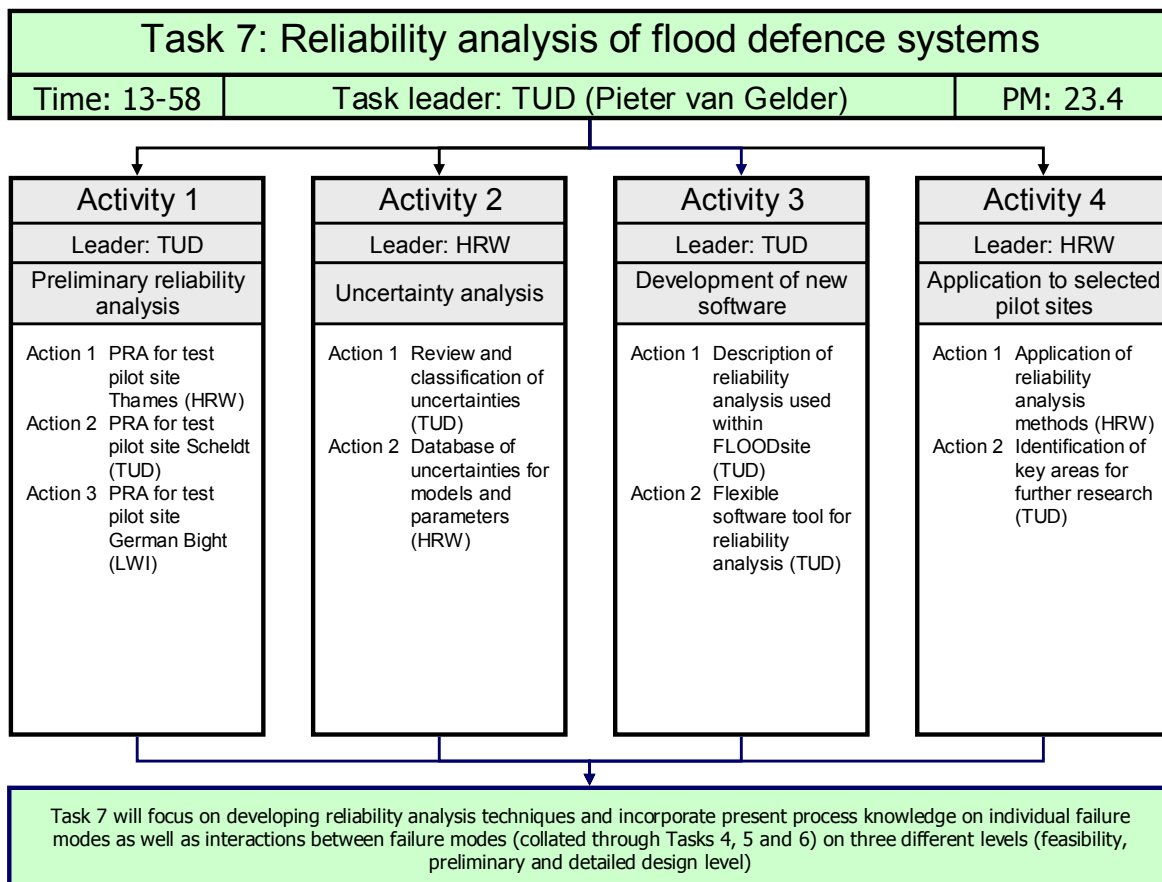


Figure 1.1 Organisational overview of Task 7

The work described within this report represents output under Action 1 of Activity 1.

1.2 Background to the Preliminary Reliability analysis on the Thames

Flood risk analysis methods widely receive attention as a valuable means to obtain insight in the most vulnerable areas in a floodplain, see HR Wallingford (2004a), Vrijling (2001). Within flood risk assessment, methods to determine the reliability of a single flood defence and of flood defence systems as a ‘snapshot in time’ are well established, e.g. Lassing et al. (2003). Reliability analysis of flood defences is a holistic approach considering the physics of failure processes as well as the uncertainties involved with those processes. It allows mapping of the structural performance of multiple defences in a system to a comparable measure, highlighting weaker or stronger links. In addition, reliability analysis facilitates insight into the sensitivity of the failure processes to the

different characteristics of the flood defence. Practically, that knowledge aids efficient targeting of data collection efforts and maintenance, repair and improvement measures.

Currently, within the UK, significant studies are underway into the assessment and management of flood risk within the Thames estuary (London). These studies are recognising the importance that the reliability of flood defences plays within assessment and management of flood risk. The work described here details reliability analysis that has been undertaken on a specific flood system within Thames: Dartford Creek to Gravesend. The report is structured as follows:

Chapter 2 gives an overview of the steps involved in a reliability analysis of this kind.

Chapter 3 describes the main structure types that are found along the Dartford Creek to Gravesend flood defence line: earth embankments, concrete walls and anchored sheet pile walls. The general shape of the structures, their primary function, the historical failures and main deterioration processes are addressed. The chapter concludes with a discussion of the main data sources: the flood defence geometry, soil conditions and hydraulic boundary conditions.

Chapter 4 details the fault tree, failure mechanisms and limit state equations applied in the reliability analysis of each structure type identified in Chapter 3. The top event in the fault tree is represented by failure of the structure to perform its primary function. The failure mechanisms capture the different chains of events leading to the top event.

Chapter 5 outlines the probabilistic calculation methods applied in the (system) reliability analysis. The Dartford Creek to Gravesend flood defence line is divided into a number of sections, each of which is represented by one cross section. The fault tree corresponds with those set up for the structure types in Chapter 4. For each of those sections individually a probabilistic calculation is carried out. In the second part of the chapter, methods to deal with system effects, i.e. failure of multiple sections, are evaluated.

Chapter 6 displays and discusses the results obtained with the probabilistic calculation methods outlined in Chapter 5. The results are broken down according to the main structure types: earth embankments, concrete walls and anchored sheet pile walls. For each structure type the reliability of the sections is compared. Subsequently, one section is picked to demonstrate the reliability results for: 1) the total fragility and the contribution of the individual failure mechanisms; 2) the annual probability of failure; 3) the sensitivity of the reliability to the random variables; 4) a structure specific comparison of broadscale fragility to the Dartford Creek to Gravesend fragility.

Chapter 7 provides the conclusions and recommendations following from the Dartford Creek to Gravesend flood defence system reliability analysis.

2. Overview of defence reliability analysis

Figure 2.1 depicts the steps involved in the calculation of flood defence reliability. These activities were carried out for the Dartford Creek to Gravesend flood defence system and are described below.

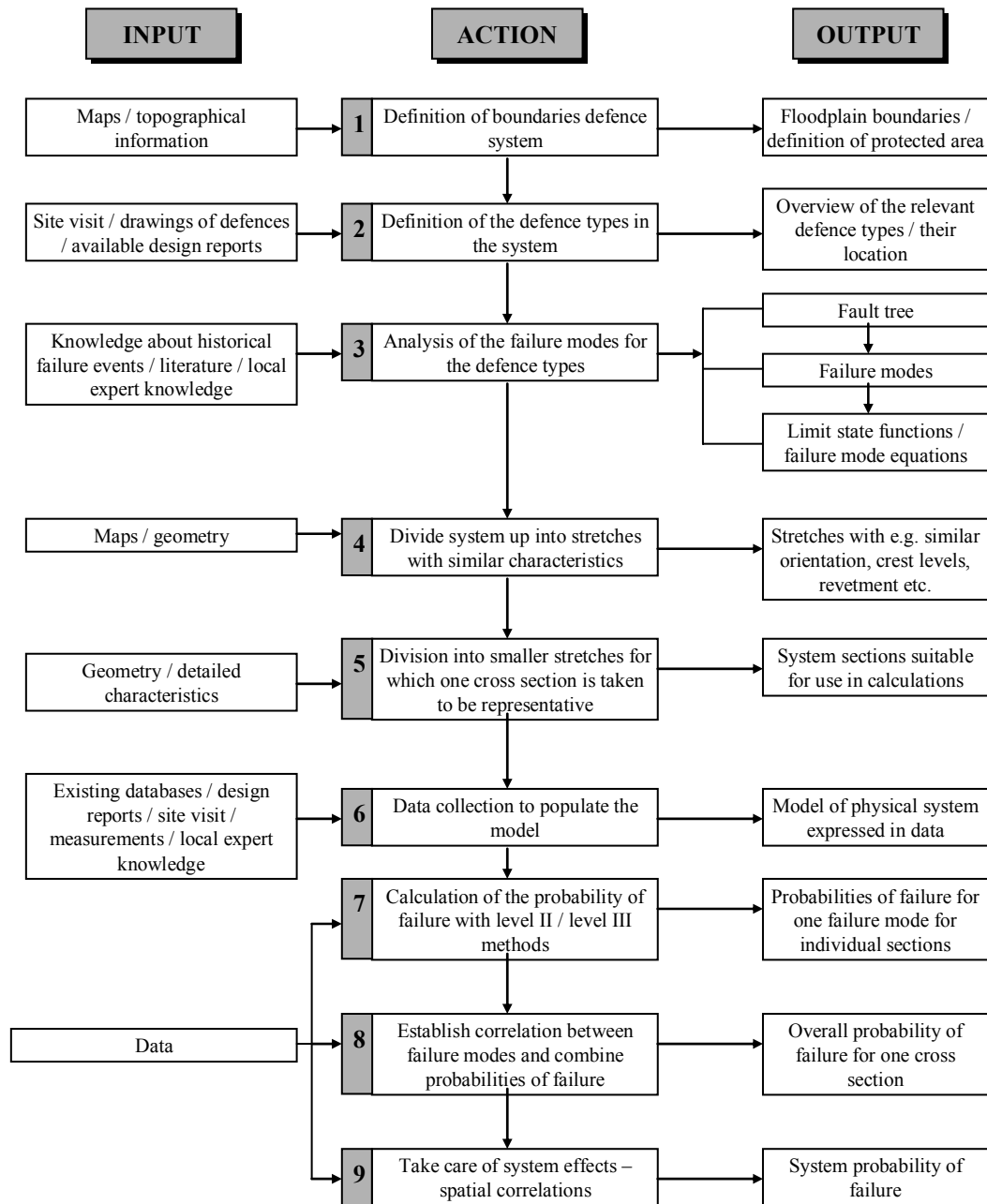


Figure 2.1. *Flow chart of activities to calculate flood defence reliability including examples of the type of input source material and the output products.*

3. Description of the Dartford Creek to Gravesend flood defence system

3.1 Introduction to the Site

In the late 1970s and beginning 1980s the flood defences along the Thames Estuary were subject to a major improvement scheme. After 30 years of service there are approximately another 20-30 years before systematic refurbishment of the current flood defence system is required. The next generation of flood defences, ideally in place in 2030, will be designed to last in excess of 2100. In recognition of the time-consuming nature of design and construction of such large scale works, recently the Thames Estuary 2100 project (TE2100 project) was launched to guide this process.

This study focuses on the Dartford Creek to Gravesend flood defence system (see Figure 3.1). Most of the flood defence structures under analysis were built during the 1970s / 1980s improvements. The figure also provides an impression of the elevations of the floodplain. The reliability analysis focuses on the defence line between Dartford Creek and Northfleet, with a length of 10.6 km. The defence line is divided in the following main flood defence types:

- Earth embankments: 6.7 km
- Concrete walls: 1.9 km
- Sheet pile walls: 2.1 km
- Floodgates, over 26 individual gates between 2.5 and 12 meter wide.

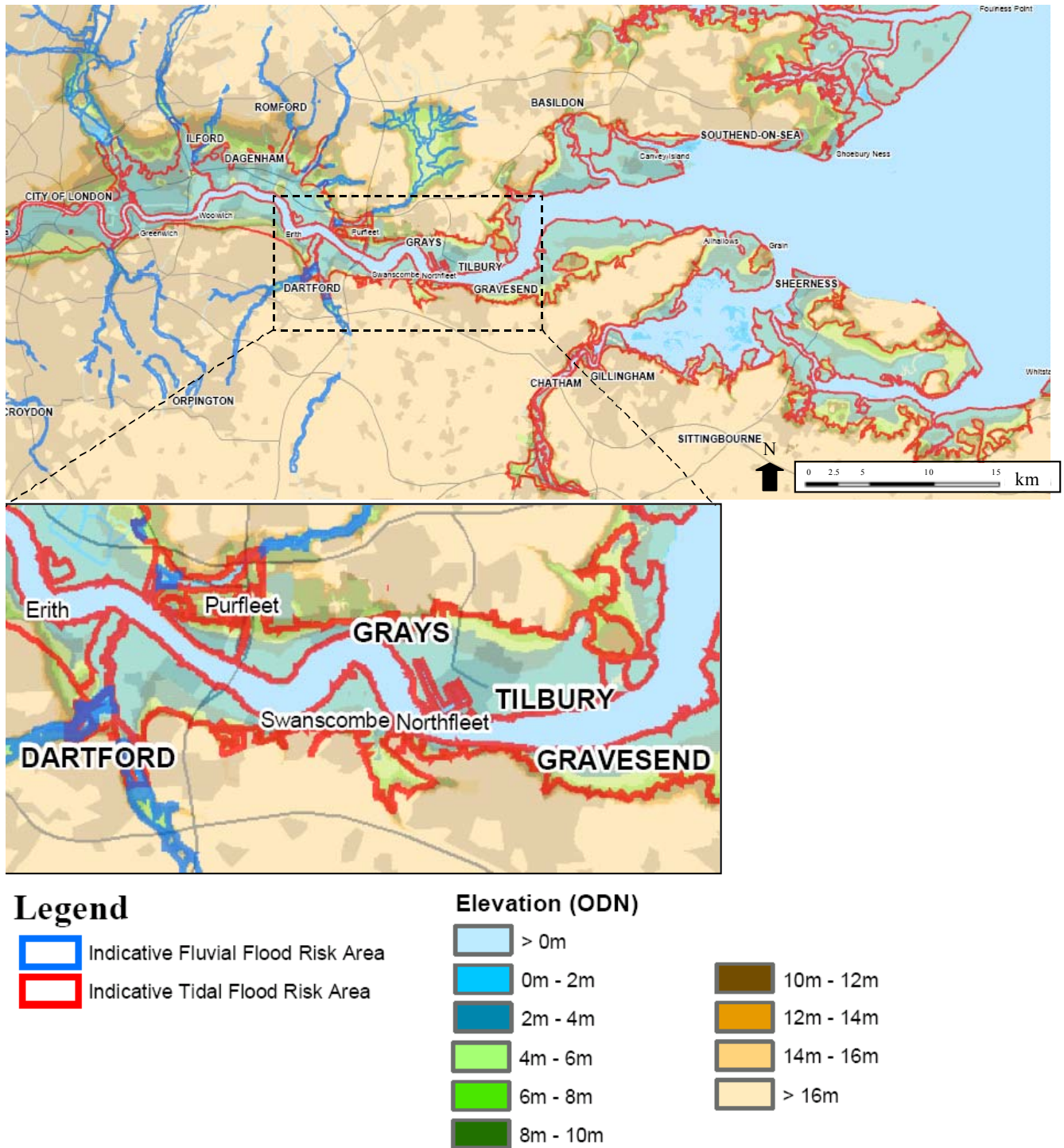


Figure 3.1 The location of the Dartford Creek to Gravesend site in the Thames Estuary (top). An indication of the elevations of the floodplain (below). The floodplain elevations relate to a highest recorded water level of about OD+4.9m near Swanscombe and of about OD+5.1m near Erith.

The sheet pile and concrete structures mainly protect private frontages. The floodgates are usually meant to provide access to docks through those private frontages. Over the years active use of the docks along the Dartford Creek to Gravesend frontages has decreased to almost none at present.

Figure 3.2 shows the elevation of the defence line and the division into the main defence types. The elevation is compared between those recently surveyed and those indicated on as designed / constructed drawings of the improvements in the '70s and '80s.

The '70s and '80s improvements to the Thames Estuary flood defences were triggered by the storm that took place in January 1953. Gilbert & Horner (1984) report: "This land was liable to catastrophic flooding because the land was sinking compared with the sea level, while there were, at rare intervals, abnormally high sea levels due to freak meteorological conditions".

According to Gilbert & Horner (1984) the area around London is sinking due to two main factors. Firstly, Southeast England is situated on a tectonic plate which was pressed down during the ice age by the ice cap. The retreating ice lifted the weight, resulting in rotation of the plate about its axis between the Severn and the Tyne, causing Scotland to rise and Southeast England to sink. Secondly, London is founded on a clay lid covering a gravels, sand and chalk basin. This basin was used in the past for water extraction with, as a result, an increasingly drying clay layer and the settlements associated with that drying out process. The water extractions were stopped because of these detrimental effects. Since then, the groundwater levels started to recover and, ironically, this process is expected to lead to groundwater flooding in the near future.

Gilbert & Horner (1984) indicate as the three main reasons for the 'abnormally high sea levels':

- Sea level rise due to melting polar ice and climate change.
- Increasing tidal ranges as a result of estuarial processes, initiated by the sinking tectonic plate.
- High surges occurring at the North Sea during unusual circumstances. Low pressure depressions developing off the coast of Canada moving across the Atlantic usually disappear to the North towards Norway. However, if the presence of such a depression north of Great Britain coincides with a strong north-westerly wind, the low pressure surge is funnelled into the North Sea. The consequence is high sea water levels at the North Sea.

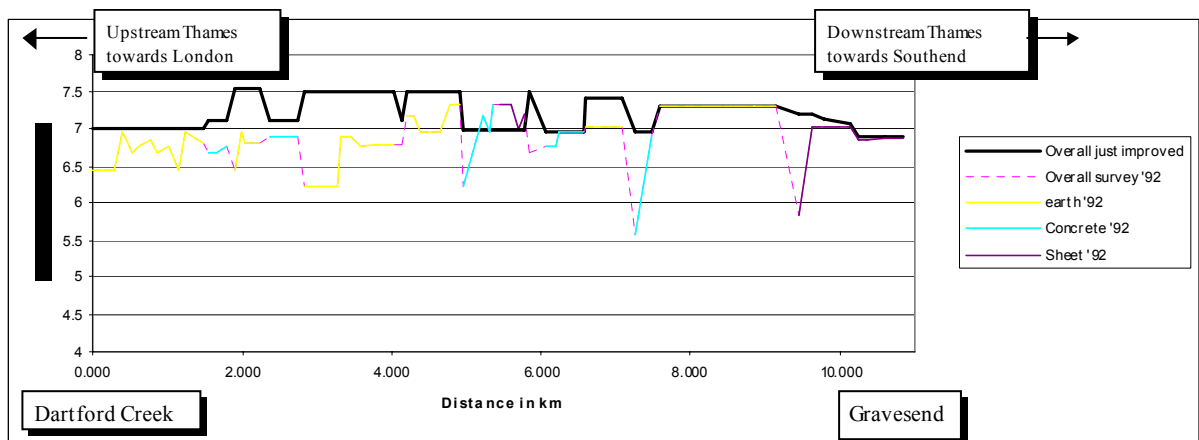


Figure 3.1 *Elevation of the defence line between Dartford Creek to Gravesend: after '70s / '80s improvements (in black) versus the recently surveyed defence line (dashed purple). The latter indicates the stretches of the different flood defence types.*

High tidal water levels at the North Sea caused by the above mentioned reasons are further amplified in the Thames Estuary after being funnelled into the trumpet shaped estuary.

3.2 Historical failure events

In this section some of the historical flood defence failures are discussed. These indicate what the weaknesses of the flood defence system are. The most recent severe storm events were the floods in 2000 and those in 1953. In 2000 along the Thames Estuary mainly overtopping occurred without structural failure. In relation to 1953 and the '70s and '80s improvements the following failure events are reported:

- 1953 – Overtopping of the crest, seepage into fissures and cracks followed by decreasing shear strength and slope instability of earth embankments (see also Figure 3.3). Crest levels then corresponded with the current lower crest. Improvements aimed to provide a 1 in 1000 year standard of protection.
- 1953 – uplifting and piping behind the earth embankments of the impermeable clayey and peaty layers. As part of the improvements, pipes were applied in ditches behind the embankments reaching into the water conductive layers below the impermeable layers. The water can drain into the ditch, thus relieving the hydraulic uplifting pressures underneath the impermeable layers. Presumably filters are applied at the bottom of the pipes to prevent erosion of the material in the water conductive layer.
- 1970s-1980s – during the construction of the improvements a stretch just downstream of Gravesend failed due to slope instability of earth embankments. The construction works were carried out under strong time limitations. Due to this time constraint, the weight of the new defences was applied too quickly, leading to insufficient drainage of the weak clayey and peaty layers (and therefore insufficient recovery of the strength of the foundational soil).



Figure 3.3. *Example of a 'crack' in an earth embankment in 1955, with in the background Littlebrook powerstation.*

3.3 Description of structure types and failure mechanisms

3.3.1 Earth embankments

General description

The earth embankments along the Dartford Creek to Gravesend defence line typically have two crests. In the late '70s and early '80s the Thames Estuary defences were improved. The lower riverward crest is the old pre-improvement defence line, the higher landward crest has been constructed as part of the improvements. The defences are founded on weak clayey and peaty soil layers with a thickness in the order of magnitude 14 to 20 m. Those impermeable layers are in turn founded on a water conductive layer formed by sandy or chalky layers. To avoid the occurrence of deep seated slip circles during and after construction, berms were applied on the inside and outside toes of the defences to provide for sufficient stabilising weight. See Figure 3.4. for an example cross section and Figure 3.5. for an impression of the recent state of the earth embankments.

Function

The primary function of the earth embankments along the Dartford Creek to Gravesend flood defence line is: protecting against flooding by retaining water.

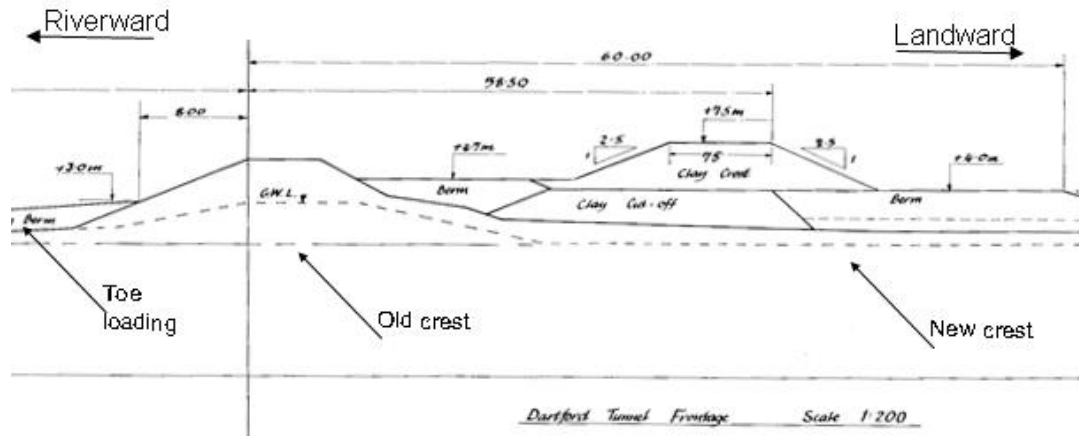


Figure 3.4 Typical cross section of earth embankments between Dartford Creek to Gravesend

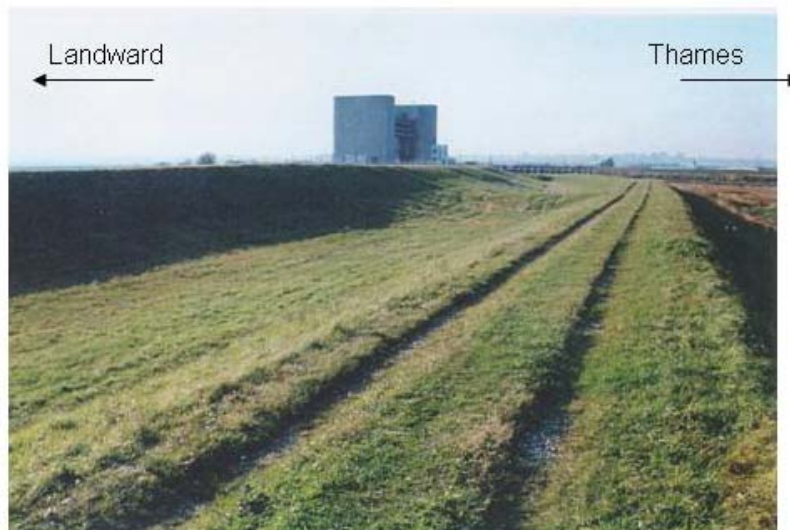


Figure 3.5. View along the current embankment just downstream of Dartford Creek, in the background the Dartford Creek barrier can be seen

Site specific failure mechanisms / deterioration

The failure events that took place in the past all relate to the earth embankments. They provide an indication of the failure mechanisms that are at least of interest:

- Overtopping / overflow discharges leading to failure of the rearslope, possibly caused by slope instability in combination with seepage in existing cracks and fissures.
- Uplifting of the permeable layers behind the earth embankment, followed by collapse due to piping.
- Slope instability, e.g. due to changing outside water level conditions possibly in combination with seepage in (horizontal) fissures, or due to rapid drawdown.

The following time-dependent processes are at least relevant for further investigation:

- Fissuring / cracking and their role in the most relevant failure mechanisms

- Crest level settlements, long term: the compressible clayey and peaty soil layers lead to substantial settlements due to the '70s and '80s improvements. Settlements in the order of magnitude of 0.5 to 1 meter took place over about 30 years.
- Crest level settlements, short term: In some of the areas, local people use the earth embankments for motor crossing, leading to damage to the crest and grass on the inside slope.
- Long term changes in the bathymetry of the Thames, causing different local hydraulic boundary conditions
- Activities encroaching on the earth embankments slopes, e.g. static loading introduced by a demolition yard stacking cars on the lower end of the slope.

3.3.2 Concrete walls

General description

The reinforced concrete walls were built as part of the Thames Estuary flood defence improvements in the '70s and '80s. An example of a concrete wall along the Dartford Creek to Gravesend defence line is given in Figure 3.6. Sheet piles applied underneath the concrete structure prevent seepage/piping and mobilise the soil between the piles for extra stability. Variations on the concrete structure shown in the figure are:



Figure 3.6. *Example of a concrete wall along the Dartford Creek to Gravesend site, downstream of Greenhithe*

- Application of a single sheet pile sometimes in the form of an anchored sheet pile.
- A mirrored version of the structure shown in Figure 3.7 with the vertical wall on the landward side rather than the Thames side.

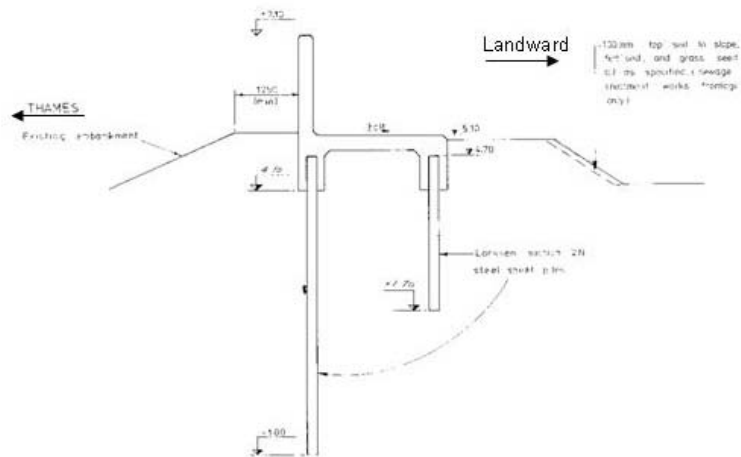


Figure 3.7. Typical cross section of the concrete wall. Two other variations on this cross section are: 1. cross section as shown in this figure but then mirrored, 2. anchored sheet pile cut offs, to mobilise more stability



Figure 3.8. Impression of damage to concrete wall caused by loading of a building site: 1. cracking of the concrete as the reinforcement is not designed for this type of loading, 2. uneven settlements along the defence line due to the activities on the site behind the wall, 3. joint failure due to uneven settlements / activities

Function

The primary function of the concrete walls along the Dartford Creek to Gravesend flood defence line is: protecting against flooding by retaining water. In most cases the concrete wall is combined with a larger earth embankment structure.

Site specific failure mechanisms / deterioration

Past failure events of concrete walls along the Dartford Creek to Gravesend defence line are not known. Problems with concrete wall structures are currently mainly caused by backfilling of the concrete wall as part of residential developments. The concrete wall is not designed for this type of loading, resulting in: cracking / spalling of the concrete (there is no reinforcement to deal with the tensile stress on the opposite side of the wall), uneven settlements and the associated failure of joints. See Figure 3.8 for an overview of the problems.

3.3.3 Sheet pile walls

General description

Sheet pile walls were built / improved as part of the Thames Estuary flood defence improvements in the '70s and '80s. Figure 3.9 and Figure 3.10 show an example of a sheet pile wall applied along the Dartford Creek to Gravesend defence line. In some cases old frontages in the form of for instance masonry walls are still present in the ground behind the current sheet pile walls, the space in between the walls backfilled with concrete. In other cases, the old frontage was used to anchor the sheet pile walls in or the rubble of the old frontage was used as backfill material.

At the time of the construction of the defence improvements, parts of the frontage between Dartford Creek and Gravesend were docks. Because of the function as a dock, besides the typical sheet pile wall a large variation of sheet pile wall cross sections and combinations with concrete structures occur. By now, the frontages are not in use as docks anymore.

Another type of sheet pile wall occurs without anchors as part of an earth embankment. The sheet pile wall then provides an additional 0.5 to 1.0 m freeboard without demanding extra space associated with a sloped elevation.

Function

The primary function of the sheet pile walls along the Dartford Creek to Gravesend flood defence line is retaining ground. Protection against overtopping is a secondary function as the sheet pile frontages border high grounds and rather fulfilled a role as part of the docks.



Figure 3.11. Overview of potential problems with sheet pile walls: 1. ALWC in the splash zone, 2. residential developments have caused 25% of the anchors to fail, 3. the boat left behind disturbs the local loading conditions

Site specific failure mechanisms / deterioration

There is no mention of failures of sheet pile walls in the past 25 to 30 years. The sheet pile walls have not been painted or otherwise significantly maintained during their lifetime. As a result Accelerated Low Water Corrosion (ALWC) has corroded the surface of the sheet pile walls over the course of 25 to 30 years. Corrosion has also reduced the diameter of the ground anchors.

Other problems are caused by residential developments which damage ground anchors. At Greenhithe this has caused one out of four anchors to fail. An overview of the problems is given in Figure 3.11.

3.3.4 Floodgates

General description

As the frontages between Dartford Creek and Gravesend partly had a function as a dock during the '70s and '80s improvements, sufficient passages from the floodplain to the Thames had to be ensured. For this reason, over 26 floodgates were built into the flood defence line (Figure 3.12.). By now, some of these floodgates are permanently in a closed position and some were replaced by fixed defences as part of commercial or residential developments. Others are part of a telemetry system and need to be closed to prevent flooding. The width of the opening varies from smaller gates, for instance 2.5 m, to larger gates of 12 m and wider.



Figure 3.12 Example of a 'bookholder' floodgate

Site specific failure mechanisms / deterioration

Human error and the resulting failure to close the gates is often cited as the main problem with floodgates. The floodgates are all connected to a telemetry system. That system can be subject to failure in several ways, e.g. human involvement or electrical failure.

Piping is one of the modes of structural failure. Underneath the sill of the floodgates seepage sheet pile screens are applied. The amount of seepage through the gates might also cause problems.

If poorly maintained, structural failure can be a problem, but most floodgates are in good condition.

3.4 Data sources

3.4.1 Geometry

Available information sources

Geometry representation is based on the following information sources:

- As built or design drawings stemming from the 1970s and 1980s. Especially comprehensive as built documentation of the sheet pile, concrete and composite structures along private frontages is available. For earth embankments the cross sectional representation is qualitatively less in terms of spatial density and conclusiveness, e.g. in the form of final design drawings rather than the as built versions. The earth embankments are in addition harder to georeference.
- Crest levels are, in this report, based on crest level surveys from the 1990s. Under TE2100 recently a new survey was carried out; the results of this survey are not incorporated in this report.
- Photogrammetric information from 2000 / 2001 is available across the flood defences and the floodplain. This information does not pick up on structures with a width smaller than 0.5 – 1 meter, e.g. concrete walls or wave return walls. It provides extra feedback on the cross sectional representation of the earth embankments.

Comments on quality and inference of the information source

A number of issues play a role in the level of quality and inference involved with geometrical data. Some can be more easily mitigated than others:

- The level of detail of the survey, e.g. the magnitude of measurement errors and whether the measurement covers the complete cross section or only the crest levels.
- As already mentioned above, the nature of the information source i.e. as built or design drawing determines the confidence in that source. In addition, the possibility to geo-reference the data is an important issue to consider.
- The spatial density of available as built or design drawings. The representation of flood defence structures along private frontages tends to be quite dense. In contrast, the availability of design drawings tends to be spatially less dense and the quality limited.
- Three dimensional effects such as bends in the alignment of the flood defences affect local reliability but are hard to model: e.g. concentration of flow or wave impact.

3.4.2 Soil conditions

Available information sources

A summary of the main sources of information on soil conditions underpinning the reliability analysis in this report is given below. The data were retrieved from the EA Addington office archive. More comprehensive and structured information must be available with BGS.

- Borehole data
- Design for settlement and instability of earth embankments along Dartford Creek to Greenhithe
- Lab tests of samples at various locations
- Investigation of tidal uplift pressures in gravel layer underlying the impermeable layers
- Some sparse information on grain sizes

The interpolation procedure that was followed to establish the geotechnical conditions for the defence line is explained in more detail below.

- Geo-referencing boreholes.
Match borehole locations to the appropriate cross section along the defence line. Geo-referencing the borehole records is not always straightforward when the original plan with boreholes is not available. Among design drawings of the improvement scheme in the 1970s several overview plans of boreholes are available. These pinpoint exact borehole locations and provide soil layer descriptions. This information was used for this reliability analysis. When there was insecurity about the borehole location, the information was not incorporated.
- Classification of the soil layers from the borehole descriptions into generic types.
Lab tests on some soil samples were carried out in the 1970s / 1980s. This provides an impression of similarities between soil properties among different soil layer descriptions. In the 1970s for the earth embankments along a stretch of 1 km downstream of Dartford Creek such a soil classification was made. The results of that classification were then used to underpin design calculations. This classification was adopted in this reliability analysis to classify the soil descriptions from the boreholes into generic types. Lab test results are also available at other locations, but were not used for the following reasons:
 - Problems with geo-referencing
 - Some lab test results, e.g. triaxial tests, require interpretation or extra work to turn them into useful soil properties
 - Interpolation of the borehole holes and soil classification to cover the whole defence line.

The resolution of borehole locations and a simplified clay-peat-sand/gravel soil classification were used to interpolate soil layers. The levels of the soil layers were linearly interpolated. Among one soil classification type, the soil properties are taken equal for the interpolated layers.

Figure 3.13 shows a plot of the interpolated soil layers, the defence crest levels as they were designed / built in the 1970s / 1980s and the crest levels from a recent survey.

The interpolated soil layers show that a pack of impermeable layers with a thickness of about 15 meter overlies a gravel / sand layer. The impermeable layers mainly consist of clay. At some locations the clay is silty, at other locations the clay is organic. Peat lenses, 0.5 to 1 meter thick, occur regularly - sometimes two lenses in one cross section.

Comments on quality and inference of the information source

The soil data, strata structure as well as soil properties, used in this study aim to roughly inform the flood defence reliability calculations. It is noted that these data need a lot more attention and refinement. An indication of the issues is given below:

- The resolution of the boreholes needs to be sufficiently dense to capture the spatial variability. The uncertainties in the reliability analysis pick up on the variability of the layer elevation. However, irregularities in the form of lenses can easily be missed out but play a critical role in slip surfaces.
- Geo-referencing of the original borehole information turned out to be a problem.
- There are two angles to the desired detail in soil classification. There is a trade-off between the aim to have as detailed information as possible and on the other hand the feasibility of investigating many different types of soil layers. This trade-off impacts on the amount of different soil types that get lumped together in one class and hence get assigned the same soil properties.
- The quality of the measurements and the approximations that need to be made in procedures to derive soil properties for calculations.
- For one soil type the number of samples that can be tested is limited.

3.4.3 Hydraulic boundary conditions

Available information sources

A joint probability study of water levels and wind speeds was carried out for the sea conditions at the mouth of the Thames Estuary, HR Wallingford (2004b). This study provides a Monte Carlo simulation of joint couples of wind speed and water level given four different wind directions: North East, South East, South West, North West. The simulations are based on joint water level and wind speed data sets that cover a period of about thirty years. According to HR Wallingford (2004b) the effect of the river discharge on the local water levels is negligible downstream of Tilbury. In this report it is therefore chosen to leave the discharge out of the analysis.

Local water levels given a number of different sea water levels at the mouth of the Thames Estuary were provided from TUFlow / Isis calculations. Several locations along the Dartford Creek to Gravesend flood defence system are represented in those results. The sea water levels span a sufficiently large range to represent extreme sea water levels.

The two information sources described above are combined to find local water levels during the reliability calculations. A simulation of a water level at one of the locations along the defence line can be derived through linear interpolation between water levels and defined locations.

To derive local wave conditions a simple shallow water wave prediction model (formulae according to Bretschneider) is used. That prediction is based on the local water level, bathymetrical information, fetch and reduced estuarial wind speeds according to HR Wallingford (1999). Local bathymetrical information was derived from a larger bathymetry study carried out for TE2100 covering the Thames River over the course of the twentieth century. Fetches were measured from a map. Being quite far upstream of the Thames Estuary, the local wave climate is not severe. The wave conditions thus calculated are in the order of magnitude of those presented in HR Wallingford (1999) for the Dartford Creek to Gravesend flood defence system.

Comments on quality and inference of the information source

The quality of the local water level predictions depends on a number of factors:

- The quality of the statistical model of the wind speeds and water levels at the mouth of the Thames Estuary. Especially the following types of issues are important:
 - the availability of data to fit the statistical model to, in case of the Thames Estuary the data cover a sufficiently long period of about thirty years;
 - the quality of the representation in the extreme tails of the statistical distribution;
 - decisions with respect to the dependency structure and the distribution function.The quality of the statistical model is often hard to judge for more extreme values as these events tend to be less populated with data.
- The quality of the local water level predictions given sea water levels at the mouth of the estuary. The following types of issues are important:
 - the detail of representation of the river bathymetry and the physical processes;
 - the data availability at different locations along the Thames to calibrate and validate the numerical model against, especially for more extreme water levels sufficient data availability is questionable;
 - the applicability of the physical relations to more extreme local water level predictions;
 - whether it is justified to linearly interpolate between two locations which are defined in the numerical model to find local water levels at other locations, depending e.g. on the variability in vegetation or foreshores, the slope along the river, the distance between two defined locations, etc.;
 - whether it is justified to linearly interpolate between two simulated water levels at one location;
 - local surge effects are not taken into account
 - funnelling effects causing extra surge due to a wind field directed upstream (westward) of the Thames Estuary.

The quality of local wave conditions depends on factors such as:

- the quality of the water level predictions along the river;
- the quality of the wave prediction model, which is in this case a rather simple model;
- data availability to calibrate and validate the wave prediction model against;
- whether a detailed representation of the river bathymetry is applied;
- whether depth limited effects on waves are taken into account;

the appropriateness of the representation of the local wind field.

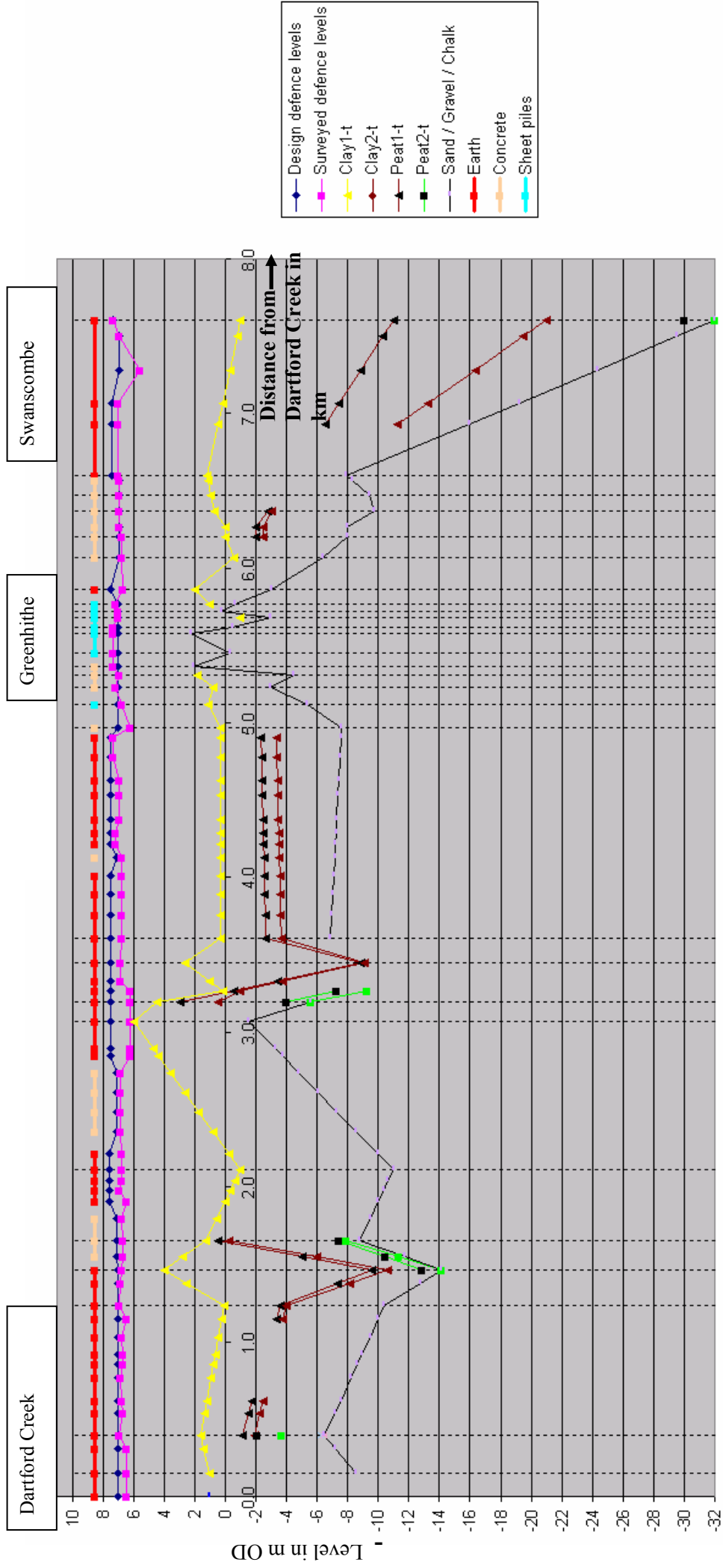


Figure 3.13 Overview of interpolated soil layers, the crest levels of the flood defence structures from as designed / as built drawings and the crest levels derived from a 1990s crest level survey.

4. Main flood defence types and their failure mechanisms

The previous chapter described the main characteristics of the Dartford Creek to Gravesend flood defence system: the flood defence types and known historical failures / deterioration processes, the hydraulic and geotechnical environment. This chapter goes into the failure mechanisms that are incorporated in the reliability calculations: fault trees are presented to capture the mutual relations, individual failure mechanisms are described and the associated equations are developed.

4.1 Fault trees, failure mechanisms and limit state equations

A flood defence structure is designed to fulfil several functions during its lifetime. Different chains of events can lead to the situation that a flood defence fails to perform its functions. Such a chain of events is referred to as a failure mechanism. These failure mechanisms and the mutual logical relations can be structured in a fault tree. The failure mechanisms lead to a top event in the fault tree: failure to perform one or more of its functions. Fault trees can be used to underpin quantified probabilistic calculations and are also applied in practice to qualitatively inform for instance Reliability-Centred Maintenance.

A central concept in reliability-based design of flood defences is a limit state equation. A limit state equation can either represent a full failure mechanism or one step in a larger chain of events. The reliability of the defence is in this approach represented by a combination between the strength of the defence and the loading of the defence structure in the form of the following limit state equation:

$$Z = R - S$$

In which S expresses the loading and can for example be a function of the hydraulic loading conditions or the ground pressures behind a vertical wall. R represents the strength the flood defence structure and can be a function of e.g. the thickness of the revetment blocks or the crest level. $Z \leq 0$, when loading exceeds the strength, defines failure according to the limit state equation.

4.2 Earth embankments

4.2.1 Representation of the structure

Two types of earth embankments occur along the Dartford Creek to Gravesend defence line: a combination of a riverward and landward earth embankment (referred to as double crested) and the regular earth embankment (referred to as single crested). The basic failure mechanisms and equations of the single and double crested earth embankment are similar. Differences occur between fault trees and some of the details in the failure mechanisms. In appendix A the detailed fault tree is given for single earth embankments.

Figure 4.1 shows the representation of the double crested earth embankment structure. How the three different water level zones impact on the reliability analysis is explained in the next section on fault trees. The embankments are generally founded on a pack of impermeable layers overlaying a water conductive sand or gravel layer. At some locations the water overpressures in the sand / gravel layer are drained by a pipe.

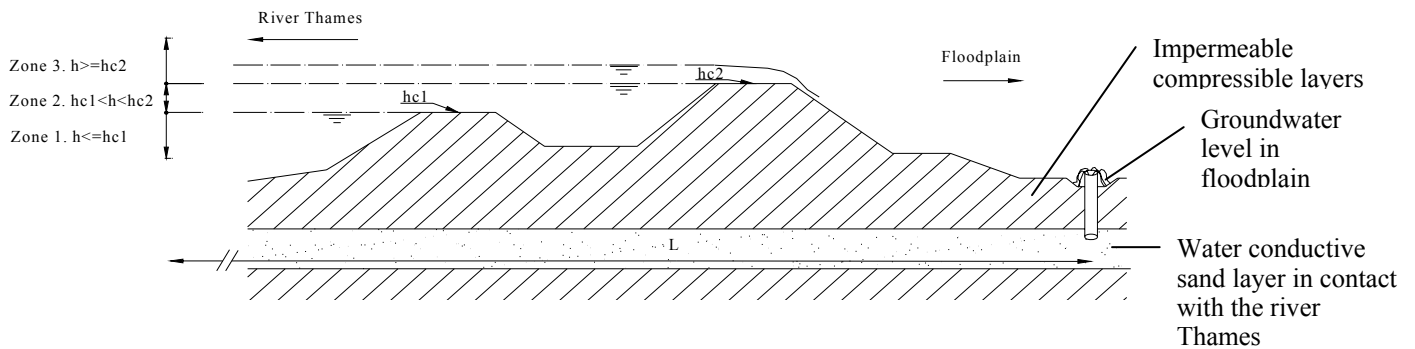


Figure 4.1 Representation of double crested earth embankments. Characteristics of process models or fault trees change according to the three different water level zones

4.2.2 Fault tree

The primary function of the earth embankments is to protect the hinterland against flooding. Failure, or the top event in the fault tree, is defined when the earth embankment structurally breaches and flooding occurs. Excessive overtopping discharges which cause damage are therefore not considered in this study.

Figure 4.2 illustrates the simplified fault tree for double crested earth embankments used in the reliability calculations. The fault tree approach changes for water levels lower and higher than the riverward crest level. The following comments are made with regard to the fault tree for double crested earth embankments.

- For water levels lower than the riverward crest level, failure of both of the two embankments must occur before breach occurs.
- For water levels higher than the riverward crest level only failure of the landward embankment is required for breach. In this case it still matters whether the riverward embankment has failed prior to the second. The presence of the riverward embankment affects e.g. the wave overtopping conditions or the pore pressures of the landward embankment. This effect is not taken into account in the calculations in this study.

4.2.3 Discussion failure mechanisms

The following failure mechanisms are discussed for the earth embankments, limit state equations can be found in Appendix B:

- Wave overtopping / overflow followed by erosion
- Uplifting
- Piping
- Slope instability

Wave overtopping / overflow followed by erosion

Water discharges due to wave overtopping or overflow respectively hit or scour the inside slope of the embankment. The loading of the inside slope damages the grass turf. After the grass has been damaged, the embankment body is exposed to the overtopping/overflowing water. In the end, if this erosion process continues long enough, the embankment breaches. The duration of this erosion process depends on the duration of the overtopping discharges during the storm.

Uplifting

In the Thames Estuary an embankment is often founded on a pack of impermeable layers overlying a water conductive sand or gravel layer. Uplifting occurs when the upward hydraulic force in the water

conductive layer exceeds the cumulative weight of the impermeable layers. The hydraulic force bursts the impermeable layer upward. In the Thames Estuary, pipes applied in ditches behind the embankment relieve the upward hydraulic force.

Piping

Bursting of the impermeable layers opens the doorway for the water in the water conductive layers. Driven by the hydraulic head between the water level outside the embankment and in the floodplain, the water seeps up, carrying particles from the water conductive sand layer. If this process can carry on long enough, pipes form underneath the embankment undermining the foundation. This can eventually lead to collapse of the embankment.

Whether there will be a piping process depends on whether the water conductive layer is connected to the water level at the Thames – defining the seepage length. For the Dartford Creek to Gravesend site this seepage length depends on the bathymetry of the river as well as the variability of the thickness of impermeable layers. As a first approximation the width of the embankment was taken plus half the width of the river.

Slope instability

An increase in pore pressures in the earth embankment over a period of time can lead to slope instability. The increase in pore pressures can have several causes, e.g. rainfall over a longer period of time, rising river water levels, rapidly receding tides, overtopping discharges seeping into fissures, etc.

The characterisation of the pore pressure distribution depends on the situation of interest. As a first estimate of factor of safety of slopes often Bishop's slip circle method is used. Bishop's factor of safety approach can also be set up in a probabilistic model, although that brings some complications. The grid encapsulating the pool of more likely slip circles needs to be located beforehand.

Once the optimal grid is found, the method is computationally intensive and takes a long time to run. Therefore only an indication is provided of the probability of failure with this method rather than generating full fragility.

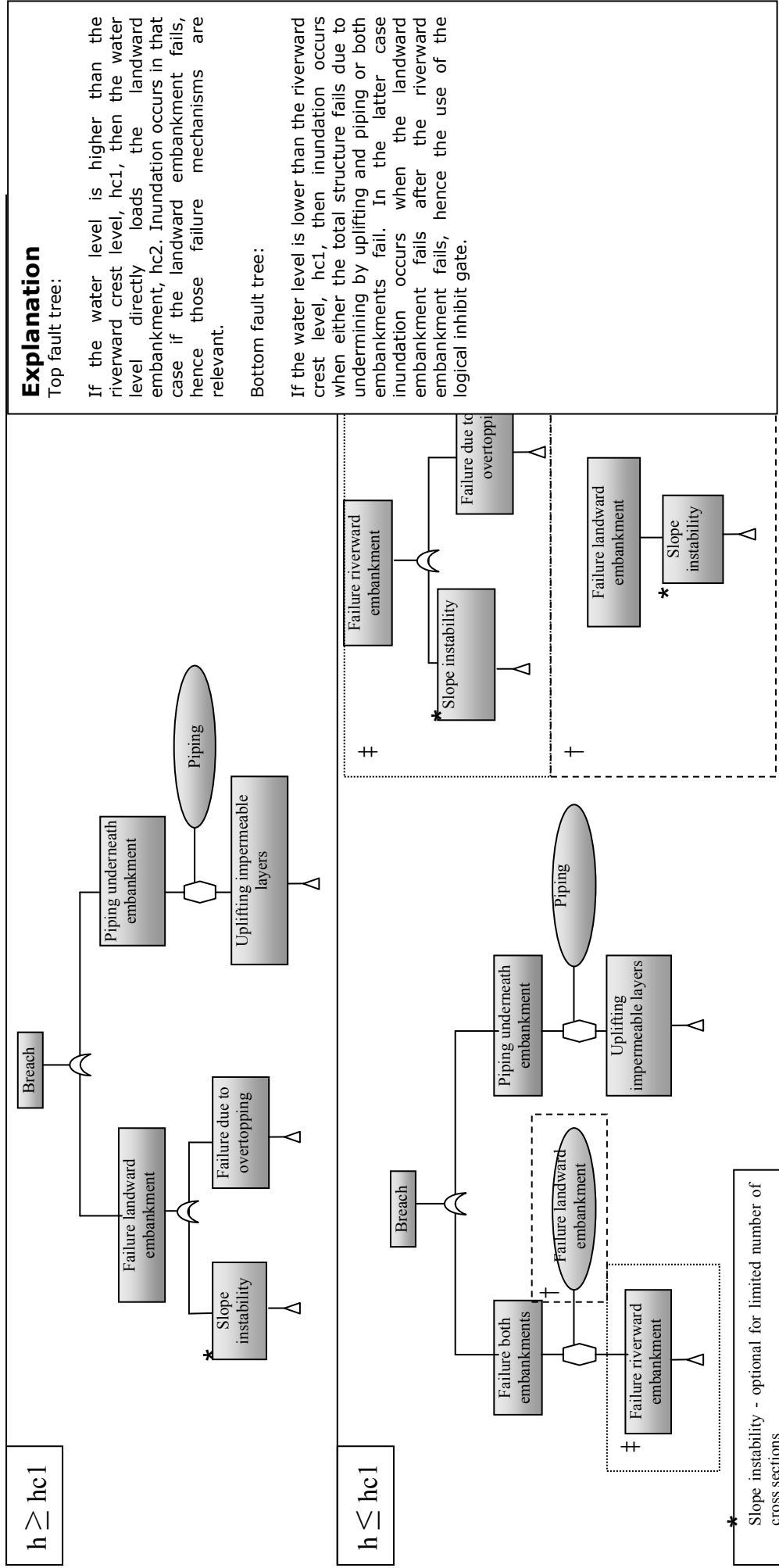
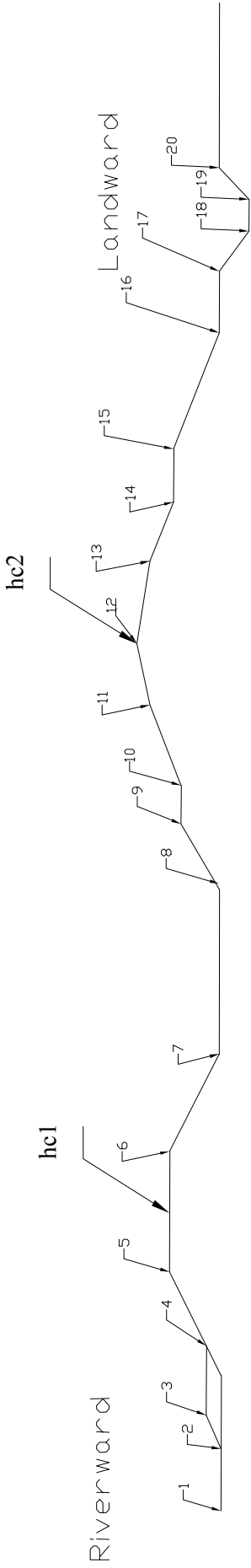


Figure 4.2 Fault trees for double crested earth embankments as applied in the limit state functions

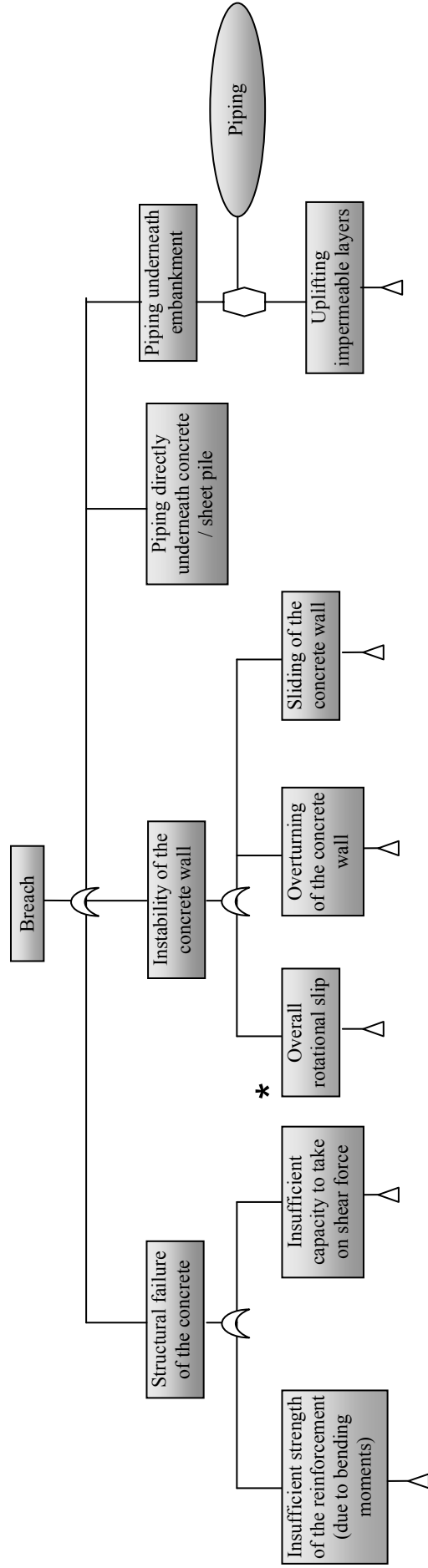
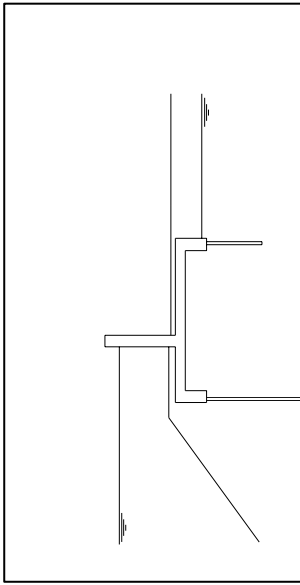


Figure 4.3 Fault trees for concrete walls as applied in the limit state functions

4.3 Concrete walls

4.3.1 Representation of the structure

The way in which the forces on the reinforced concrete wall structure are represented depends on whether ground is mobilised underneath the concrete structure, between either the sheet pile cut-off or concrete extensions. The ground is only mobilised if the connections of the extensions with the concrete structures have been detailed for bending moments. The technical drawings of the details of the sheet pile – concrete wall connections for the Dartford Creek to Gravesend concrete walls confirm that these are designed for bending moments. The applied concrete extensions are in most cases not that long, and are also detailed for bending moments. The structure can then be decomposed as shown in Figure 4.3. This decomposition leads to the forces H1 to H8 and V1 to V3, which are explained below.

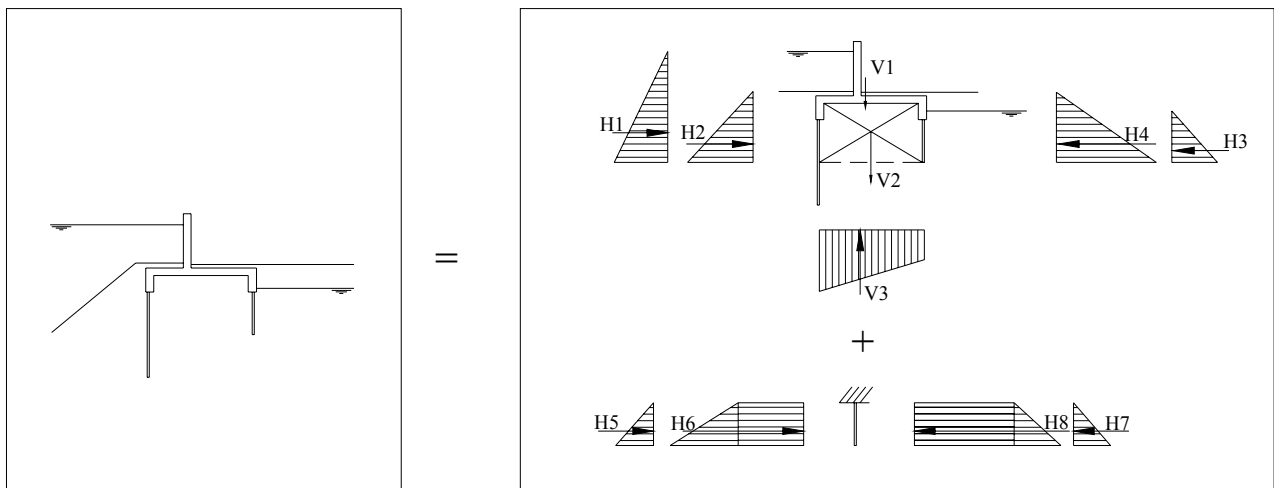


Figure 4.3 *Decomposition of concrete wall in case of mobilised foundational soil. The horizontal grain forces on the main structure are active and passive on respectively the river- and landside. The horizontal grain forces on the sheet pile wall extension are active and passive on respectively the land- and riverside.*

A description of the different horizontal forces exerted on *the main structure* - concrete wall and mobilised ground – is as follows:

- H1 = horizontal hydraulic force exerted by the river water level
- H2 = active horizontal grain force exerted by the ground on the riverside
- H3 = horizontal hydraulic force exerted by the groundwater on the landside
- H4 = passive horizontal grain force exerted by the ground on the landside

The horizontal forces on the *sheet pile cut-off* that does not mobilise ground is modelled as follows:

- H5= horizontal hydraulic force exerted by the river water level on the sheet pile cut off
- H6= passive horizontal grain force exerted by the ground on the sheet pile cut off on the riverside
- H7= horizontal hydraulic force exerted by the groundwater on the sheet pile cut off on the landside
- H8= active horizontal grain force exerted by the ground on the sheet pile cut off on the landside

Vertical forces are as follows:

- V1= The vertical weight of the concrete structure, the location of the centre of gravity should also be established
- V2= The vertical weight of the mobilised ground between the extensions, as explained above, the details of the connections should be designed for bending moments

V3= Upward hydraulic force exerted by the water pressures in the ground underneath the concrete structure. The distribution is taken linear, between the river water level and groundwater level behind the concrete wall.

4.3.2 *Fault tree*

The primary function of the concrete walls is to protect the hinterland against flooding. Failure, or the top event in the fault tree, is defined when the concrete wall structurally fails and flooding occurs. Excessive overtopping discharges which cause damage are therefore not considered in this study. It is additionally noted that the concrete walls along the Dartford Creek to Gravesend are part of a larger earth embankment structure. Structural failure of the concrete wall alone may not in all cases lead to a full breach.

Figure 4.4 illustrates the fault tree implemented for concrete walls along the Dartford Creek to Gravesend flood defence line. The failure mechanisms are described in more detail in the next section.

4.3.3 *Discussion failure mechanisms*

The following failure mechanisms are discussed in relation to the reinforced concrete walls, limit state equations can be found in Appendix B:

- (Wave) overtopping followed by erosion
- Uplifting and piping underneath the earth embankment
- Sliding of the concrete wall
- Overturning of the concrete wall
- Overall rotational instability of the concrete wall
- Failure of the vertical concrete slab due to bending moments
- Failure of the vertical concrete slab due to shear stress
- Piping directly underneath the sheet pile wall cut-off

(Wave) overtopping followed by erosion

Overtopping followed by erosion has not been incorporated for these concrete walls. Firstly, the concrete walls are part of a very wide earth structure which is extensively protected by asphalt / concrete pavements or roads. Secondly, the nature of the failure mechanism is different from that applied to earth embankments: the erosion process undercuts the foundation of the concrete wall leading to instability. Appropriate representation needs further investigation.

Uplifting and piping underneath the earth embankment

At some locations it is more appropriate to include these failure mechanisms than at others. For example along the frontage at Greenhithe the failure mechanisms are not incorporated. The village of Greenhithe can be considered as high ground. However, at other locations the concrete wall does form part of a wider earth embankment and is the combination of uplifting and piping relevant.

Sliding of the concrete wall

When the water level reaches the concrete wall, a horizontal hydraulic force is exerted against the wall. This force can initiate sliding of the concrete structure. Resisting forces are the weight of the structure and the pressures of the ground keeping the structure into place.

Overturning of the concrete wall

When the water level reaches the concrete wall, a horizontal hydraulic force is exerted against the wall. This force can overturn the concrete structure. Resisting forces are the weight of the structure and the pressures of the ground keeping the structure into place.

Overall rotational instability of the concrete wall

When the water level reaches the concrete wall, a horizontal hydraulic force is exerted against the wall. This force exerts a destabilising force against the concrete structure. Depending on the geotechnical properties of the foundational soil and the pore pressures, an overall slip circle can initiate, leading to instability of the wall. As a simplified analysis Bishop's slip circle analysis is used to estimate a factor of safety. Intersection of simulated slip circles with one of the sheet pile cut-off / concrete extensions should be avoided and therefore poses a minimum restraint on the radii of the slip circles. Given the time-consuming nature, these calculations were not carried out.

Failure of vertical concrete slab due to bending moments

The horizontal hydraulic force exerted by the river water level and the ground resting against the riverside of the concrete wall cause bending moments in the vertical slab of the wall. The concrete structure consists of blocks of a length of for instance 10 meter long, sealed by joints. These joints are not designed to transfer forces between the blocks of concrete structure. The vertical slabs are therefore only supported by the foundational slab of the structure. The bending moment for which the reinforcement should be designed is then present at the base of the vertical slab. See Figure 4.5.

Failure of the vertical slab occurs when there is insufficient reinforcement to take on the tensile stress due to the bending moment.

Failure of the vertical concrete slab due to shear stress

The horizontal hydraulic force exerted by the river water level and the ground resting against the riverside of the concrete wall cause shear stress at the base section of the vertical slab. The concrete structure consists of blocks of a length of for instance 5 meter long, sealed by joints. These joints are not designed to transfer forces between the blocks of concrete structure. The vertical slabs are therefore only supported by the foundational slab of the structure. The horizontal force is therefore transferred at the base of the vertical slab. See Figure 4.5.

Failure of the vertical slab occurs if the concrete cross section has insufficient width or shear strength to take on the horizontal force. Concrete slabs are usually not equipped with reinforcement for shear stress, that is confirmed by technical drawings of the Dartford Creek to Gravesend concrete walls.

Piping directly underneath sheet pile cut-off

Failure due to piping directly underneath the sheet pile cut-off is taken into account if the water level exceeds the ground water level in the earth bank behind the wall. This ensures a positive water head over the concrete structure, which drives the piping process. One of the requirements is that the water level persists long enough for the piping process to initiate. In this context two issues are worth noting:

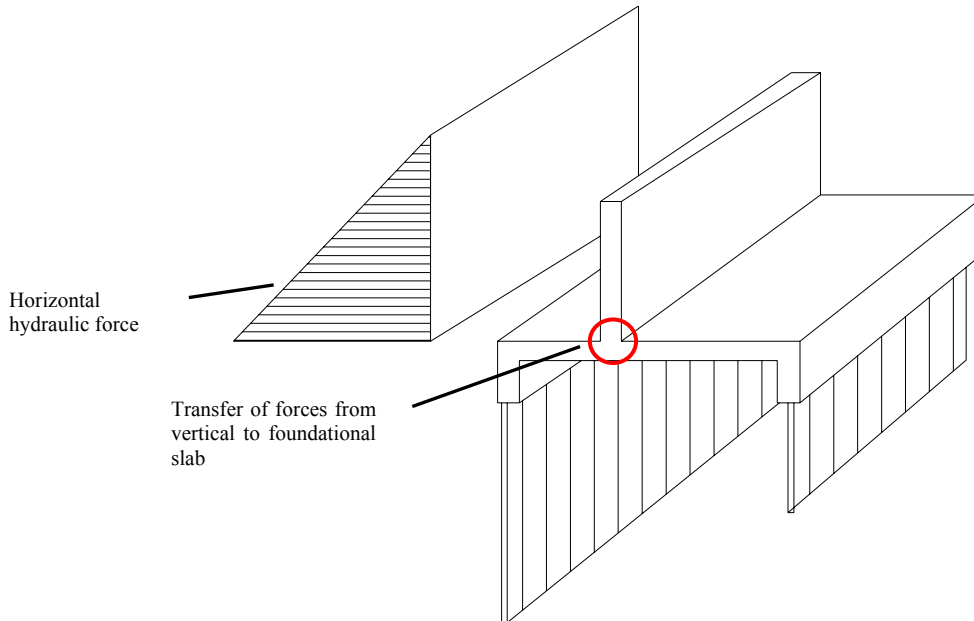


Figure 3.5 One 'block' of concrete wall structure indicating location of transfer of forces between vertical slab to foundational concrete slab.

- The local water levels in this study stand for the high water level during a storm. It depends per storm or surge situation how long such a high water level prolongs.
- Whether or not the piping process initiates depends amongst other factors on the permeability of the soil / the presence of permeable strata. This is currently not taken into account in the model.

4.4 Anchored sheet pile walls

4.4.1 Representation of structure

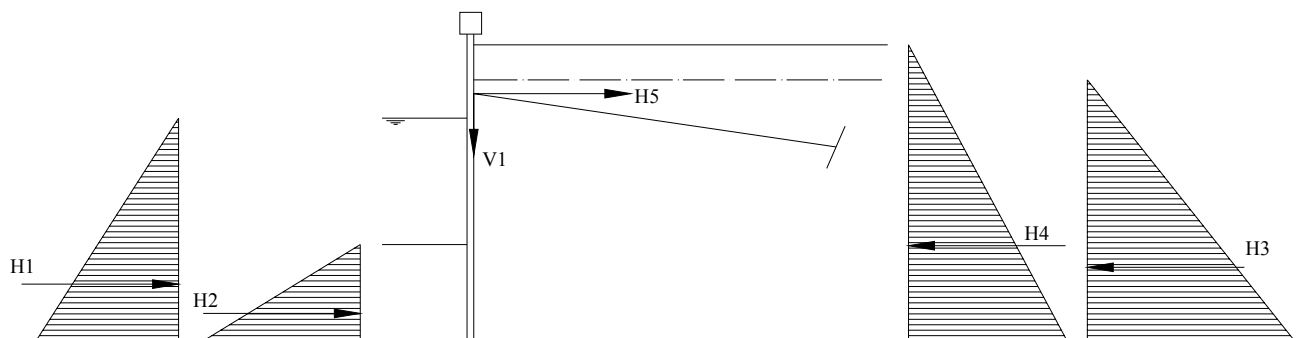


Figure 3.6 Representation of forces acting at anchored sheet pile structure

The representation of the forces in the reliability analysis of anchored sheet pile walls is as shown in Figure 4.6. The presence of remains of old frontage walls behind the anchored sheet pile wall is ignored in this study. Two notes are made with respect to this representation:

- The effect of the presence of such a wall on the reliability of the anchored sheet pile wall can vary. If the old wall e.g. still partly has a retaining function, it relieves the sheet pile wall. In other cases the old wall can introduce backfill pressures in the form of rubble.
- In some cases old river frontages have been used to anchor the tie rod of the sheet pile wall. In such a case the failure mechanism of anchor failure due to insufficient shear strength in the soil is irrelevant.

Description of the forces on the anchored sheet pile wall in figure 3.6:

- H1= horizontal hydraulic force exerted by the river water level
- H2= passive horizontal grain force exerted by the ground on the riverside
- H3= horizontal hydraulic force exerted by the groundwater on the landside
- H4= active horizontal grain force exerted by the ground on the landside
- H5= horizontal force in the tie rod
- V1= vertical force in the tie rod – to be taken into account in failure due to bending moments in the sheet pile

4.4.2 Fault tree

The primary function of the sheet pile walls is to retain ground. Failure, or the top event in the fault tree, is defined when the sheet pile wall structurally fails and therefore does not retain the ground it was designed to. The probability of failure is therefore not representative of the probability of breach. The latter is not applicable as the sheet pile walls protect high grounds. However, structural failure of the sheet pile walls does imply less protection against overtopping during high water events.

Figure 4.7 illustrates the fault tree implemented for anchored sheet pile walls along the Dartford Creek to Gravesend flood defence line. The failure mechanisms are described in more detail in the next section.

4.4.3 Discussion failure mechanisms

The following failure mechanisms are discussed in relation to the anchored sheet pile walls, limit state equations can be found in Appendix B:

- (Wave) overtopping followed by erosion
- Uplifting and piping underneath the earth embankment
- Breaking of sheet pile wall due to bending moments
- Insufficient shear strength of the soil near the anchorhead: sliding of the anchor
- Insufficient strength of the tie rod: breaking of the anchor
- Rotation around the toe of the sheet pile
- Overall rotational failure of the anchored sheet pile wall

(Wave) overtopping followed by erosion

Overtopping followed by erosion has not been incorporated for these anchored sheet pile walls. The anchored sheet pile walls are per definition part of a very wide earth structure which provides support to the tie rod. These banks can usually be considered as high ground.

Uplifting and piping underneath the earth embankment

At some locations it is more appropriate to include these failure mechanisms than at others. For example along the frontage at Greenhithe the failure mechanisms are not incorporated. The village of Greenhithe can be considered as high grounds. Anchored sheet pile walls in this study only occur along the frontages of industry / villages / towns. On the other hand cantilevered sheet pile walls are often applied as part of a narrower earth bank. Uplifting and piping may be of relevance there. This issue is discussed in the next section.

Breaking of sheet pile wall due to bending moments

The ground that is retained, the groundwater, the river water level and the tie rod exert pressure on the sheet pile wall. Those pressures cause bending moments in the sheet pile wall. Failure occurs if the capacity of the sheet pile cross section is exceeded by the actually occurring bending moments. From the maximum occurring bending moment in the anchored sheet pile a maximum tensile stress in the sheet pile wall can be derived, using the moment of inertia and the height of the section. That maximum occurring tensile stress is compared against the tensile strength of the sheet pile steel.

Insufficient shear strength of the soil near the anchorhead: sliding of the anchor

Tie rods of the Dartford Creek to Gravesend anchored sheet pile walls are usually anchored in the soil using an anchor head. The anchor head transfers the force from the tie rod to the soil. Failure occurs if the stress exerted by the anchor head exceeds the shear strength of the soil. The shear strength of the soil depends on e.g. the depth of the anchor head, the size of the anchor head and the soiltype.

Insufficient strength of the tie rod: breaking of the anchor

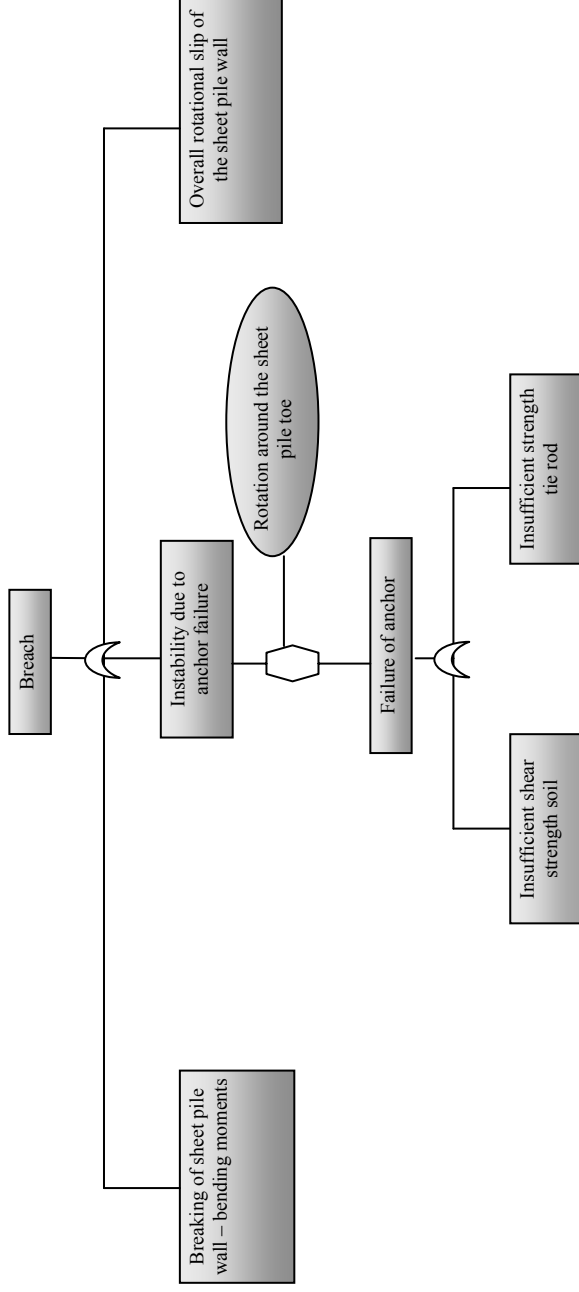
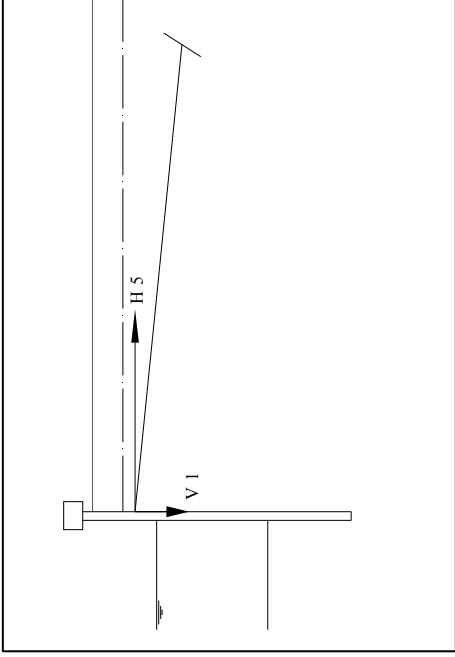
The tie rod supports the sheet pile wall in taking on the forces. Failure of the tie rod occurs if the stress occurring in the tie rod exceeds the tensile strength of the steel. Corrosion can play a large role in reducing the tie rod cross section near the connection with the sheet pile wall. Especially when this connection is located near the splash zone.

Rotation around the toe of the sheet pile

Whether the sheet pile wall collapses after failure of the tie rod depends on the moment equilibrium around the toe of the sheet pile. Failure occurs if the moments as a result of the ground and groundwater pressures are larger than those as a result of the ground and water level on the river side.

Overall rotational failure of the anchored sheet pile wall

Overall rotational failure of the anchored sheet pile takes place if a slip circle occurs encapsulating both the anchor and the sheet pile. Bishop's slip circle method can be used to make an estimation of the factor of safety. The slip circles cannot intersect with the tie rod and the toe of the sheet pile, this poses a constraint on the choice of slip circle radius. Given the time-consuming nature, these calculations were not carried out.



* Rotational instability - optional for limited number of cross sections

Figure 4.7 Fault trees for anchored sheet pile wall as applied in the limit state functions

5. Single cross section and system reliability methods

The previous chapters dealt with the definition of the flood defence system boundaries, the structure types and their failure mechanisms. The next steps are:

- To discretise the flood defence line into stretches with similar characteristics.
- To represent each stretch with one cross section.
- Collect data for this cross section according to the structure type and its defined failure mechanisms.
- Perform reliability calculations, in this study level III Monte Carlo simulations were applied.

5.1 Single cross section reliability method

5.1.1 Method to establish fragility and the annual probability of failure

In chapter 3 limit state equations were derived for individual failure mechanisms as a function of a process-based model for strength and loading. A generalised expression is given below:

$$Z = R - S \quad (5.1)$$

Whereby R represents strength and S represents loading. Failure occurs when $Z < 0$. The definition of failure depends on the functions of the structure in question. The concept of fragility calculates the probability of failure given a range of different conditions of source variables. The annual probability of failure takes the probability distribution functions of the source variables into account. The probability of failure due to a failure mechanism described by a strength and loading model can be calculated with the integral below. The limit state equation is hereby represented by a function f of a vector of random variables:

$$P_f = \int_{Z \leq 0} f(\vec{X}) d\vec{X} \quad (5.2)$$

This integral can usually not be analytically solved. To approximate the probability of failure therefore a level III crude Monte Carlo method is applied according to CUR190 (1997).

Often several failure mechanisms in a cross section can lead to failure of a structure. These mechanisms share similar properties introducing mutual correlations. In Monte Carlo simulations correlation is straightforwardly dealt with by using the same variable values for one simulation. In Figure 4.1 is shown how joint probabilities of failure for several failure mechanisms in one cross section are calculated.

In the Monte Carlo simulations of fragility the probability of failure is calculated conditional on the source variables (related to the Source-Pathway-Receptor-Consequences model). When calculating annual probabilities of failure, in contrast, the probability distribution functions of the source variables are included in the simulation. The annual probability of failure is separately calculated given each wind direction, and merged into one by combining them with the probability of the wind direction:

$$P_{f;annual} = P_{NE} \cdot P_{f;annual;NE} + P_{SE} \cdot P_{f;annual;SE} + P_{SW} \cdot P_{f;annual;SW} + P_{NW} \cdot P_{f;annual;NW} \quad (5.3)$$

Wherein $P_{f;annual}$ is the total annual probability of failure, P_{NE} , P_{SE} , P_{SW} , P_{NW} are the probabilities of the wind directions North East (NE: $0^\circ - 90^\circ$), South East (SE: $90^\circ - 180^\circ$), South West (SW: $180^\circ - 270^\circ$), North West (NW: $270^\circ - 360^\circ$), and $P_{f;annual;NE}$, $P_{f;annual;SE}$, $P_{f;annual;SW}$, $P_{f;annual;NW}$ are the annual probabilities of failure given the four previously mentioned wind directions.

5.1.2 Method to establish sensitivity indices

A by-product of level II FORM calculations are alpha-values. These indicate the contribution of the uncertainty of a random variable to the total probability of failure. A Monte Carlo simulation allows a less accurate derivation of alpha values. One method that can be employed is to hold on to the random draw for $Z < 0$ with the highest joint density in the normal space. The alpha-values can then be derived by dividing the standard normal values by the reliability index. During the Monte Carlo calculations this method did not provide meaningful alpha-values. The FORM method was therefore used to establish the appropriate alpha-values.

Alpha values indicate how the probability of failure can be most effectively reduced by taking out the uncertainty of a particular random variable. The nature of this uncertainty can be for instance variability in time, in case of water levels or waves, in space due to poor borehole resolution or in knowledge.

In Buijs et al. (2005) another indicator is proposed, see definition below. This sensitivity index represents the normalised sensitivity to change of the failure space to a change in one of the random variables. It provides insight into the sensitivity of a failure mechanism to improvement, deterioration, inspection or other monitoring.

$$\Delta_{X_i} = \varepsilon \cdot \mu_{X_i} \cdot \int_{Z \leq 0} \frac{\partial Z}{\partial X_i} \cdot f_x(\vec{X}) d\vec{X} = \varepsilon \cdot \mu_{X_i} \cdot E\left(\frac{\partial Z^-}{\partial X_i}\right) \quad (5.4)$$

In which Δ_{X_i} is the delta-value of variable X_i , $\varepsilon \cdot \mu_{X_i}$ is a percentage of the mean value, $\partial Z / \partial X_i$ is the partial derivative of the limit state equation to the variable X_i , $f_x(\vec{X})$ the joint density function of the vector of random variables \vec{X} , $E(\partial Z / \partial X_i)$ is the expectation of the partial derivative of Z to X_i in the failure region of the limit state equation.

The partial derivative depends on the unit of the random variable, the multiplication with $\varepsilon \cdot \mu_{X_i}$ eliminates the dependency on the unit. Instead of a percentage of the mean value other types of increments can be considered such as: the increment of a deterioration process affecting X_i , a correction after an inspection, the change in the design variable in the light of an improvement study.

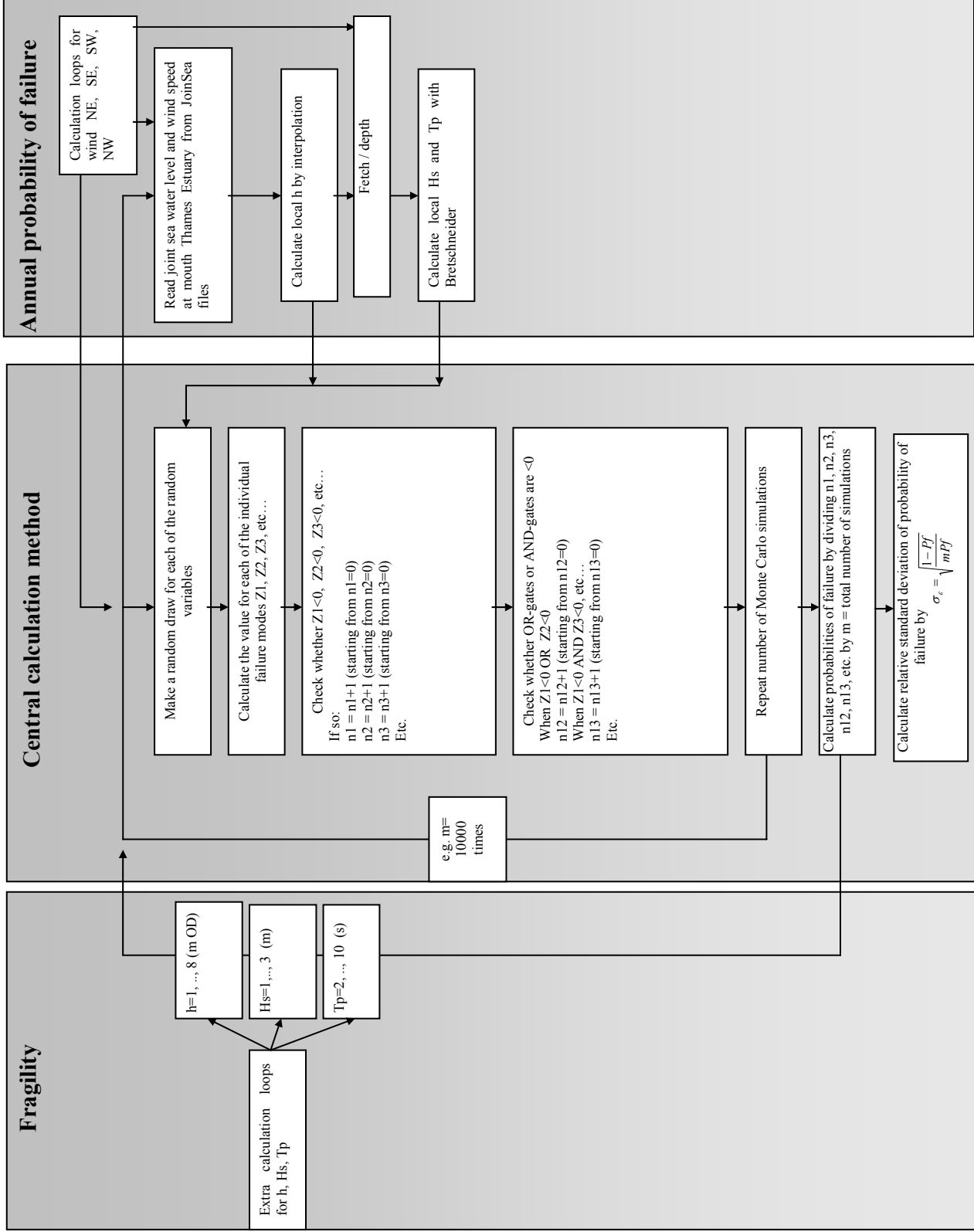


Figure 5.1 Flow chart with steps to calculate fragility and the annual probability of failure

5.2 Evaluation of defence length reliability methods

5.2.1 Introduction to length effect

Material properties, geometry, vegetation, hydraulic boundary conditions or other characteristics that make up flood defence reliability are similar along the flood defence line. Because of these similarities, failure tends to occur simultaneously over certain defence stretches and breach locations tend to be spatially related.

Theoretically the length effect is represented by the probability of failure of a series of flood defence cross-sections, within any given defence length. Each stretch along the flood defence line can be subdivided into an infinite number of cross sections. If flood defence sections are assumed to be independent the joint probability of failure keeps on decreasing when including more sections. If the flood defence sections are correlated, the joint probability of failure decreases less sharply than in the independent case. Depending on the type of correlation structure the joint probability of failure converges to an equilibrium value, see also Chun-Ching Li (1993).

The theoretical approach to the length effect investigated in this study consists of the following components:

- Statistical model of the length effect:
 - Spatial autocorrelation function
 - Multivariate normal distribution function
- Calculation method

These components are discussed in more detail below.

Spatial autocorrelation function

In this study the spatial behaviour of the flood defence properties is characterised by the two models described next. Two frequently used spatial correlation functions are shown in figure 4.2. The first model concerns a correlation that diminishes with distance or converges to a constant value. The equation for this model is given below:

$$\rho(\Delta x) = \rho_x + (1 - \rho_x) \exp\left(-\frac{\Delta x^2}{d_x^2}\right) \quad (5.5)$$

The second model uses a correlation that remains constant with distance.

The application of these two correlation models and their limitations is illustrated by the categories of flood defence properties below:

- Water level and wave conditions are taken to be fully correlated along the flood defence line. This assumption is made as the local hydraulic climate is driven by the same overall sea water

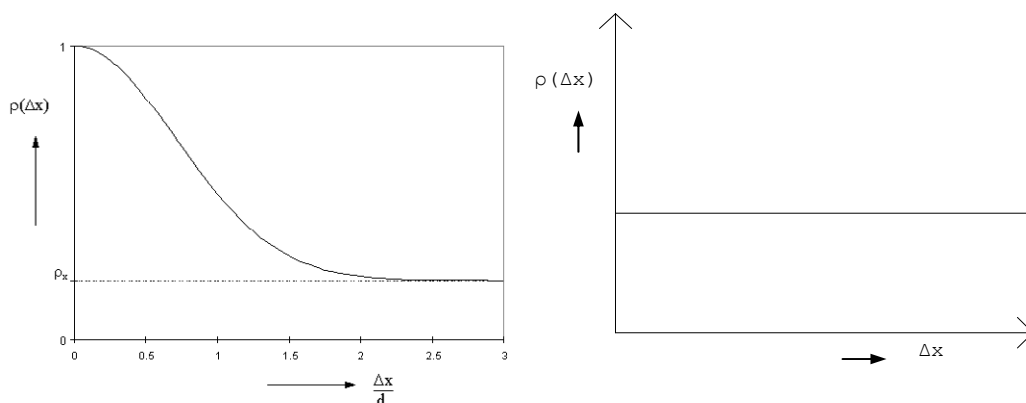


Figure 4.2 Two types of correlation functions

level and wind field. The appropriateness of this assumption depends on factors such as the quality of the representation of the bathymetry, local wind field variations or the quality of the numerical model.

- Soil properties are characterised by a correlation function that reduces to a constant value with distance. On the other hand, local variations in the form of lenses or highly variable soil properties cannot be captured by this model. In addition, a constant correlation may be more appropriate if earth structures are e.g. similarly compacted over a particular stretch.
- Man-made material properties such as concrete wall properties are taken to be fully correlated for the length of a unit such as a concrete wall.

Multivariate normal distribution function

In this study the multivariate normal distribution function is applied to calculate the joint probability of failure of correlated cross sections. It can also be used to combine several failure mechanisms in one cross section into one overall probability of failure. That approach leads to a linearised limit state equation formulated in the standard normal space by an equivalent reliability index and a set of alpha-values.

The main advantages of the multivariate normal distribution function are:

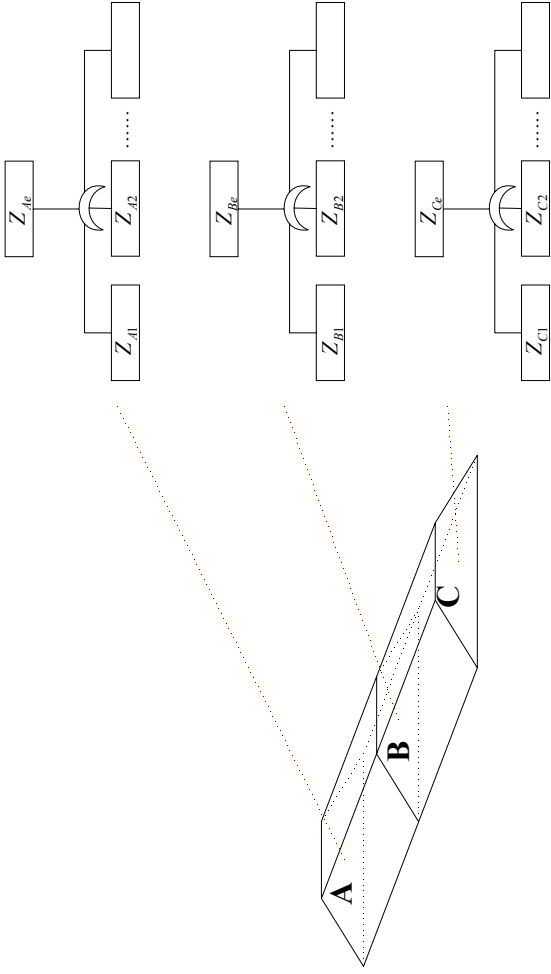
- The probability of failure and the contributions to uncertainty of random variables herein can be characterised by a linearised limit state equation in the standard normal space. A multivariate normal distribution function is then a convenient representation of the correlation.
- The multivariate normal distribution function offers a flexible correlation structure that is transparent and easy to deal with in calculations.

On the other hand, the multivariate normal distribution function represents the correlation in the normal space. It is not clear to which extent the correlation in the normal space relates to that in the physical space.

Calculation method

Figure 5.3 provides an overview of the calculation procedure for the length effect. Two issues deserve mentioning in the context of formulating an equivalent beta and set of alpha-values for one cross section. Firstly, the method to derive equivalent alpha-values is empirical rather than theoretical. Secondly, to calculate the bivariate normal distribution function either an approximate level-II method according to Hohenbichler et al. (1983), or a Monte Carlo integration method can be used. The results obtained with both methods were compared and do not deviate too much.

With regard to the length effect calculations between two cross sections two issues are further addressed in section 5.3. Firstly, the stretch between two cross sections must be subdivided into a sufficient number of sections to capture the system effect. The grid must therefore be fine enough. On the other hand, it is preferable to keep the grid coarse to limit the calculation time. A second question is whether the correlation between subsections can be assumed to be constant over a particular stretch, or should be represented in more detail.



Calculation of joint probability of failure for cross sections A, B and C

- Combine the individual failure mechanisms for one cross section to one equivalent limit state equation Z_{Ae} . To this end the procedure in box 1 can be used.
- Repeat the procedure under the previous bullet for all cross sections: A, B and C.
- Further discretise the defence line between A, B and C into smaller sections to make a better approximation of the system effect.
- ρ_{A_i, B_k} is the autocorrelation for the k-th random variable between two subsections on the length between cross section A and B. This autocorrelation can be derived by using the functions as outlined in the main text.
- The equivalent limit state equations for the cross sections and autocorrelations are then available from the previous steps. Derive the joint probability of failure of cross sections A, B and C by using the procedure described in box 2.

1

$$Z_{A1} = \beta_{A1} + \alpha_{A11}u_{A11} + \alpha_{A12}u_{A12} + \dots = \beta_{A1} + \sum_{k=1}^n \alpha_{A1k}u_{A1k}$$

$$Z_{A2} = \beta_{A2} + \alpha_{A21}u_{A21} + \alpha_{A22}u_{A22} + \dots = \beta_{A2} + \sum_{k=1}^n \alpha_{A2k}u_{A2k}$$

$$\rho_{Z_{A1}, Z_{A2}} = \sum_{k=1}^n \alpha_{A1k} \alpha_{A2k} \rho_{Aijk}$$

$$\Phi(-\beta_{Ae}) = \Phi(-\beta_{A1}) + \Phi(-\beta_{A2}) - BIN(-\beta_{A1}, -\beta_{A2}, \rho_{Z_{A1}, Z_{A2}})$$

$$Z_{Ae} = \beta_{Ae} + \alpha_{Ae1}u_{Ae1} + \alpha_{Ae2}u_{Ae2} + \dots = \beta_{Ae} + \sum_{k=1}^n \alpha_{Aek}u_{Aek}$$

2

$$\rho_{Z_{Ae}, Z_{Be}} = \sum_{k=1}^n \alpha_{Aek} \alpha_{Bek} \rho_{A_i, B_k}$$

$$\mathbf{R}_{A,B,C} = \begin{bmatrix} 1 & \rho_{Z_{Ae}, Z_{Be}} & \rho_{Z_{Ae}, Z_{Ce}} \\ \rho_{Z_{Be}, Z_{Ae}} & 1 & \rho_{Z_{Be}, Z_{Ce}} \\ \rho_{Z_{Ce}, Z_{Ae}} & \rho_{Z_{Ce}, Z_{Be}} & 1 \end{bmatrix}$$

$$\Phi_{j \circ \text{int}}(-\beta_{j \circ \text{int}}) = MIN(-\beta_{Ae}, -\beta_{Be}, -\beta_{Ce}, \mathbf{R}_{A,B,C})$$

Figure 5.3. Calculation procedure for the length effect

5.2.2 Influence of variations in length effect approach to flood defence reliability

Three main components of the approach to calculate the length effect were discussed in 5.2.1. This section looks into the influence of variations in that approach on flood defence reliability results. The following aspects are discussed:

- The difference between the joint probability of independent sections and that taking length effect into account.
- Statistical model of the length effect:
 - Spatial autocorrelation function – the influence of different assumptions about the function on the joint probability of failure of defence sections. This influence provides insight both in assumptions about the autocorrelation function as well as inferences made due to lack of data availability.
 - Multivariate normal distribution function – the application of different multivariate distribution functions is not subject to further investigation here.
- Calculation method – a number of aspects are further addressed:
 - The resolution of the discretisation for a sufficient representation of the system effect.
 - The assumption of a constant correlation between subsections or a more detailed correlation function. This assumption is considered in conjunction with the use of a Monte Carlo integration method versus a level II approach based on Hohenbichler et al. (1983)

All results presented in this text concern an earth embankment structure with a section length of 85 meter. The 85 meter stretch is subdivided into smaller sections with a slice width as displayed in the figures.

Length effect versus independent flood defence sections

Figure 5.4 shows the difference between an approach taking independent sections and correlated sections into account. It demonstrates the sharply increasing joint reliability index in case of independent sections compared to the correlated situation.

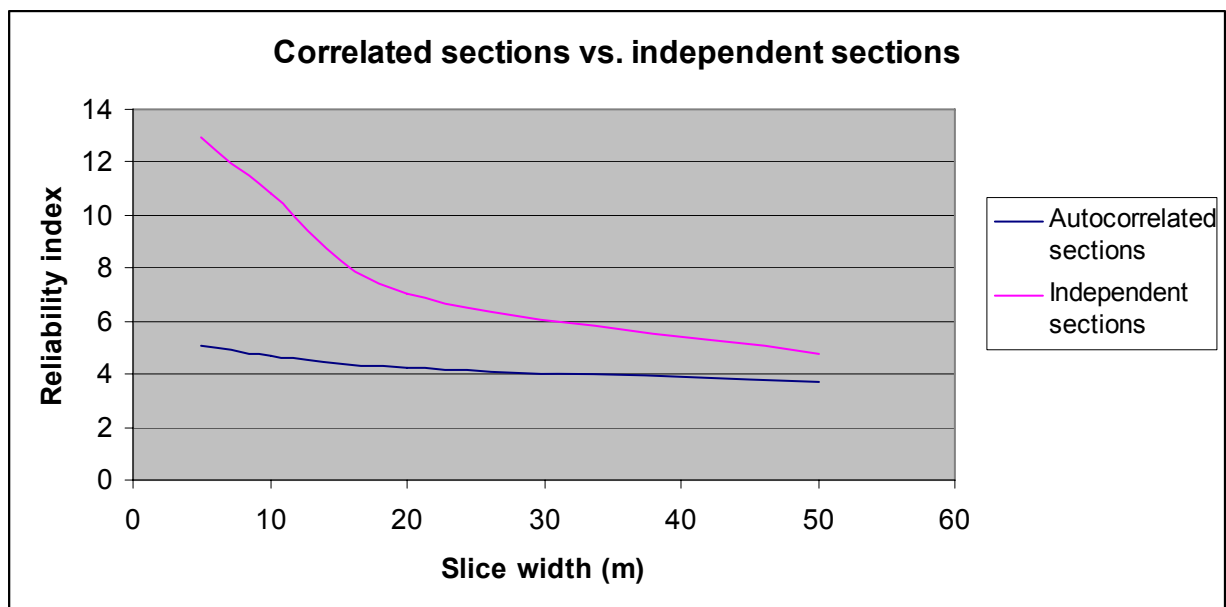


Figure 5.4 Joint reliability index for independent and autocorrelated sections given different slice widths

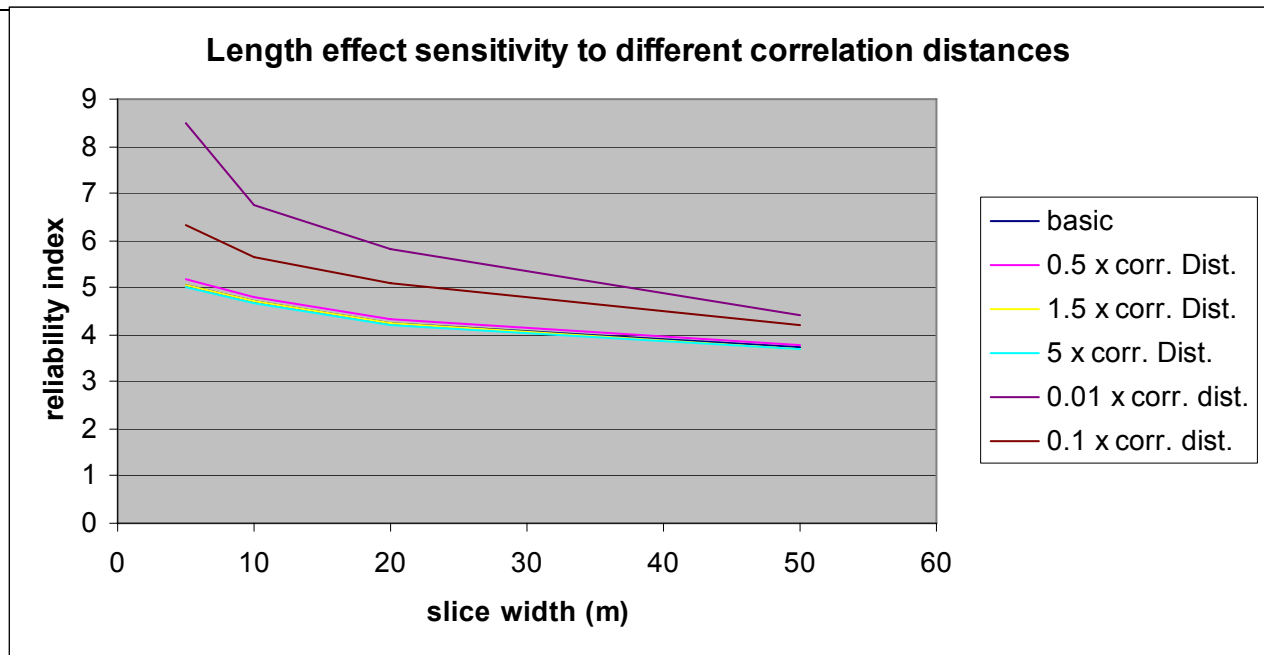


Figure 5.5 Sensitivity of the length effect to different correlation distances

Influence of the spatial autocorrelation function

In Figure 5.5 the length effect is calculated for different correlation distances. The figure indicates that under the assumed correlation structure in the base case, the correlation ρ_x in equation 5.5 has a strong influence on the length effect. This indication is supported by the following:

- The results show that for a very strong reduction in correlation distance (0.01 x corr.dist) the joint reliability index behaves more independently. Still, in that case the joint reliability index is below that of the fully independent one indicated in Figure 5.4.
- Only a very strong reduction in correlation distance appears to have an influence on the results.
- The sections are heavily correlated under the assumed correlation structure in the base case. Applying much higher correlation distances does not have much effect.

The influence of the correlation distance on the joint reliability was also considered for a flood defence stretch of 158 meter. The results show similar behaviour as compared to that of the 85 meter stretch used in Figure 5.5.

The required discretisation resolution of the flood defence length

According to Chun-Ching Li (1993) the length effect converges to equilibrium for correlation functions that are differentiable in the origin. In general, this equilibrium tends to be reached for a discretisation with a slice width of roughly one fifth of its correlation distance.

Although equation 5.4 is differentiable in the origin, Figures 5.4 and 5.5 demonstrate that the joint reliability index still increases for smaller slice widths. From these results therefore no conclusive recommendations can be made about the appropriate discretisation resolution of the length effect.

Simplified correlation versus detailed correlation

Figure 5.6 shows the comparison between the approach assuming a constant correlation among sections and the approach based on a detailed representation of the correlation. In the latter case, sections that are located further apart behave more independently. The constant correlation representation is calculated with the approach according to Hohenbichler et al. (1983). The detailed correlation representation is calculated by means of a Monte Carlo integration method.

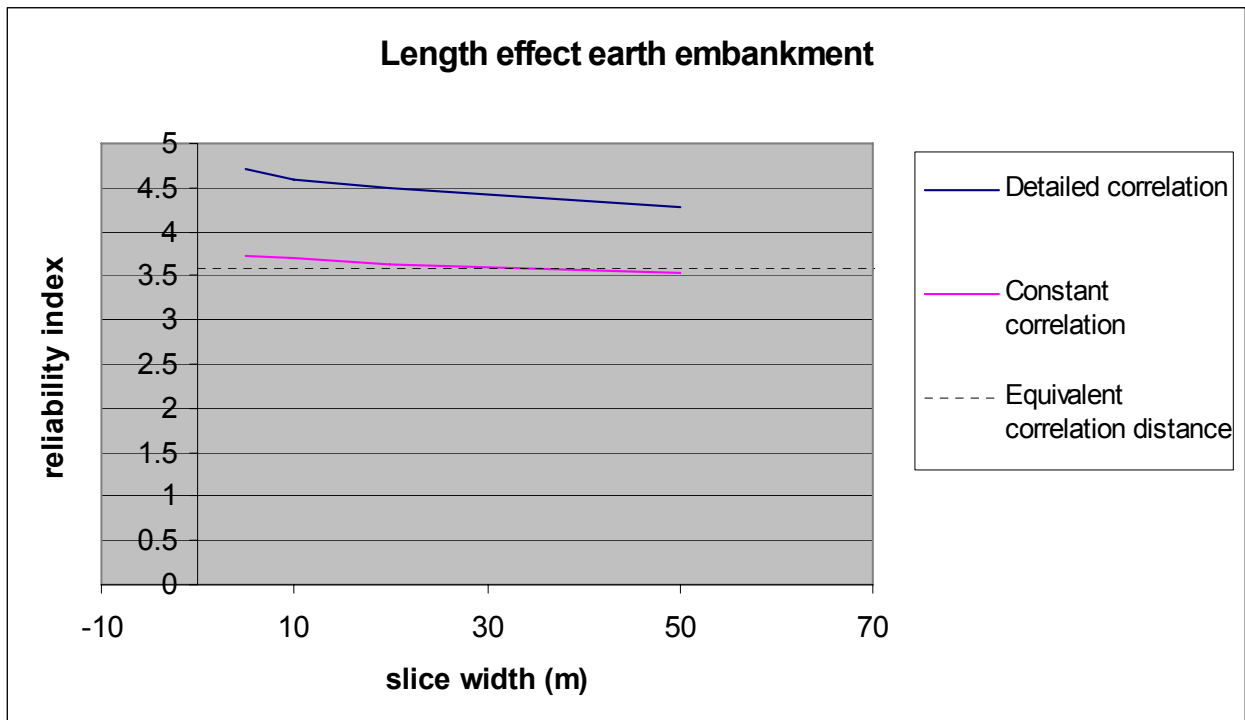


Figure 5.6 Monte Carlo integrated approach versus simplified approximation for the length effect of earth embankments

The difference between the two representations is clearly seen in Figure 5.6, wherein the detailed correlation representation displays much higher joint reliability indices than the constant correlation representation.

One method to estimate a slice width for discretisation in length effect calculations is based on determining the equivalent correlation distance. How the results based on the equivalent correlation distance relate to the other two approaches is shown in Figure 5.6. The equivalent correlation distance results in relatively low joint reliability indices and therefore provides a conservative discretisation.

Role of spatial correlation in flood risk assessment

Firstly, a flood risk assessment procedure is described that incorporates the length effect, see Figure 5.7. Secondly, a number of practicalities regarding this flood risk assessment procedure are given.

Before going into the flood risk assessment procedure and its practicalities, a distinction is made between breach initiation and breach formation. These two definitions apply to a defence structure with as primary function the prevention of flooding.

Breach initiation marks the point when the flood defence fails to perform its primary function. In this research the probability of (structural) failure equals the probability of breach initiation. The applied limit state equations and process-based models intend to underpin that probability of breach initiation.

Breach formation is the process of breach growth that follows after breach initiation. This process influences the development of the inundation in the floodplain, and hence the damage inflicted during a storm.

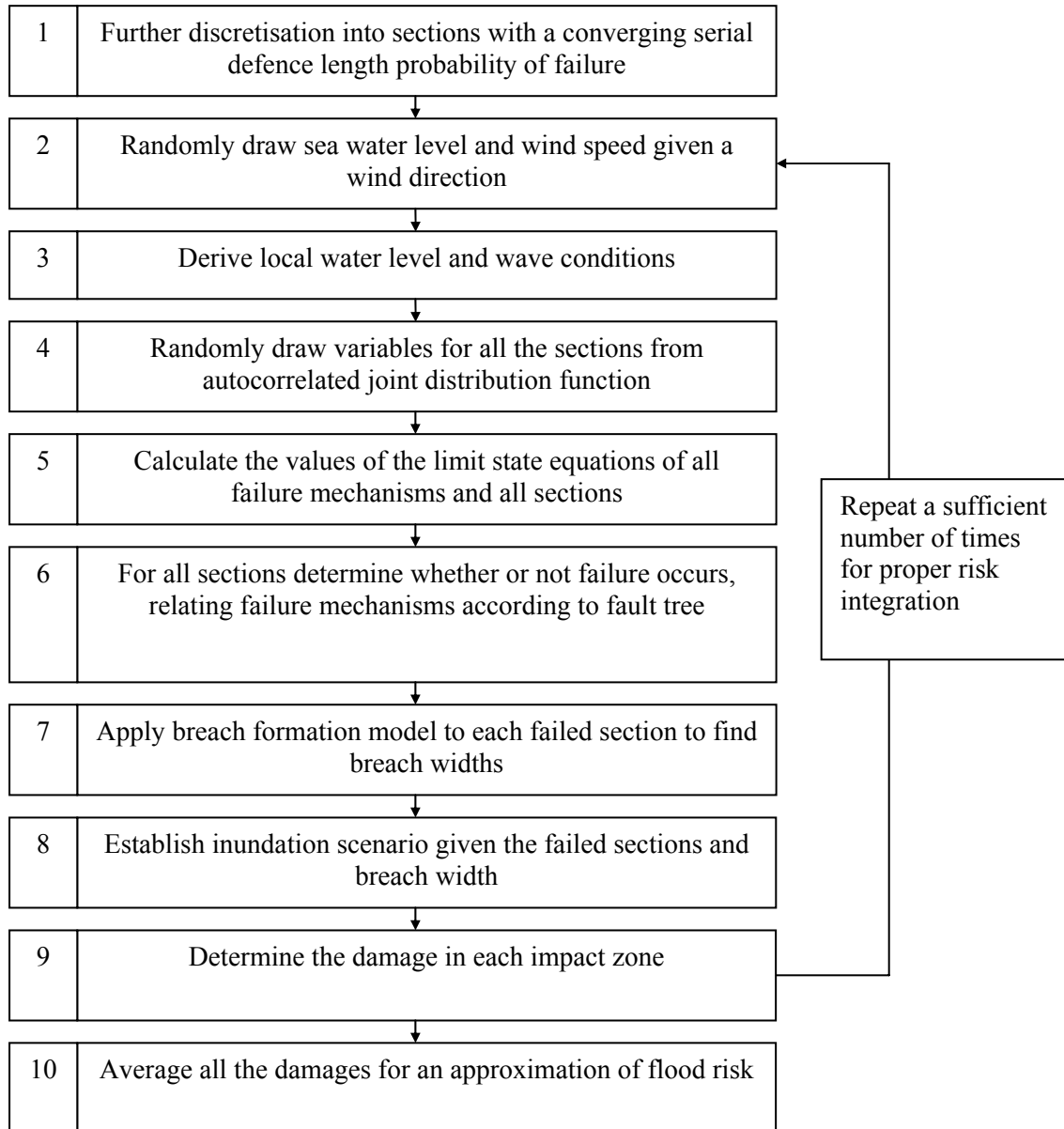


Figure 5.7 Flow chart for flood risk assessment procedure incorporating length effect

Flood risk assessment procedure incorporating length effect

The flood risk assessment procedure that incorporates the length effect is shown in Figure 5.7. This figure is discussed in more detail in the text below. The procedure takes over at step 5 in the flow chart in Figure 2.1, the point where the flood defence line is divided into stretches for which one cross section is representative.

Step 1) In order to capture the length effect the flood defence line is further discretised into smaller sections. The size of the sections is chosen such that the serial defence length probability of failure converges. Spatial autocorrelation is a function of distance and is derived between the midpoints of these sections.

Step 2) Water levels at the sea and the wind field drive the local hydraulic boundary conditions in the estuary.

Step 3) Local water levels and wave conditions are determined given the sea water level and wind field resulting from the previous step. To this end a numerical model can be used.

Step 4) Random variables are autocorrelated among the sections which result from step 1. A joint distribution function captures this autocorrelation among the sections. The autocorrelation among the sections is taken into account by drawing for each random variable from the (spatial) joint distribution function.

Step 5) All the (autocorrelated) variables are then defined for each section. These values can be used to calculate the process-based models in the limit state equations for the failure mechanisms. This calculation points out for each failure mechanism whether failure occurs given this draw.

Step 6) The logical relations between the failure mechanisms in the fault tree then define whether the total flood defence section fails given this draw. This provides an overview of the occurrence of breach initiation in the sections along the flood defence line.

Step 7) A breach formation model is applied to each section. The breach initiation is modelled to take place at the midpoint of the failed sections. Current knowledge in breach formation does not provide insight in the behaviour of interacting breach growth processes. As a simplification superposition of breach growth processes can be applied.

Step 8) Determine the behaviour of the inundation in the floodplain during the breach growth process.

Step 9) Establish the damage done in each impact zone by the inundation during the breach growth process.

Step 10) Average the damages for each impact zone to find an estimate of the flood risk. A sufficient number of Monte Carlo simulations are required for a proper approximation of the flood risk.

Practicalities regarding the proposed flood risk assessment procedure

A number of practicalities associated with the flood risk assessment procedure proposed in Figure 5.7 are listed below.

- The current spatial correlation model is synthetic, as demonstrated in sections 5.2.1 and 5.2.2.
 - Information about the real autocorrelation between flood defence sections is hard to retrieve. The spatial resolution of e.g. soil properties is often coarse. Even if more detailed information is available, further elaborate analysis is required.
 - In addition, correlations are captured by the flexible and easy computable multivariate normal distribution function. In reality other multivariate distributions might be preferable, but may make the flood risk calculation more complex.
 - Simplifying assumptions made in the calculation procedure can have quite an influence on the results.
- However, an assumption about the independency of defence sections is equally synthetic. This is supported by the fact that literature suggests that autocorrelation of e.g. soil properties occurs in many situations. The results in section 5.2.2 show that taking autocorrelation into account has a significant impact on the joint reliability of sections compared to the fully independent case.
- A fine discretisation of the flood defence line in conjunction with the Monte Carlo simulations leads to the occurrence of a large number of section failure combinations. A large database of inundation scenarios is required to support that diversity in failure combinations. The feasibility of such a database is currently questionable

6. Discussion of the results

In Chapter 5 the method applied to establish single cross section reliability and system reliability were discussed. This chapter goes into the results that were obtained with the calculations. The discussion of the results is organised as follows:

- Reliability analysis of the structure types
 - Earth embankments
 - Concrete walls
 - Sheet pile walls
- System reliability analysis

The flood defence line between Dartford Creek and Northfleet was discretised into sections according to the steps shown in Figure 2.1. Data-wise these sections are represented for the full length by one cross section. The sections are numbered as presented in Figure 6.1. The flood defence line between section 68 and 78 consists of a very wide bank of fly ash and was not considered in the structural reliability analysis. The data availability was poor from section 78 on to Gravesend, this stretch is therefore not addressed in the results.

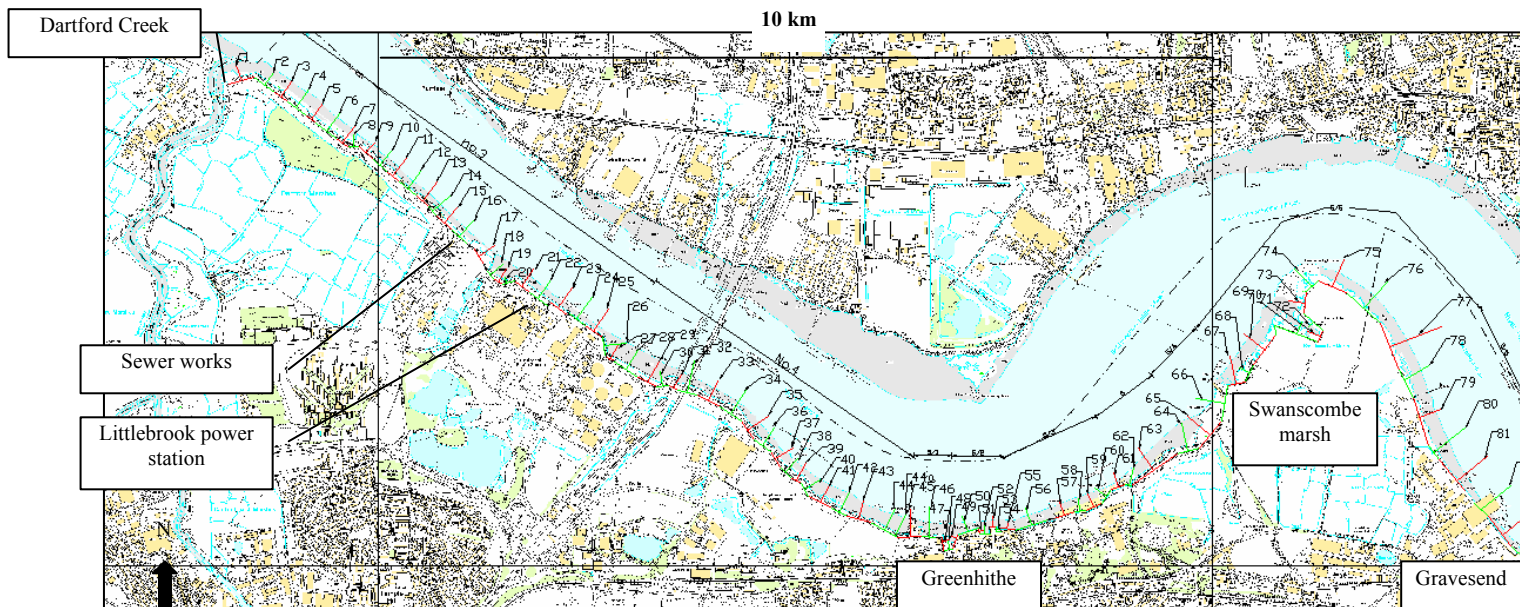


Figure 6.1 Discretised flood defence line between Dartford Creek and Northfleet. The numbered red and green lines represent the sections included in the calculations.

6.1 Description of the products of the reliability analysis

In the following sections for each of the structure types the results listed below are discussed. A general indication of the practical significance of the results is also given below.

- *The fragility* provides insight in the likely behaviour of the flood defence given different source conditions. A steep curve signifies more certainty about the conditions under which the flood defence will fail. A shallow curve relates to a larger range of uncertainty about the conditions under which the flood defence will fail. In addition it shows the most prevalent failure mechanism under different circumstances. Its practical significance is closely tied to the type of application:
 - Design from scratch requires consideration of all failure mechanisms for a range of relevant design standards.

- Maintenance monitors the flood defence to check whether the fragility is within an acceptable envelope.
- Improvement and repair requires insight in which part of the fragility does not meet the acceptable envelope and which failure mechanisms are causing the problems. The effect on fragility of different improvement options can subsequently be compared within a cost-benefit framework.
- Evacuation requires information about the likelihood of a flood given a storm situation.
- *The total probability of failure* allows comparison of the reliability of flood defence sections among different locations in contrast to the fragility. Fragility does not incorporate the likelihood of the local hydraulic boundary conditions in the probability of failure. Two flood defence sections can have the same fragility but suffer from different hydraulic loading and hence will have a different annual probability of failure.
- *Sensitivity of the reliability to the random variables* is considered in two ways. Firstly, alpha-values indicate the contribution of individual random variables to the overall uncertainty. Secondly, delta-values indicate the sensitivity of the reliability to an incremental change in the individual random variables. The results from the total probability of failure include the contribution and sensitivity of the hydraulic boundary conditions. This sensitivity information is a useful addition to that coming from the fragility calculations. The value of alpha and delta-values is explained in more detail below:
 - Alpha-values conventionally indicate the contribution of the uncertainty of a random variable to the overall probability of failure, be it one point on the fragility or the annual probability of failure. The alpha-values show how to target efforts to effectively reduce the probability of failure. Some uncertainties are more readily reducible than others. Spatial uncertainties in the crest level can e.g. be reduced by increasing the resolution and quality of measurements. Variations in wave conditions across different storms can e.g. be reduced by sheltering the flood defence with a breakwater.
 - Delta-values indicate the sensitivity of the probability of failure to an incremental change in one of the random variables, as explained in Buijs et al. (2005). These values show the sensitivity of the reliability in a change in mean value or standard deviation of a random variable. This information supplements the alpha-values in several ways. A first example is when random variables contribute little uncertainty but have a large impact on improving the probability of failure in design or improvement schemes. A second example is when the mean value or standard deviation of a random variable (low in uncertainty contribution) is misjudged. In addition to variables that contribute large uncertainties, highly influential variables should be targeted in data collection activities. A last example is changes induced by deterioration processes, the sensitivity to these changes are not fully reflected by the alpha-values.
- *Dartford Creek to Gravesend fragility is compared to broad scale fragility* to assess whether the broad scale fragility is in the appropriate order of magnitude. Broad scale fragility is a generalised representation of the structural performance of a specific class of flood defence structures.

6.2 Reliability analysis of the earth embankments

A reliability analysis was carried out for 42 earth embankment sections. An overview of the annual reliability for all of the earth embankment sections is provided in Figure 6.2. Section 4 is the weakest earth embankment section in terms of annual probability of failure. For section 4 and more generally for all earth embankment sections, the failure mechanism driven by uplifting and piping dominates the overall reliability. Section 4 serves as an illustration of more detailed results from the reliability analysis.

6.2.1 Fragility

Figure 6.3 shows the fragility curve for section 4. The failure mechanism driven by a combination between uplifting and piping dominates the total fragility curve. The probability of failure is plotted against the water level, rather than against other hydraulic boundary conditions. Wave conditions

occur in the wave overtopping discharge which is only considered for water levels below the crest level. It is evident from Figure 6.3 that the probability of failure due to overtopping for water levels below the crest level is negligible. In addition, flood spreading scenarios currently do not take the effect of the wind field into account. The wind field therefore does not feature in the overall risk

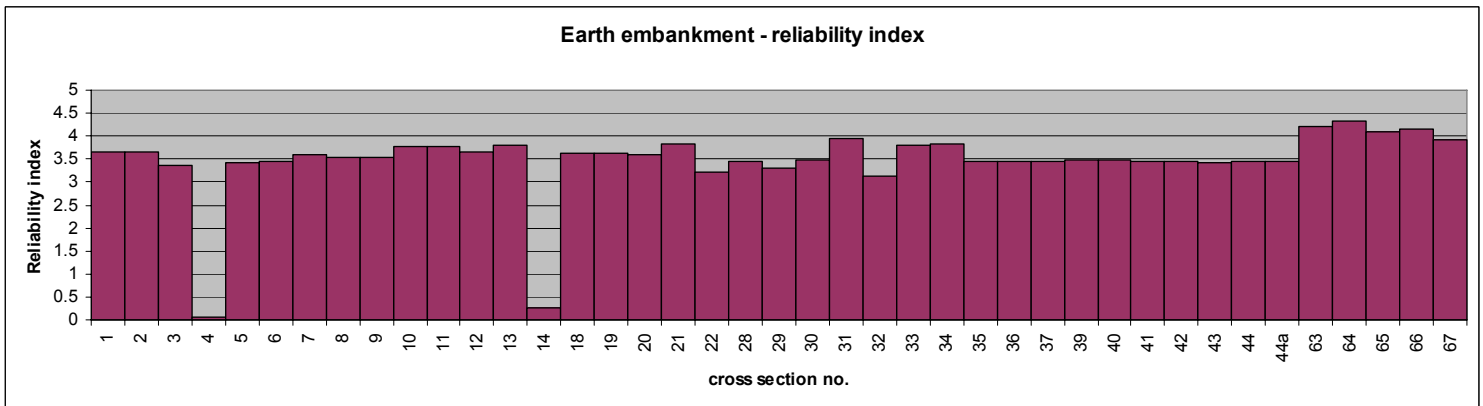


Figure 6.2 The results of the reliability analysis for the earth embankment sections. The numbers correspond with those shown in figure65.1. Section 4 is the weakest section.

integration problem.

As a point of reference, an indication of the highest recorded water level, which is believed to correspond with the 1953 flood, is given in the figure. According to these results, during a big storm it

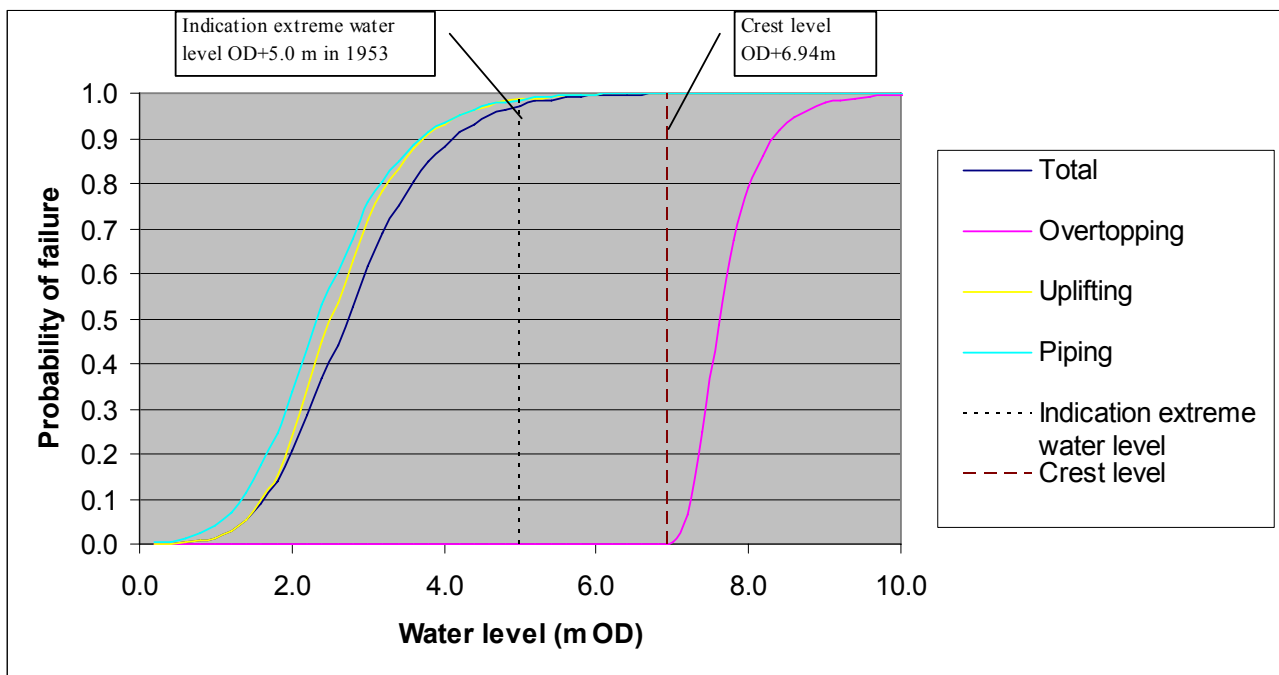


Figure 6.3 Fragility for earth embankment section 4. The failure mechanism driven by a combination of uplifting and piping dominates the total fragility curve.

is very likely that there will be problems with uplifting and piping at the location of section 4. These results should however be considered in the light of the following issues:

- The ditch behind the earth embankments is equipped with drainage pipes that relieve the uplift pressures underneath the earth embankment. This effect is acknowledged by taking a reduction

on the head of the water levels over the embankment into account. Further in-depth analysis is required to fully incorporate the drainage pipes in the reliability analysis.

- The borehole information used in this reliability analysis is generally patchy and based on interpolation. In addition, the geometrical information used for this earth embankment stretch is poor.

For a low water level along this stretch an indication of the probability of failure due to inside slope instability is calculated at 0.038. This probability will increase for higher water levels, depending on the condition of the earth embankment. However, the embankment consists of two crests and therefore behaves as a parallel system. In order to cause inundation, failure of both crests needs to be considered as a combination of several failure mechanisms.

Figure 6.4 presents the standard deviation of the fragility for overtopping, uplifting and piping given the choice of 10,000 Monte Carlo simulations for each water level step. Below a water level of OD+1.2m the standard deviation of the fragility is between 5 and over 30% of the fragility. To improve the results, the number of simulations should be increased for these water levels. To make the calculation of fragility more efficient, the number of Monte Carlo simulations can be varied for different water level intervals. The choice for the number of simulations per interval depends on the required level of accuracy.

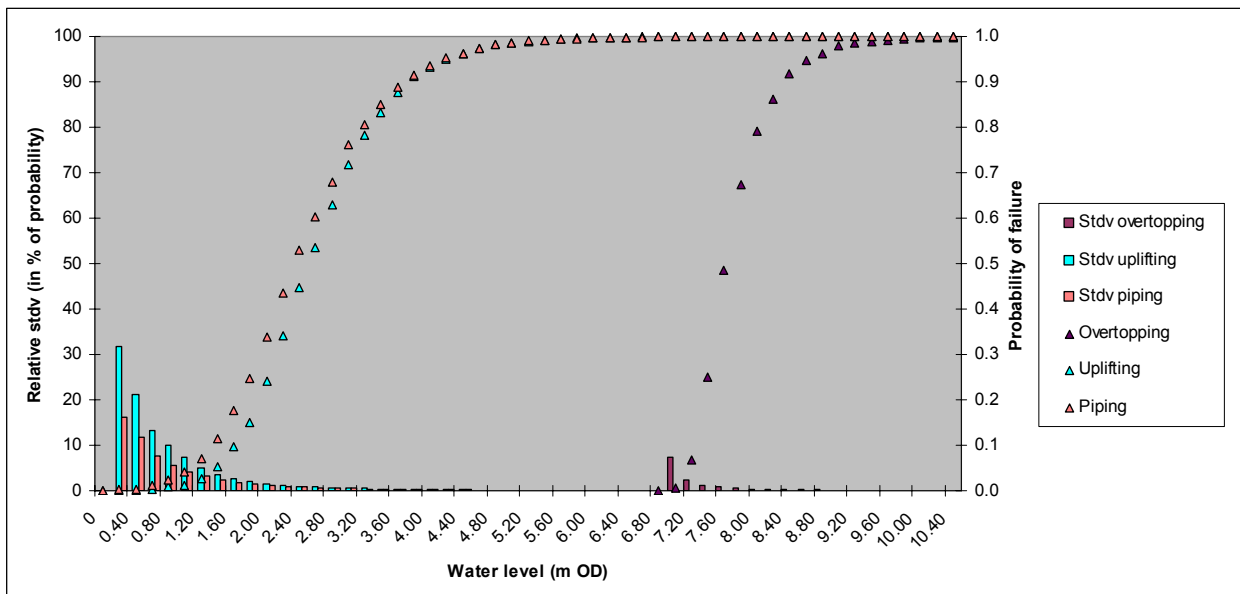


Figure 6.4 Plot of the relative standard deviation of the fragility for overtopping, uplifting and piping. E.g. for a water level of OD+0.4m the standard deviation of the fragility is about 32% of the fragility.

6.2.2 Annual probability of failure

Figure 5.5 provides the annual probability of failure for the wind directions. As mentioned before, the combination of uplifting and piping dominates the total annual probability of failure. The total annual probability of failure of section 4 is 0.47. This probability is rather high considering that then approximately every two years failure due to uplifting and piping is expected. Possible reasons to adjust the probability of failure are mentioned in the bullet list under the previous discussion of fragility: 1) the presence of water head reducing pipes in the ditch behind the embankment; 2) flawed borehole and geometrical data.

Table 6.1 lists the standard deviations of the failure modes overtopping, uplifting and piping given the choice of 100,000 Monte Carlo simulations. The standard deviation associated with the overtopping failure mechanism is several orders of magnitude of the total annual probability of failure. The number

of Monte Carlo simulations must be increased for this failure mechanism to ensure more confidence in the output.

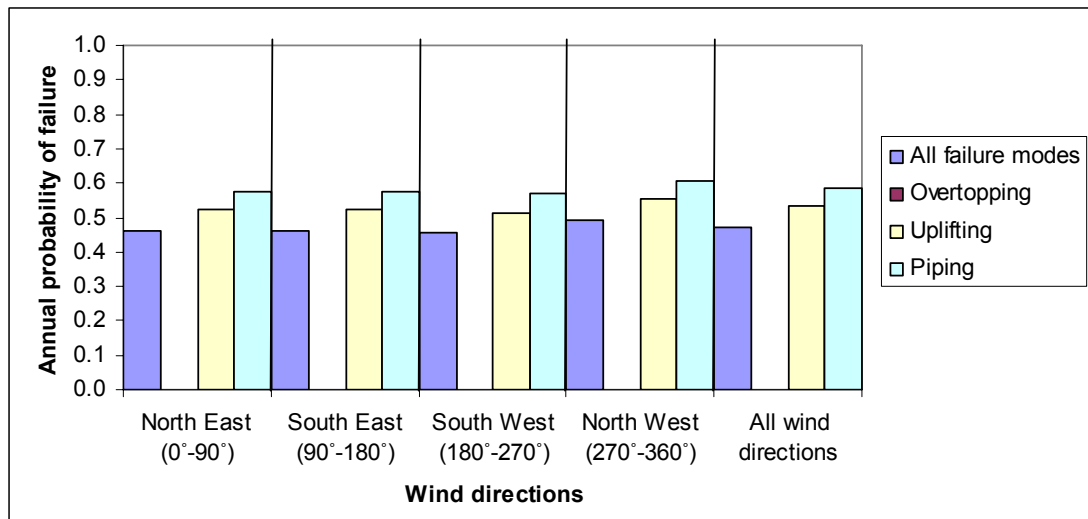


Figure 6.5 Section 4, annual probability of failure for each wind direction. Total annual probability of failure is dominated by the combination between uplifting and piping.

6.2.3 Sensitivity of the reliability to the random variables

Below for each failure mechanism the alpha-values and delta-values obtained with the fragility and annual probability of failure calculations are discussed. The alpha-values and delta-values obtained with the calculation of the annual probability of failure given the four wind directions are similar. Therefore it suffices if Figure 6.6 displays the alpha-values obtained given one wind direction. The North East, NE, is chosen for this purpose.

Uplifting

The alpha-values of the uplifting failure mechanism are given in the top plot in Figure 6.6. The random variables are defined in the box next to Figure 6.6. Two observations are made with regard to the alpha-values:

- The density of the impermeable layers, γ_{wet} , has the highest alpha-values among the fragility results (from $h=OD+2m$ to $h=OD+14m$).
- The alpha-values of the water level, h , and γ_{wet} are most relevant for the annual probability of failure of NE.

The delta-values of the uplifting failure mechanism are shown in the top plot in Figure 6.7. The definition of the random variables corresponds with those given in the box next to Figure 6.6. Three observations are made with regard to the delta-values:

- h , γ_{wet} and the density of the water, γ_w , have the highest delta-values. This observation applies to both the fragility and the annual probability.
- The higher the water level in the fragility, the more sensitive the probability is for a change in the water level.
- The delta-values of the annual probability of failure are in the order of magnitude of those between $h=OD+3.0m$ and $h=OD+4.0m$ in the fragility. That corresponds with the water levels found on average in the Monte Carlo simulation of the water levels and wind speeds.

Piping

The alpha-values of the piping failure mechanism are given in the middle plot in Figure 6.6. The random variables are defined in the box next to Figure 6.6. Two observations are made with regard to the alpha-values:

- Gamma_wet contributes most to the probability of failure in the fragility results.
- h and gamma_wet both contribute most to the annual probability of failure due to piping.

The delta-values of the piping failure mechanism are shown in the middle plot in Figure 6.7. The definition of the random variables corresponds with those given in the box next to Figure 6.6. Three observations are made with regard to the delta-values:

- h, gamma_wet and gamma_w have the highest delta-values.
- The sensitivity to h increases with increasing fragility.
- The delta-values of the annual probability of failure are in the order of magnitude of those between $h=OD+3.0m$ and $h=OD+4.0m$ in the fragility.

Overtopping

The alpha-values of the overtopping failure mechanism are given in the bottom plot in Figure 6.6. The random variables are defined in the box next to figure 5.6. Three observations are made with regard to the alpha-values:

- The water level, h, and the model uncertainty of the critical discharge model, mqc contribute most to the annual probability of failure due to overtopping.
- In the fragility results the variables that contribute most to the probability of failure due to overtopping are: mqc, the storm duration, ts and the grass root depth, dw.
- There is no contribution from variables associated with the wave overtopping model according to Owen. The probability of failure due to overtopping is therefore dominated by the overflow and erosion model. Two causes can be found for this observation. 1) The wave climate at the river is insufficiently rough to cause wave overtopping discharges that lead to structural failure. 2) The wave overtopping must occur at the landward crest of the earth embankment. A condition is that the water level exceeds the riverward crest. The difference between the landward and riverward crest is very small ~ 0.5 meter.

The delta-values of the overtopping failure mechanism are shown in the bottom plot in Figure 6.7. The definition of the random variables corresponds with those given in the box next to Figure 6.6. Two observations are made with regard to the delta-values:

- The fragility results and the annual probability of failure are most sensitive to changes in h and the crest level hc.
- The sensitivity to h increases with increasing fragility, whilst the sensitivity to hc decreases.

Overview

The sensitivity results explain why section 4 has a high annual probability of failure relative to its neighbouring sections. The total annual probability of failure as well as the total fragility is dominated by a combination of the failure mechanisms uplifting and piping. Both these failure mechanisms are very sensitive to gamma_wet in terms of its uncertainty contribution and a change in mean value / standard deviation. After revisiting the data it turns out that section 4 is founded on a number of peat layers. These strata considerably reduce the saturated density of the impermeable layers, gamma_wet, relative to neighbouring sections.

In terms of improvement it is better to focus on increasing the density of the impermeable layers rather than e.g. the thickness. Additionally, the fragility and annual probability of failure are very sensitive to the water level. The reduction of the water level pressures with drainage pipes is therefore an effective solution.

Data collection activities should be concentrated according to these results on the stratification of the impermeable layers and density measurements.

Deterioration of e.g. a filter in the drainage pipes is for this location relevant.

6.2.4 Comparison of Dartford Creek to Gravesend fragility to broad scale fragility

As discussed above, broad scale fragility is a generalised representation of the structural performance of a specific class of flood defence structures. In case of the earth embankments class 45 applies, which is described as: fluvial wide embankment with turf front, crest and rear protection. The class 45 broad scale fragility is compared to the fragility of the Dartford Creek to Gravesend earth embankment sections. This comparison provides insight in whether the broad scale fragility is in the appropriate order of magnitude.

Figure 6.8 plots the broad scale fragility against the fragility results of the Dartford Creek to Gravesend earth embankments. The figure also highlights the strongest and weakest sections. The following comments are relevant with respect to the broad scale fragility:

- In the lower water level region the overall fragility is driven by the combination of uplifting and piping. Broad scale fragility underestimates the probability of failure for practically all Dartford Creek to Gravesend sections in the lower region. That region corresponds with the prevalent hydraulic boundary conditions, but with less damaging consequences of inundation.
- In the higher water level region of fragility, where the probability of failure is dominated by the overtopping failure mechanism, the broad scale fragility overestimates for practically all sections. That region corresponds with the very extreme hydraulic boundary conditions, but with more damaging consequences of inundation.

Generally speaking, even if the broad scale fragility is better representative of more detailed fragility (i.e. in terms of averaging), the flood risk assessment can be distorted. For instance, if the weaker sections are all grouped and protecting an area with high economic consequences, whilst the stronger sections protect an area with lower economic consequences.



h=	water level (mOD)
Dimp=	thickness impermeable layers (m)
gamma_wet=	volumetric weight of saturated soil (kN/m ³)
gamma_w=	volumetric weight of water (kN/m ³)
fg=	groundwater level (mOD)
m_u=	model uncertainty uplifting (-)
L=	Seepage length (m)
eta=	constant of White (-)
d70=	sand diameter of water conductive layer in piping (m)
k_s=	permeability of water conductive sand layer (m/s)
m_p=	model uncertainty piping (-)
theta=	resistance angle sand (°)
hc=	crest level inland crest (mOD)
cw=	crest width (m)
tano=	tangent riverward slope (-)
tani=	tangent landward slope (-)
cg=	erosion strength grass (ms)
cRK=	erosion strength clay (ms)
dw=	grass root depth (m)
Pt=	pulsating effect of overtopping discharge
r_l=	roughness landward slope (m)
ts=	storm duration (hours)
m_qe=	model uncertainty critical discharge model (-)
r_o=	roughness riverward slope (-)
beta1=	angle of incoming waves (°)
A, B=	empirical coefficients Owen's wave overtopping
m_qo=	model uncertainty wave overtopping (-)

Figure 6.6 Alpha-values given different water levels on fragility for overtopping, uplifting and piping.

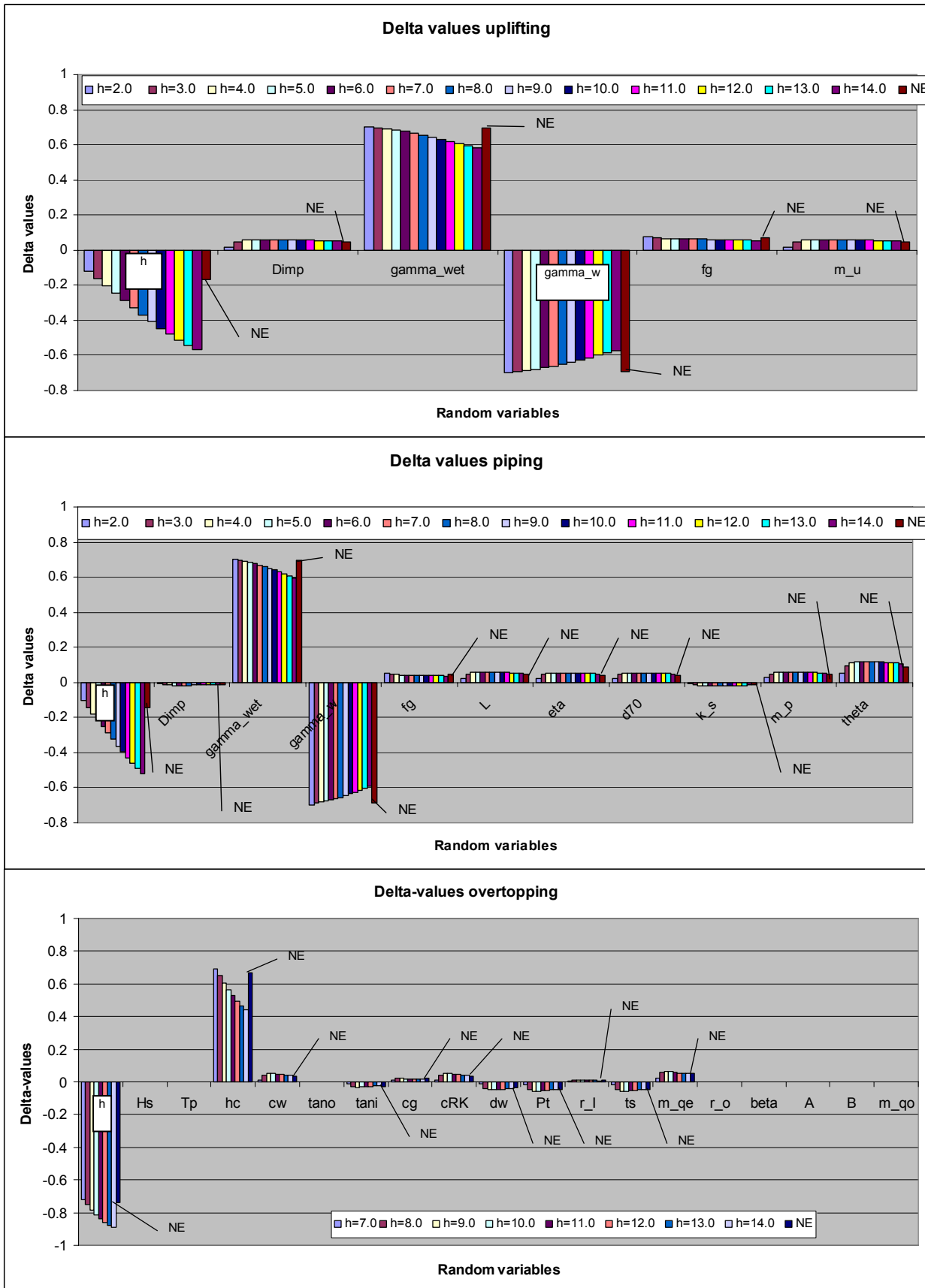


Figure 6.7 Delta-values given different water levels on fragility for overtopping, uplifting and piping. For definition of random variables see Figure 6.6.

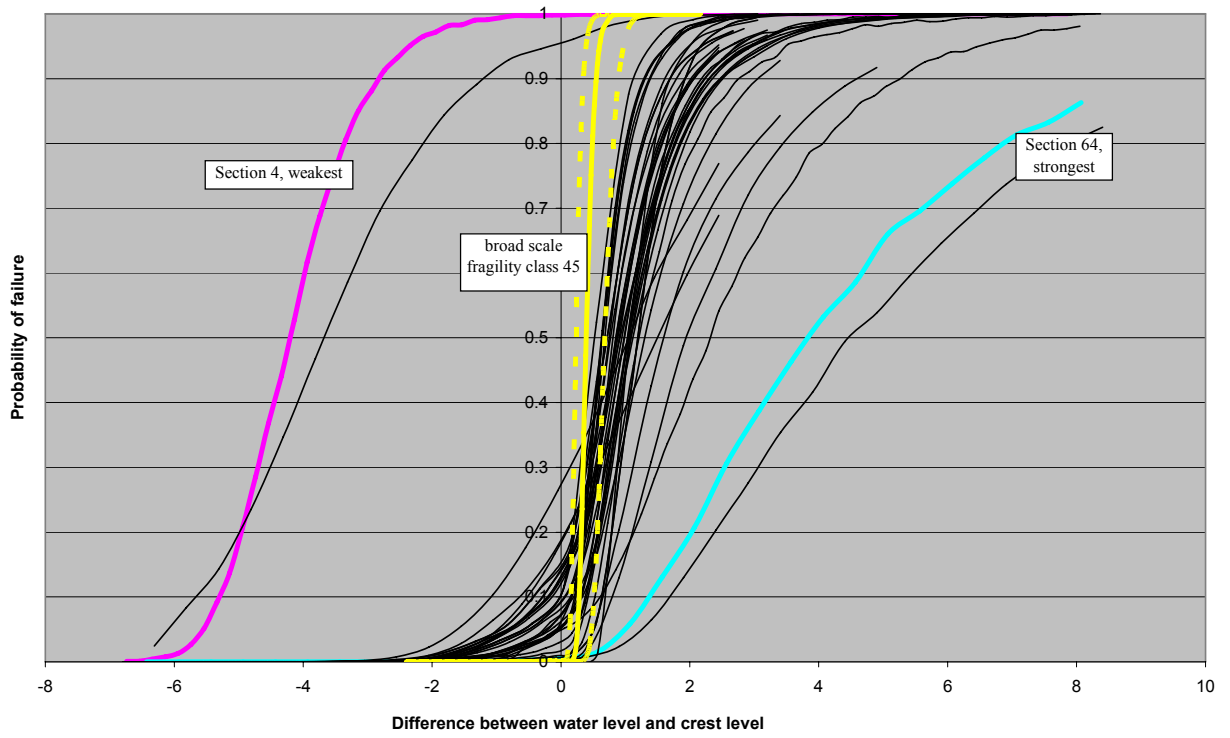


Figure 6.8 *Broad scale fragility, class 45, compared to the fragility of the Dartford Creek to Gravesend earth embankments. The broad scale fragility with upper and lower bounds, weakest section, 4, and the strongest section, 64, are highlighted.*

6.3 Reliability analysis of the concrete walls

Figure 6.9 displays the three main concrete wall types subject to analysis in this research. On the map in Figure 6.1 the types relate to the following stretches:

- type 1 to stretch 15 to 17 (protecting sewer works), represented by section 16;
- type 2 relates to stretch 23 to 27 (protecting Littlebrook power station), represented by section 26;
- type 3 represents stretches 45a, 47 to 49 and 57 to 61 (protecting Greenhithe), represented by section 48.

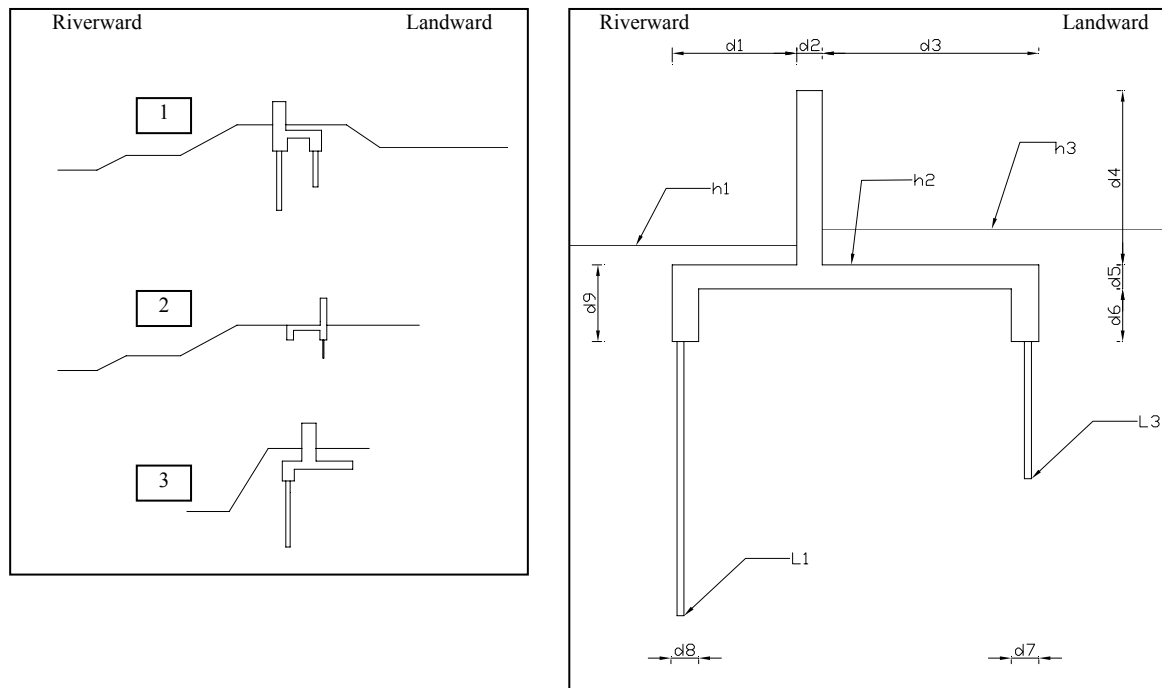


Figure 6.9 Left: three main concrete wall types in this research. Right: generic dimensions of the concrete wall types.

The generic dimensions of these types are shown on the right in Figure 6.9. The annual reliability of all concrete wall sections is displayed in Figure 6.10.

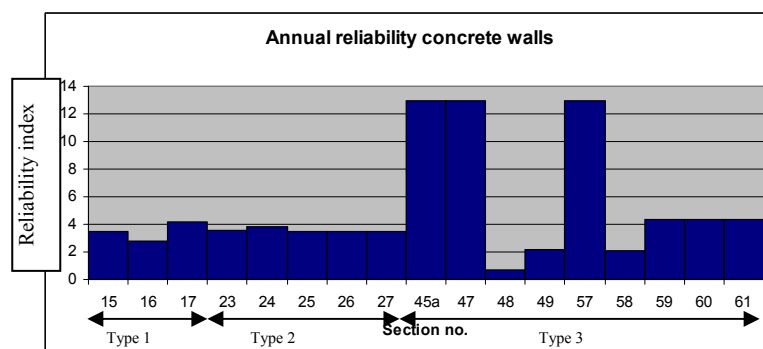


Figure 6.10 Annual reliability for the concrete wall sections along the Dartford Creek to Gravesend flood defence line. The section numbers correspond with those shown in Figure 6.1.

6.3.1 Fragility

Figure 6.11 provides the fragility curves for each of the failure mechanisms of the three types of concrete wall: sections 16, 26 and 48. For each of the types there is a different hierarchy in the prominence of the failure mechanisms. The types are discussed below. The relative standard deviation of the fragility according to Figure 6.11 is discussed as well. It indicates the standard deviation of the fragility as a percentage of the fragility itself.

Hierarchy in failure mechanisms for type 1 (section 16)

Type 1 concrete wall is applied as part of a broad earth embankment structure. Interactions between failure mechanisms of the concrete structure and the earth embankment are not considered in this study. The failure mechanisms uplifting and piping are incorporated because: 1) the combination of these failure mechanisms is an important failure mechanism for the earth embankment structures; 2) these failure mechanisms are independent from the interaction between the concrete and earth embankment structures, and can therefore be easily implemented. The following is commented with regard to the hierarchy in failure mechanisms in the fragility:

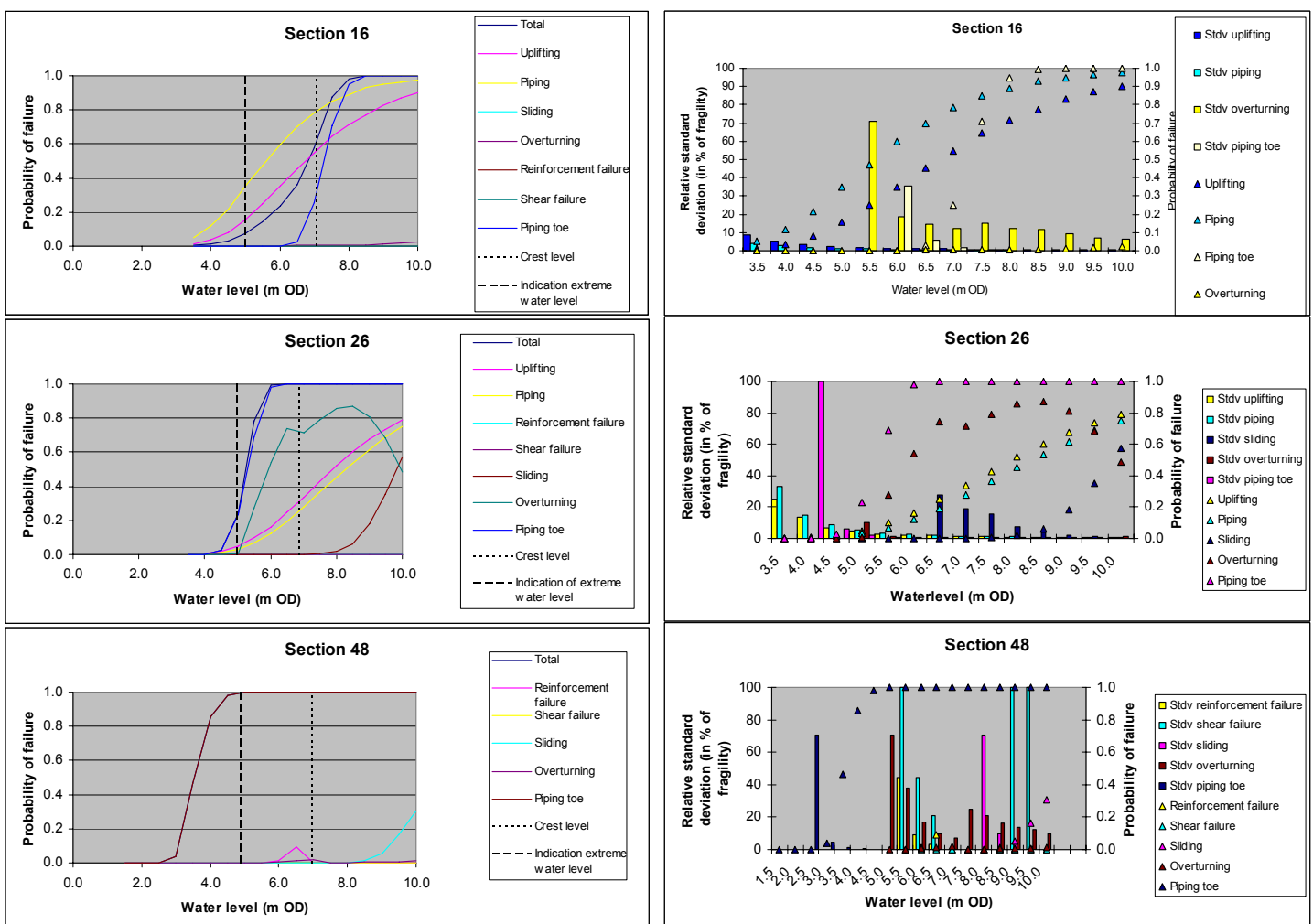


Figure 6.11 Fragility in the left hand column of figures from top to bottom: section 16, section 26, section 48 and section 58. Right hand column contains fragility and corresponding relative standard deviation of fragility for sections 16, 26, 48 and 58. The relative standard deviation indicates the variation of the fragility as a percentage.

- Uplifting and piping are prominent failure mechanisms for the lower water levels.
- As soon as the water level reaches the concrete wall the influence of piping directly underneath the toe of the concrete structure increases and overtakes that of uplifting and piping. Still, in

comparison to sections 26 and 48, the strength of section 16 for piping under the toe is good. The two seepage screens and the relatively deep foundation of the longest seepage screen explain this relatively larger strength.

- The failure mechanisms sliding and overturning have no contribution. The ground mobilised between the seepage screens provides extra strength for these failure mechanisms.

The relative standard deviations in the lower tail of the fragility for the uplifting and piping failure mechanisms are lower than 10%. The relative standard deviation of piping directly under the toe is initially 30% but decreases steeply with rising water levels. The relative standard deviation of the overturning failure mechanism ranges between 70% for the lowest water level to around 10% for higher water levels. The contribution of the latter failure mechanism is negligible; hence the impact of these variations is negligible. The standard deviation of any of the failure mechanisms can be brought down by increasing the number of simulations.

Hierarchy in failure mechanisms for type 2 (section 26)

Type 2 concrete wall is applied as part of a broad earth embankment structure, similar to type 1. Interactions between failure mechanisms of the concrete structure and the earth embankment are not considered in this study. The failure mechanisms uplifting and piping are incorporated for the same reasons as mentioned above.

- Uplifting and piping are less prominent failure mechanisms for the lower water levels than for section 16.
- Piping directly underneath the toe of the concrete structure dominates the fragility overall. The presence of only one seepage screen with a shallow foundation depth explains the high contribution of this failure mechanism, compared to section 16.
- Overturning and sliding are influential failure mechanisms for higher water levels. The difference between type 2 and type 1 is the absence of an extra seepage screen. The latter addition mobilises extra ground for the resistance. Type 2 is therefore less resilient than type 1 in terms of overturning and sliding.

The relative standard deviation of uplifting and piping starts quite high, however, the fragility is very low. The relative standard deviation of piping directly underneath the toe of the concrete structure decreases steeply with rising water levels. For overturning the relative standard deviation is generally lower than 10%. For sliding the relative standard deviation is high for water levels between OD+6.5m and OD+8m. More Monte Carlo simulations can bring the variation down if desired.

Hierarchy in failure mechanisms for type 3 (section 48)

The type 3 concrete wall is applied as part of high grounds along the frontage of Greenhithe. The failure mechanisms uplifting and piping are therefore not taken into account. The following is commented with regard to the hierarchy in failure mechanisms in the fragility:

- Piping directly underneath the toe of the concrete structure dominates the fragility overall. The presence of only one seepage screen with a shallow foundation depth explains the high contribution of this failure mechanism, compared to section 16.
- Although section 48 lacks a second seepage screen, the contributions by the failure mechanisms overturning and sliding are lower than those in case of section 26. The one seepage screen that is present has a deeper foundation level. It therefore provides more stability against sliding and overturning. The probability of overturning is for this reason negligible. The probability of sliding for high water levels is driven by upwards hydraulic force rather than instability caused by the resulting horizontal forces.
- There are marginal contributions by the failure mechanisms reinforcement failure and shear failure. The concrete structure of section 48 is therefore weaker than those of sections 16 and 26, or more exposed to hydraulic loading.

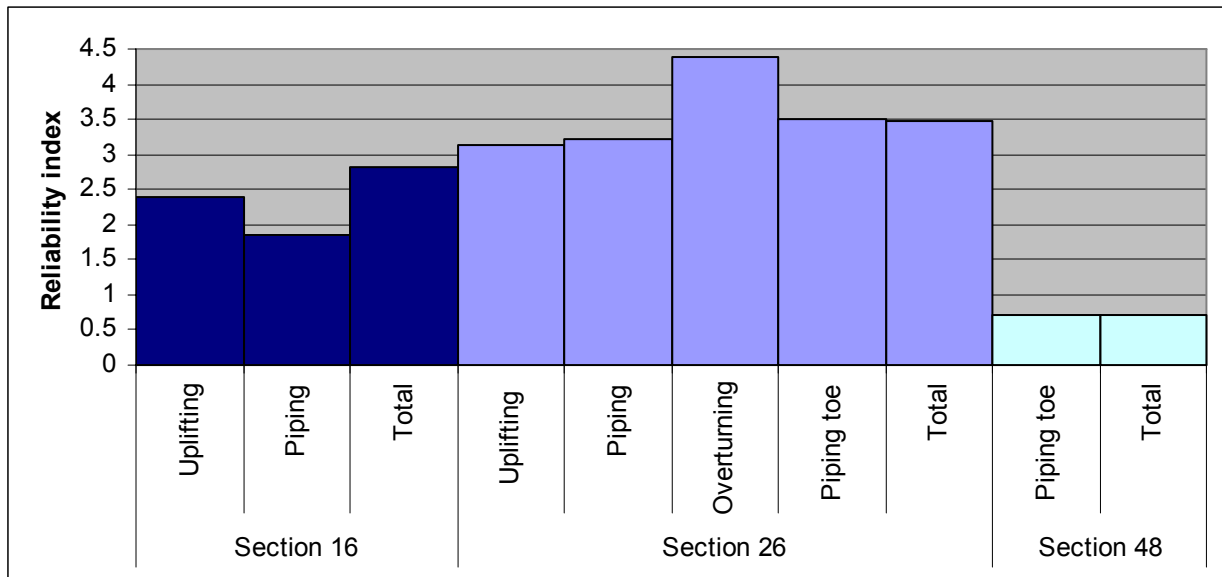


Figure 6.12 The annual reliability indices for the different types of concrete wall, and the contributing failure mechanisms.

The relative standard deviation of piping directly underneath the toe of the concrete structure starts high but decreases sharply with increasing water levels. This error is most relevant to the overall fragility. The relative standard deviation of overturning is high: generally between 20 and 60%. The relative standard deviations of the concrete failure mechanisms reinforcement failure and shear failure are very high. The relative standard deviation of the failure mechanisms can be brought down by increasing the number of Monte Carlo simulations.

6.3.2 Annual probability of failure

Figure 6.12 contains the annual reliability index for each of the types of concrete wall. The hierarchy of the prominent failure mechanisms in the lower range of the fragility for each of the concrete wall types is reflected in the annual reliability. Uplifting and piping contribute most in case of section 16. Piping at the toe of the structure, overturning and the combination of uplifting and piping drive the annual reliability of section 26. The annual reliability of section 48 is dominated by piping at the toe of the structure.

6.3.3 Sensitivity of the reliability to the random variables

Below for each of the failure mechanisms the alpha-values and delta-values obtained with the fragility calculations are addressed. As the discussion of fragility pointed out, the prominence of the failure mechanisms varies per section. Therefore section 26 is taken as an example for the failure mechanisms sliding and overturning. Section 48 serves as an example for the rest of the failure mechanisms: reinforcement failure, shear failure and piping directly underneath the toe of the concrete structure.

Sliding of the concrete structure

The alpha-values of the failure mechanism sliding of the concrete wall, section 26, are given in the top plot in Figure 6.12. The random variables are defined in the box to the right of Figure 6.12. The following observations are made with regard to the alpha-values:

- The foundation level, L1, the groundwater level, gw, and the level of the top of the concrete slab, h2, contribute most to the probability of failure due to sliding of the concrete wall.

The delta-values of the failure mechanism sliding of the concrete wall, section 26, are shown in the top plot in Figure 6.13. The definition of the random variables corresponds with those given in the box next to Figure 6.12. The following observations are made with regard to the delta-values:

- The alpha-values highlight L1, gw, and h2 as important variables. The reliability is in addition sensitive to changes in: the water level, h, the crest level, hc, the volumetric weight of the water, gamma_w, the landward toe level, L3, and the riverward ground level h1.
- The delta-values mentioned under the previous bullet either dominate the magnitude of the loading or relate to the mobilised soil underneath the structure.

Overturning of the concrete structure

The alpha-values of the failure mechanism overturning of the concrete wall, section 26, are given in the second plot in Figure 6.12. The random variables are defined in the box to the right of Figure 6.12. The following observations are made with regard to the alpha-values:

- The model uncertainties for the strength and loading models are prominent contributors to the probability of failure. These are high as currently the overturning failure mechanism is based on a very limited stability model. Important factors that are not considered are, but captured with the model uncertainty, are: other geotechnical stability failure mechanisms, the effect of wave impact on pore pressures at the foundation of the concrete wall and on the resulting horizontal forces.
- In addition to the model uncertainties the following variables contribute significantly to the probability of failure: the groundwater level, gw, the toe levels, L1 and L3, the groundwater level riverward, h1, and the level of the top of the horizontal concrete slab, h2.

The delta-values of the failure mechanism overturning of the concrete wall, section 26, are shown in the second plot in Figure 6.13. The definition of the random variables corresponds with those given in the box next to Figure 6.12. The following observations are made with regard to the delta-values:

- In addition to the variables highlighted by the alpha-values, the reliability is sensitive to the dimensions of the concrete wall.

Reinforcement failure in the concrete slab

The alpha-values of the failure mechanism reinforcement failure in the concrete slab, section 48, are given in the third plot in Figure 6.12. The random variables are defined in the box to the right of figure F6.12. The following observations are made with regard to the alpha-values:

- The model uncertainties of the strength and loading models contribute most to the probability of failure. Factors such as the horizontal force introduced by the wave impact are not taken into account and incorporated by means of the model uncertainties. The level of the top of the horizontal slab, h2, defines the freestanding height of the vertical slab and therefore relates to the magnitude of the hydraulic loading.
- The model uncertainties overshadow all other alpha-values. This blurs insight in the relevance of structural characteristics to the probability of failure. Therefore calculations were made without model uncertainties. These are given in Figure 6.14. These results point out that:
 - the area of reinforcement steel, A_s , the yield stress of the reinforcement steel, f_s , and the distance between the top of the slab and the heart of the reinforcement, d_s , contribute more than the cubic strength of the concrete, f_b .
 - in summary the characteristics of the steel and the height of the vertical concrete slab contribute more to the probability of failure than the quality of the concrete.

The delta-values of the failure mechanism reinforcement failure in the concrete slab, section 48, are shown in the third plot in Figure 6.13. The definition of the random variables corresponds with those

given in the box next to Figure 6.12. The following observations are made with regard to the delta-values:

- The reliability is more sensitive to the water level, h , and the top of the horizontal concrete slab, h_2 , which determines the vertical height of the concrete slab, than the characteristics of the concrete and reinforcement.

Shear failure in the concrete slab

The alpha-values of the failure mechanism shear failure in the concrete slab, section 48, are given in the fourth plot in Figure 6.12. The random variables are defined in the box to the right of Figure 6.12. The following observations are made with regard to the alpha-values:

- The model uncertainties of the strength and loading models contribute most to the probability of failure. Factors such as the horizontal force introduced by the wave impact are not taken into account and incorporated by means of the model uncertainties. The level of the top of the horizontal slab, h_2 , defines the freestanding height of the vertical slab and therefore relates to the magnitude of the hydraulic loading.
- The model uncertainties overshadow all other alpha-values. This blurs insight in the relevance of structural characteristics to the probability of failure. Therefore calculations were made without model uncertainties. These are given in figure 5.14. These results point out that the crest level and the tensile strength of the concrete are the most important structural characteristics.

The delta-values of the failure mechanism shear failure in the concrete slab, section 48, are shown in the fourth plot in Figure 6.12. The definition of the random variables corresponds with those given in the box next to Figure 6.12. The following observations are made with regard to the delta-values:

- The reliability is more sensitive to the water level, h , and the top of the horizontal concrete slab, h_2 , which determines the vertical height of the concrete slab, than the characteristics of the concrete.

Piping directly underneath the toe of the concrete structure

The alpha-values of the failure mechanism piping directly under the toe of the concrete structure, section 48, are given in the fifth plot in Figure 6.12. The random variables are defined in the box to the right of Figure 6.12. The following observations are made with regard to the alpha-values:

- The variables that contribute most to the probability of failure are: the groundwater level, gw , the model uncertainty, m_T , the toe levels of the structure, L_1 and L_3 , and the height of the landward ground level.

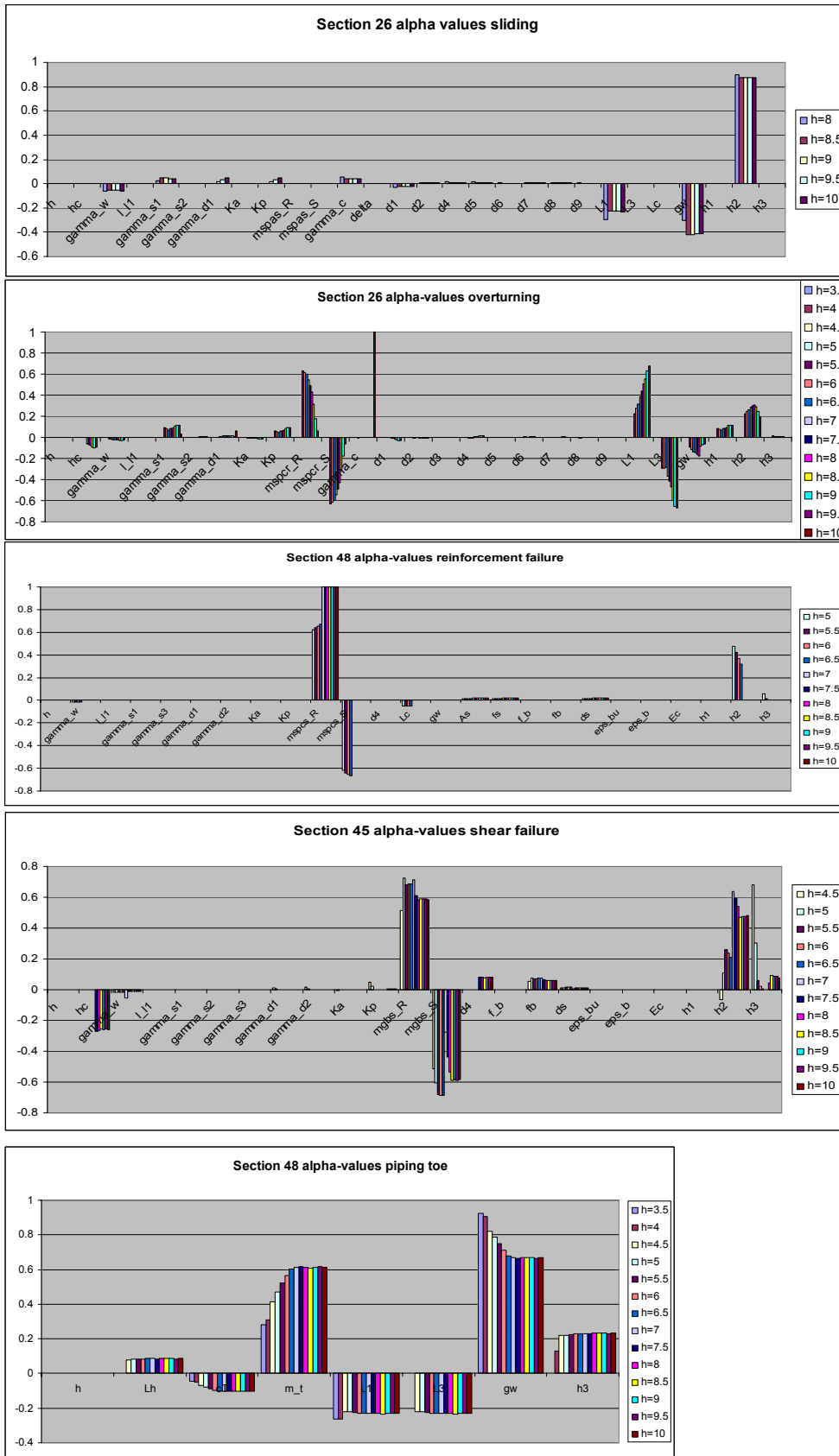
The delta-values of the failure mechanism piping directly under the toe of the concrete structure, section 48, are shown in the fifth plot in Figure 6.13. The definition of the random variables corresponds with those given in the box next to Figure 6.12. The following observations are made with regard to the delta-values:

- The reliability is most sensitive to the water level, h , and the groundwater level, gw .

Overview

Most importantly, the relevance of the variables should be considered in accordance to the hierarchy of the failure mechanism contributions. The failure mechanism piping directly underneath the concrete structure is the dominant failure mechanism. The toe levels and the relative difference between the groundwater level and river water level are thus most relevant to the reliability of the concrete wall. The hierarchy of the rest of the failure mechanisms depends on the type of concrete wall defined in Figure 6.9. Generally however, the toe levels, the height of the vertical concrete slab and the

groundwater level dominate the sensitivity. Therefore, according to these results, the concrete wall reliability is rather a product of the initial design choices than that of an inspection or monitoring strategy. In terms of manageable properties the reinforcement steel and the tensile strength of the concrete are relevant.



h=	water level (mOD)
hc=	top of concrete wall (mOD)
gamma_w=	volumetric weight of water (kN/m ³)
L1=	transition level between top and second strata (m OD)
gamma_s1=	saturated volumetric weight of top strata (kN/m ³)
gamma_s2=	saturated volumetric weight of 2nd strata (kN/m ³)
gamma_d1=	dry volumetric weight of top strata (kN/m ³)
Ka=	active horizontal grain stress coeff. (-)
Kp=	passive horizontal grain stress coef. (-)
mspas_R=	model uncertainty strength sliding (-)
mspas_S=	model uncertainty loading sliding (-)
gamma_c=	volumetric weight of concrete (kN/m ³)
delta=	friction angle between concrete structure and soil (°)
d1 to d9=	concrete wall dimensions (m), see figure 5.9
L1=	riverward toe level (mOD), see figure 5.9
L3=	landward toe level (mOD), see figure 5.9
Lc=	length of concrete wall unit (m)
h1 to h3=	ground levels (mOD), see figure 5.9
mspcr_R=	model uncertainty strength overturning (-)
mspcr_S=	model uncertainty loading overturning (-)
mspcs_R=	model uncertainty strength reinforcement failure (-)
mspcs_S=	model uncertainty loading reinforcement failure (-)
As=	area reinforcement per meter length (mm ²)
fs=	yield stress reinforcement steel (N/mm ²)
f_b=	cubic pressure strength of concrete (N/mm ²)
fb=	tensile strength of concrete (N/mm ²)
ds=	distance top of pressure zone in concrete cross section to heart reinforcement bar (m)
eps_bu=	limit elasticity for breaking concrete (-)
eps_b=	elasticity limit for plastic behaviour (-)
Ec=	Elasticity modulus (N/mm ²)
eps_b=	elasticity limit for plastic behaviour (-)
mgbs_R=	model uncertainty strength shear failure (-)
mgbs_S=	model uncertainty loading shear failure (-)
Lh=	horizontal seepage length (m)
c1=	creep ratio according to Terzaghi
m_T=	model uncertainty piping underneath toe (-)
gw=	ground water level (mOD)

Figure 6.12 Alpha-values for the concrete wall failure mechanisms. Sliding and overturning of section 26, reinforcement failure, shear failure and piping directly underneath the toe of section 48 are selected for analysis. The variables are described on the right of the figures with alpha-values.

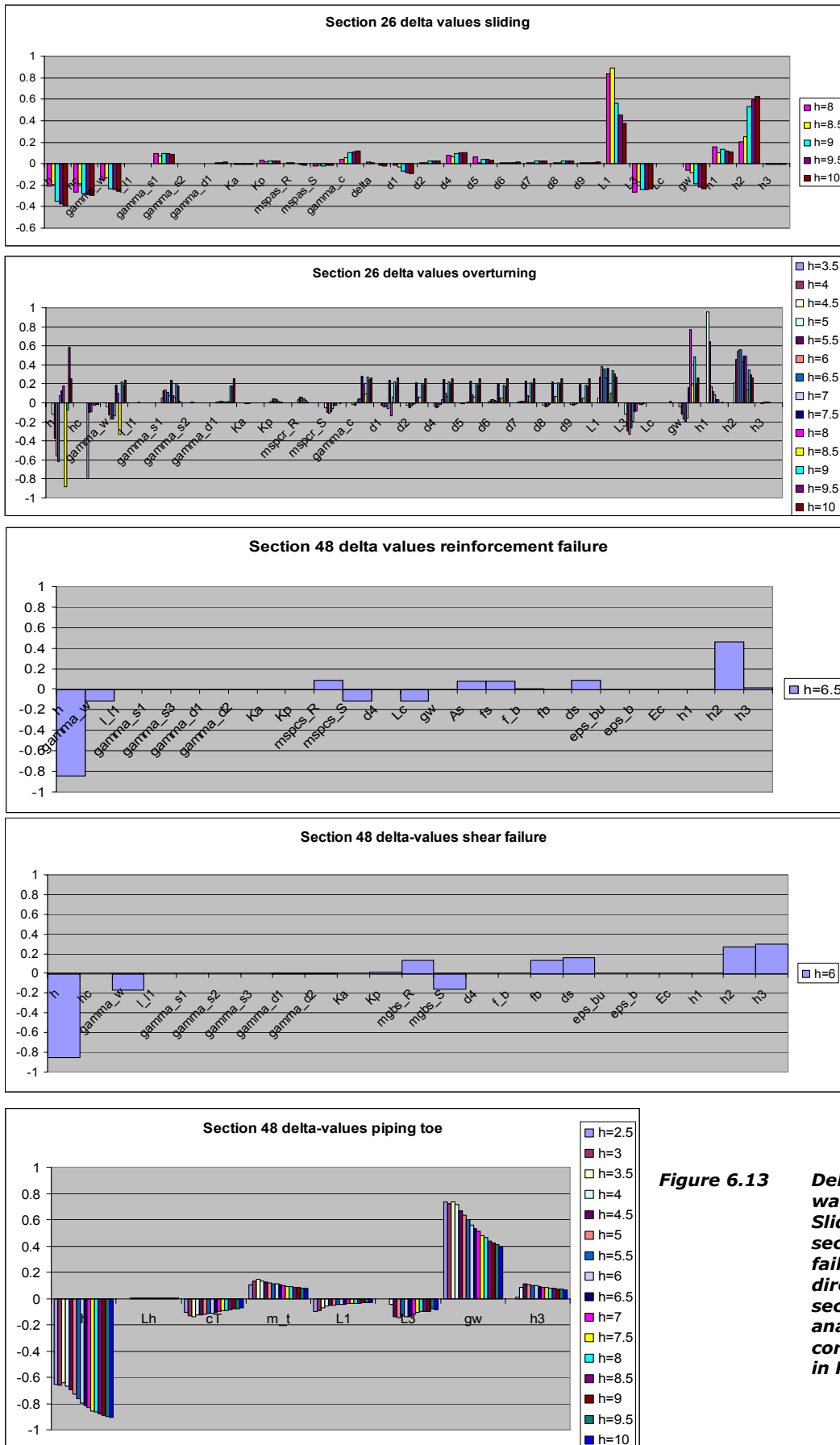


Figure 6.13 Delta-values for the concrete wall failure mechanisms. Sliding and overturning of section 26, reinforcement failure, shear failure and piping directly underneath the toe of section 48 are selected for analysis. The variables correspond with those defined in Figure 6.11.

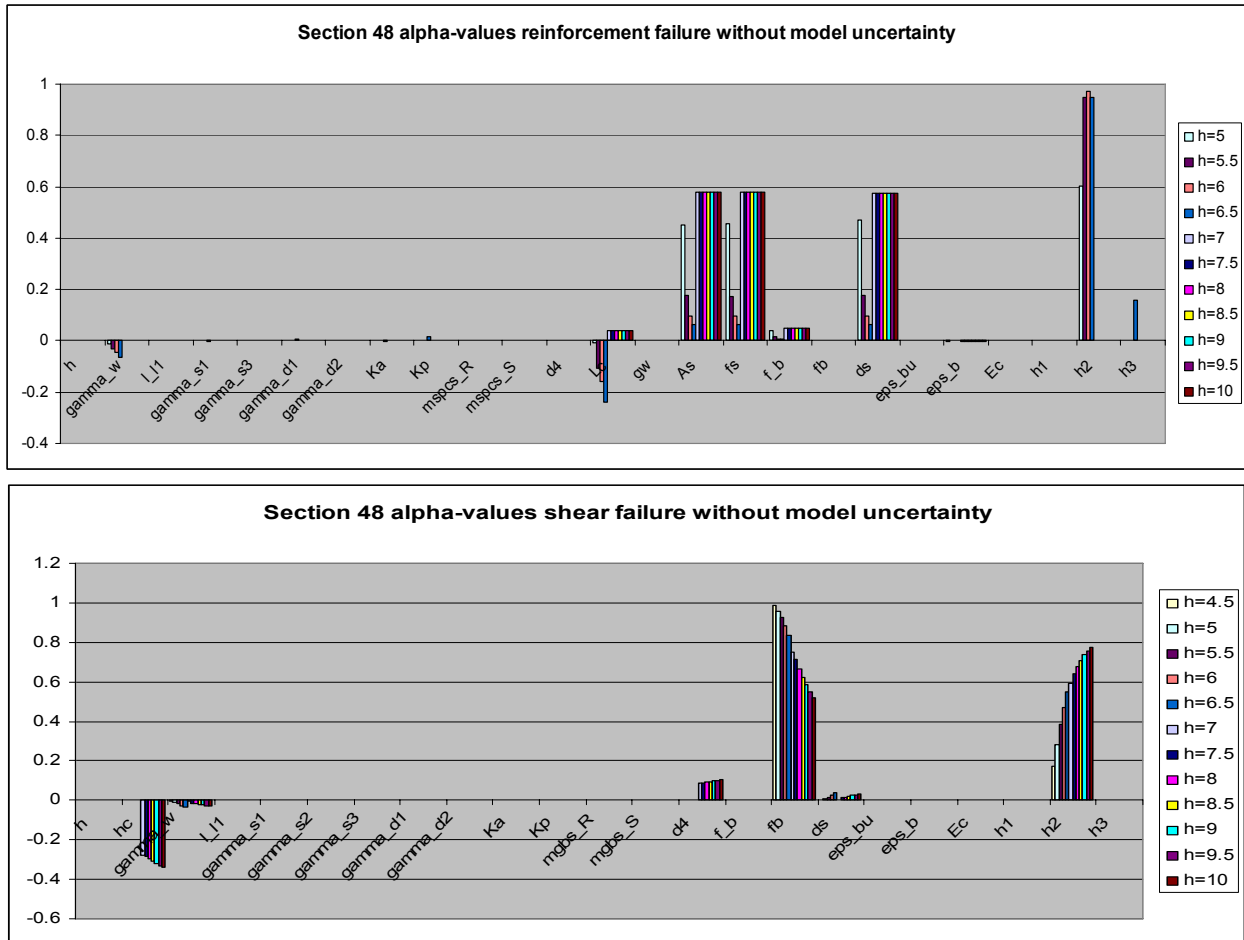


Figure 6.14 The alpha-values associated with failure mechanisms reinforcement failure and shear failure for section 48 without model uncertainties.

6.3.4 Comparison of Dartford Creek to Gravesend fragility to broad scale fragility

Broad scale fragility is a generalised representation of the structural performance of a specific class of flood defence structures. In case of the concrete walls class 41 applies, which is described as: fluvial wide vertical wall structure consisting of brick & masonry or concrete. The class 41 broad scale fragility is compared to the fragility of the Dartford Creek to Gravesend concrete wall sections. This comparison provides insight in whether the broad scale fragility is in the appropriate order of magnitude.

Figure 6.15 plots the broad scale fragility against the fragility results of the Dartford Creek to Gravesend concrete walls. The figure also highlights the strongest and weakest sections. The following comments are relevant with respect to the broad scale fragility:

- The broadscale concrete wall fragility is strong in comparison with the Dartford Creek to Gravesend concrete wall fragility. This applies to the high probability-low damage region, i.e. the low water levels, as well as to the low probability-high damage region, i.e. the high water levels. It is therefore recommended to reconsider the dominant failure mechanism for the concrete wall broadscale fragility along Dartford Creek to Gravesend. The latter is driven by the failure mechanism piping directly underneath the toe of the concrete structure failure mechanism.
- Generally speaking, even if the broad scale fragility is better representative of more detailed fragility (i.e. in terms of averaging), the flood risk assessment can be distorted. For instance, if the weaker sections are all grouped and protecting an area with high economic consequences, whilst the stronger sections protect an area with lower economic consequences.

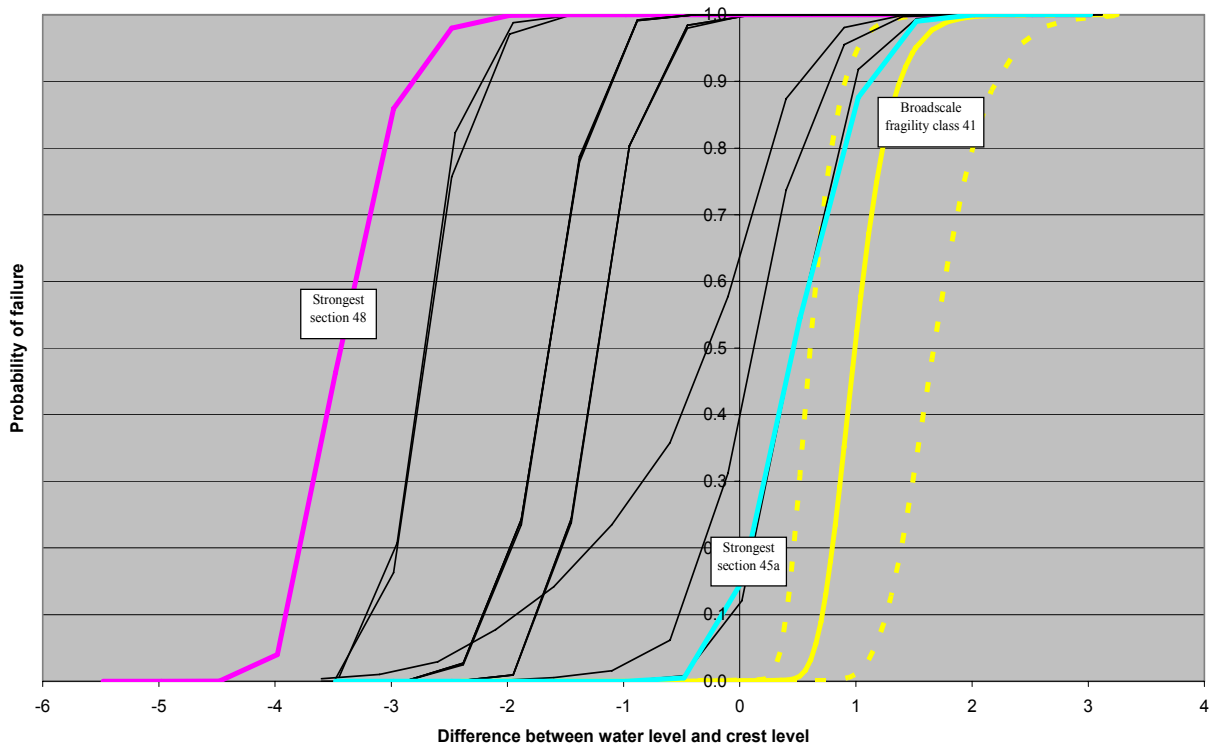


Figure 6.15 *Broadscale fragility, class 41, compared to the fragility of Dartford Creek to Gravesend concrete walls. The broadscale fragility with upper and lower bounds and the fragility of the weakest section, 48, and the strongest section, 45a are highlighted.*

6.4 Sheet pile walls

Figure 6.16 shows the annual reliability of the sheet pile wall sections taken into account in this reliability analysis of the Dartford Creek to Gravesend flood defences. The Greenhithe frontage consists of a variety of composite concrete wall – sheet pile wall structures. Each of those structure types is unique and requires a specific analysis in terms of failure mechanisms and its fault tree. For the largest part however, the frontage is made out of anchored sheet pile walls. This research therefore concentrates on the anchored sheet pile structures. The typical shape and dimensions are displayed on the right in Figure 6.16.

The role of the reliability of anchored sheet pile wall structures in flood risk assessments is different from the earth embankment or concrete wall structures. This difference is mainly the result of a different primary function: retaining ground along high grounds (Greenhithe) rather than protecting a low-lying floodplain. A number of differences are listed below:

- Failure of such flood defence structures increases the overtopping discharges, rather than causing a direct breach and inundation scenario.
- Failure of anchored sheet pile walls leads to landslides and hence local foundational instability of residence and industry. The economic consequences therefore do not necessarily relate to damage done by flooding.
- The critical situations are not necessarily related to the high water level during a storm. Extreme low water levels have a destabilising effect on anchored sheet pile walls and can also trigger failure. This study only considers high water levels during storms and therefore provides limited insight in the reliability of anchored sheet pile walls.

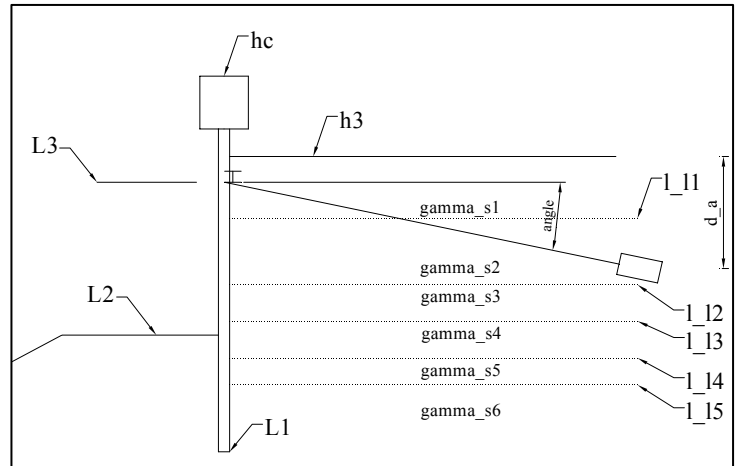
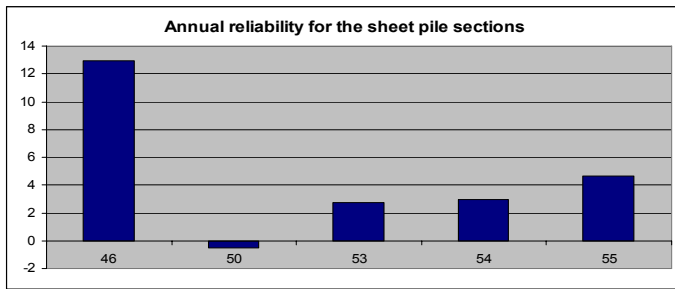


Figure 5.16 Left: annual reliability for the sheet pile sections along Dartford Creek to Gravesend. The section numbers correspond with those in figure 5.1. Right: some dimensions associated with the sheet pile wall structure.

6.4.1 Fragility

Figure 6.17 displays the fragility for section 53. The total fragility is driven by the combination of a breaking anchor followed by rotational failure of the sheet pile wall. The combination of a sliding anchor followed by rotational failure of the sheet pile has a negligible contribution. The failure mechanism breaking sheet pile contributes zero probability.

The fragility shows that the reliability of the sheet pile wall increases with a rising water level. That observation is based on the failure mechanisms underpinning this reliability analysis. It is noted that toe scouring failure mechanisms or erosion due to overtopping water jets are not taken into account. The process of toe scouring in fluvial high water situations is poorly understood. The quantification of the impact of water jets is equally challenging, even more so because of the presence of asphalt or infrastructure behind the defences.

The relative standard deviation of anchor breaking increases to 20% with a rising water level, see Figure 6.18. The relative standard deviation of rotational failure is negligible. The relative standard deviation of sliding anchor is over 10%. The variation of the probability of failure can be brought down by increasing the number of Monte Carlo simulations.

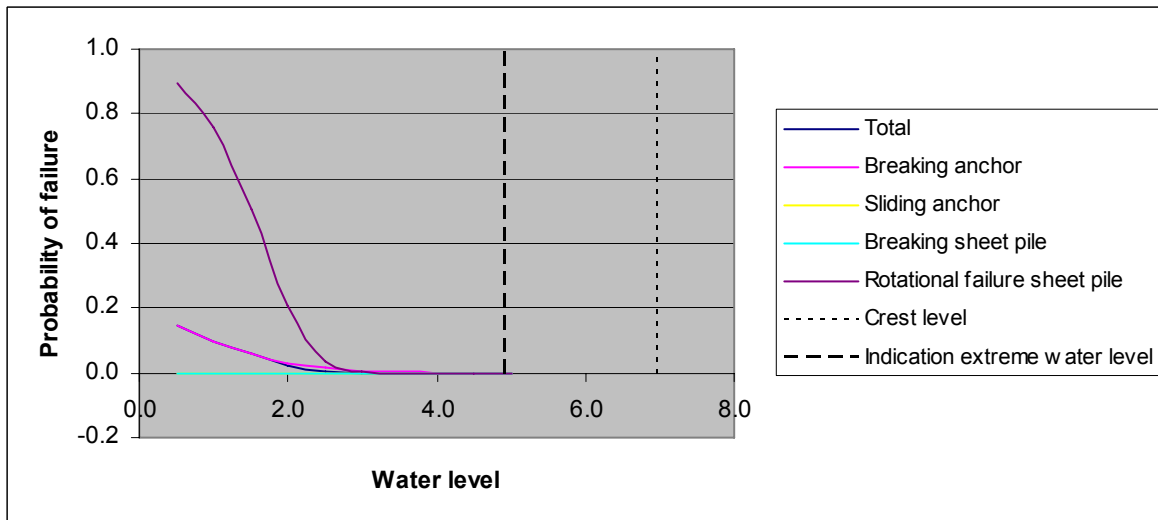


Figure 6.17 Fragility for sheet pile wall section 53. The contributions of the individual failure mechanisms to the total fragility are structured as follows: 1) the combination between a breaking anchor followed by rotational failure of the sheet pile; 2) the combination between a sliding anchor followed by rotational failure of the sheet pile; 3) breaking sheet pile wall.

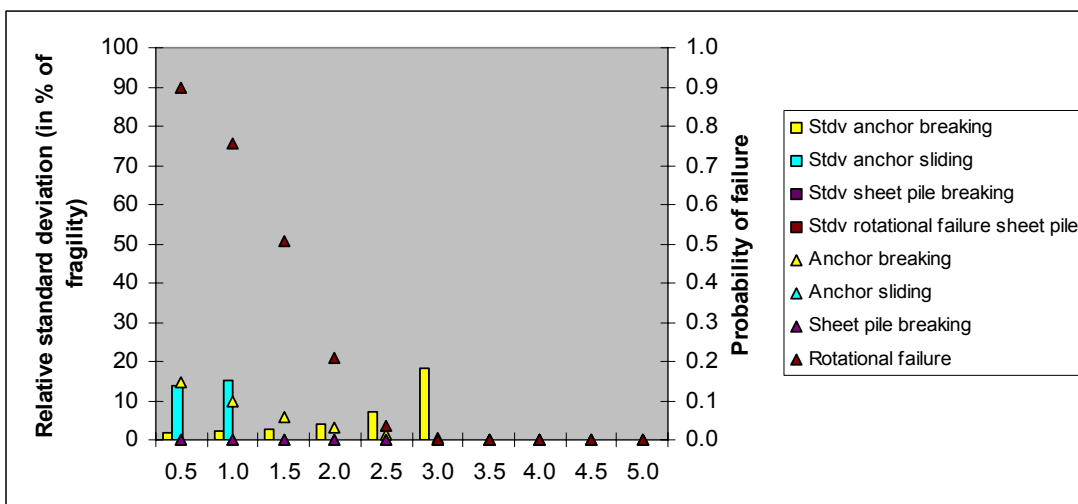


Figure 6.18 Fragility for section 53 and its relative standard deviation in percentages.

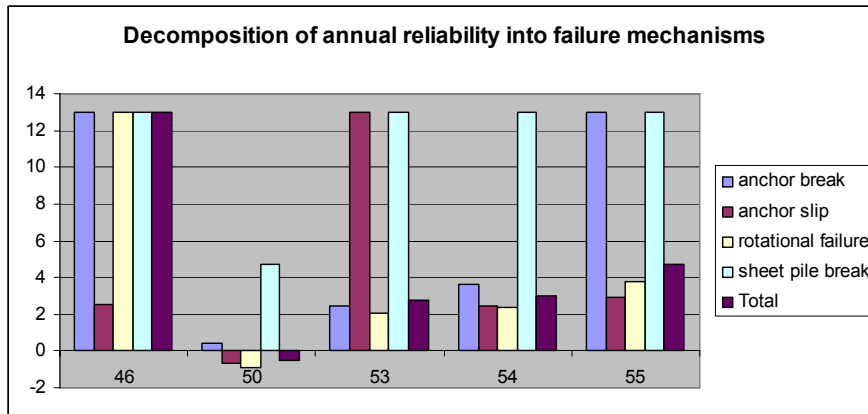


Figure 6.19 Annual reliability for the failure mechanisms anchor breaking, anchor sliding, sheet pile breaking and rotational failure following anchor failure for the sheet pile wall sections. The combinations of the failure mechanisms is equal to those applied in the fragility, see figure 5.17.

6.4.2 Annual probability of failure

Figure 6.19 provides the annual reliability for the failure mechanisms of the sheet pile wall sections. The combination of anchor failure and rotational failure determines the total annual reliability. The annual reliability of section 50 is rather unrealistic and compares to an annual probability of failure of over 0.7. For this reason section 53 is chosen for a more detailed interpretation in 6.4.1 and 6.4.3.

6.4.3 Sensitivity of the reliability to the random variables

Below for each of the failure mechanisms the alpha-values and delta-values obtained with the fragility calculations are addressed for section 53.

Anchor breaking

The alpha-values of the failure mechanism anchor breaking are given in the top plot in Figure 6.20. The random variables are defined in the box to the right of Figure 6.20. The following observations are made with regard to the alpha-values:

- The variables that contribute most to the probability of failure are: the model uncertainties of the strength and loading model, m_{shw} and sh_width , the coefficients for the horizontal grain stress, K_a and K_p , and the groundwater level, gw .
- The contributions of l_{11} to l_{14} and γ_{s1} to γ_{s5} indicate the influence of the soil strata loading the sheet pile wall, see Figure 6.16 for a visualisation of these dimensions.

The delta-values of the failure mechanism anchor breaking are shown in the top plot in Figure 6.21. The definition of the random variables corresponds with those given in the box next to Figure 6.20. The following observations are made with regard to the delta-values:

- The reliability is sensitive to changes in: the groundwater level, gw , the density of the water, γ_w , the coefficients for the horizontal grain stress, K_a and K_p , and the toe level, $L1$.
- The reliability is sensitive in equal degrees to the soil layers and ground level.

Anchor sliding

The alpha-values of the failure mechanism anchor sliding are given in the second plot in Figure 6.20. The random variables are defined in the box to the right of Figure 6.20. The following observations are made with regard to the alpha-values:

- The variables that contribute most to the probability of failure are: the model uncertainties of the strength and loading model, m_{sh} and $D50$, the area of the anchors, A_a (which determines the resulting force exerted on the soil), and the coefficients for the horizontal grain stress, K_a and K_p .

The delta-values of the failure mechanism anchor sliding are shown in the second plot in Figure 6.21. The definition of the random variables corresponds with those given in the box next to Figure 6.20. The following observations are made with regard to the delta-values:

- The reliability is sensitive to changes in: the groundwater level, gw , the density of the water, γ_w , the coefficients for the horizontal grain stress, K_a and K_p , and the toe level, $L1$.

Sheet pile breaking

The alpha-values of the failure mechanism sheet pile breaking are given in the third plot in Figure 6.20. The random variables are defined in the box to the right of Figure 6.20. The following observations are made with regard to the alpha-values:

- The model uncertainties, Q_{ac_sh} and m_{q_sh} , overshadow all other contributions by variables.
- To provide more insight in the contributions of structural variables in Figure 6.22 the alpha-values without model uncertainty are given. According to this figure, the yield stress of the sheet pile, f_y , the coefficients for the horizontal grain stress, K_a and K_p , the ground level on the riverside of the sheet pile, $L2$ and the groundwater level, gw , contribute most to the probability of failure

The delta-values of the failure mechanism anchor sliding are shown in the third plot in Figure 6.21. The definition of the random variables corresponds with those given in the box next to Figure 6.20. The following observations are made with regard to the delta-values:

- Delta-values were not obtained for this failure mechanism, as there were insufficient simulations in the failure region.

Rotational failure of the sheet pile wall, following anchor failure

The alpha-values of the failure mechanism sheet pile breaking are given in the third plot in Figure 6.20. The random variables are defined in the box to the right of Figure 6.20. The following observations are made with regard to the alpha-values:

- The variables that contribute most to the probability of failure are: the groundwater level, gw , the coefficients for the horizontal grain stress, K_a and K_p , the toe level, $L1$ and the ground level on the riverside of the sheet pile, $L2$.

The delta-values of the failure mechanism anchor sliding are shown in the third plot in Figure 6.21. The definition of the random variables corresponds with those given in the box next to Figure 6.20. The following observations are made with regard to the delta-values:

- The reliability is sensitive to changes in the density of the water, γ_w , the groundwater level, gw , the coefficient for passive grain stress, K_p , the toe level, $L1$, the soil densities, γ_{s1} to γ_{s3} , and the water level, h .

Overview

Below the most influential variables to the probability of failure of the sheet pile are listed:

- The *groundwater level* can be controlled by applying drainage measures.
- The *coefficients for the horizontal grain stress* are quantified as part of the design process. In this process the behaviour of the soil can be represented in more detail.

- The *toe level* of the sheet pile is a design variable.
- The *riverward ground level* suffers from variations induced by tidal scouring or dredging activities.
- The *yield stress* is a design variable.
- The *area of the anchor* is affected by corrosion.

6.4.4 Comparison of Dartford Creek to Gravesend fragility to broad scale fragility

Figure 6.23 shows the broad scale fragility class 43 described as wide fluvial vertical wall structures made of sheet piles, its upper and lower bounds and the fragility of the Dartford Creek to Gravesend sheet pile sections. It is noted that the fragility of section 50 is included in the plot but is not considered to be realistic.

The probability of failure in broadscale fragility cannot be directly mapped to the probability of failure of the Dartford Creek to Gravesend sheet pile wall sections:

- Sheet piles applied in wide embankments have a probability of failure driven by low water events as well as high water events. The probability of failure in broad scale fragility relates to high water events only. In addition, broad scale fragility does not take the stabilising effect of rising water levels into account.
- Broad scale fragility represents the probability of breach, leading to flood damages. The Dartford Creek to Gravesend sheet piles primarily have a ground retaining function bordering high grounds. Failure of sheet pile walls leads therefore to additional damages, i.e. landslides, to flood damages that are currently not considered in flood risk assessments.

Anchored sheet pile walls are often applied as ground retaining structures in combination with high grounds, with an additional height to reduce overtopping discharges. Failure of the sheet pile wall implies extra overtopping discharges. This effect is not taken into account in current flood risk assessments.

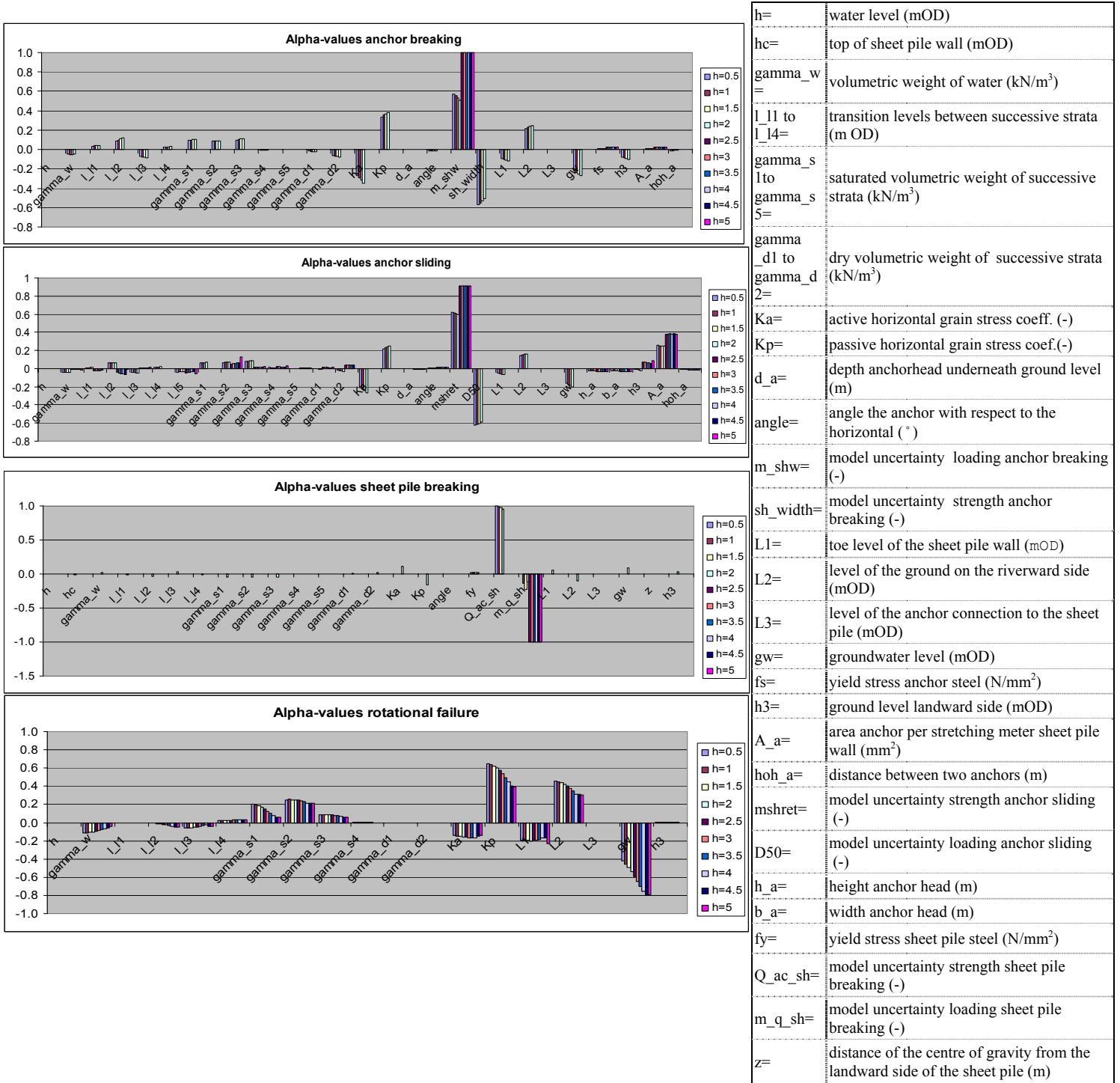


Figure 6.20 Left: plots containing alpha-values for the failure mechanisms anchor breaking, anchor sliding, sheet pile breaking and rotational failure. Right: description of the variables.

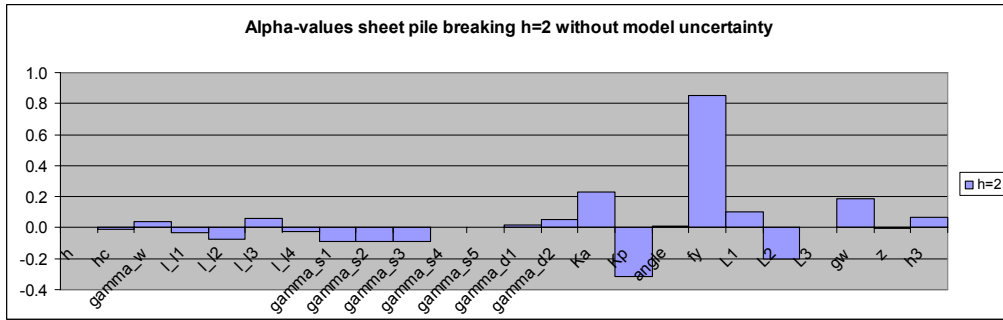


Figure 6.21 Alpha-values for sheet pile breaking without model uncertainties, provide insight in the contributions of the structural variables. A definition of the variables can be found in Figure 6.20.

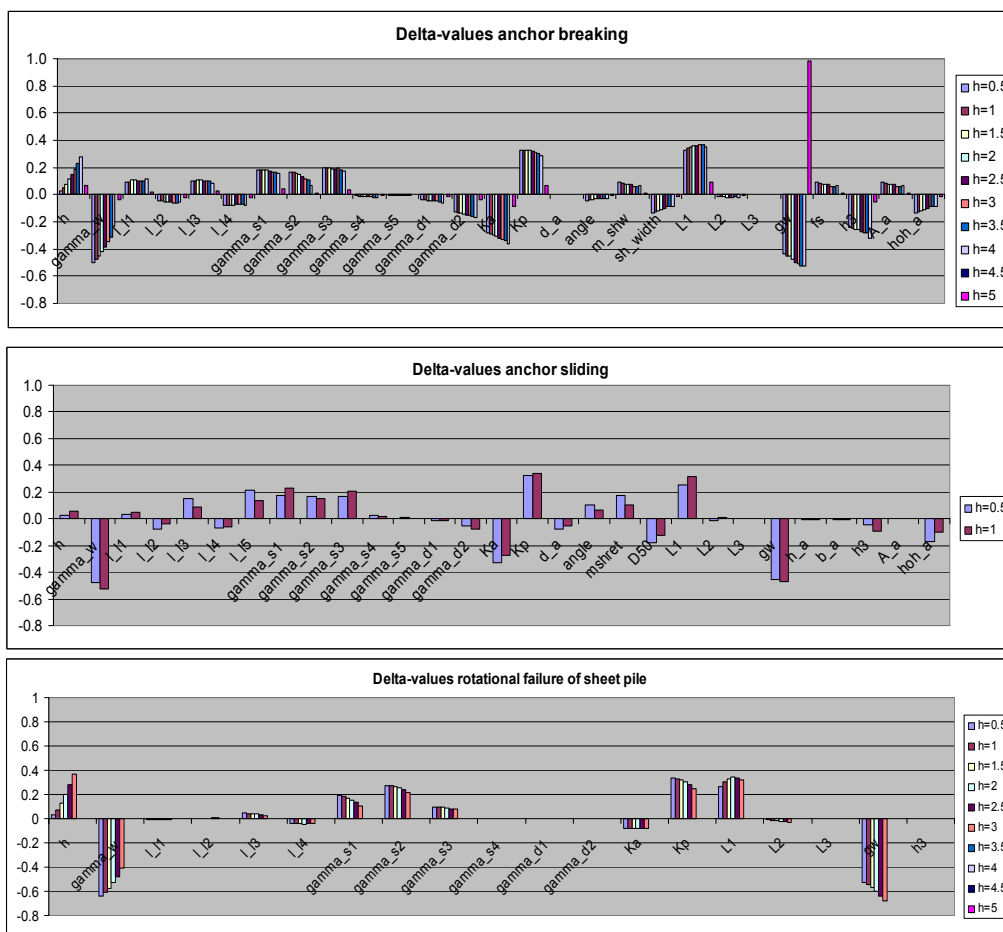


Figure 6.22 Delta-values for the failure mechanisms anchor breaking, anchor sliding and rotational failure of the sheet pile. The delta-values for sheet pile breaking are zero. A definition of the variables in the plots can be found in Figure 6.20

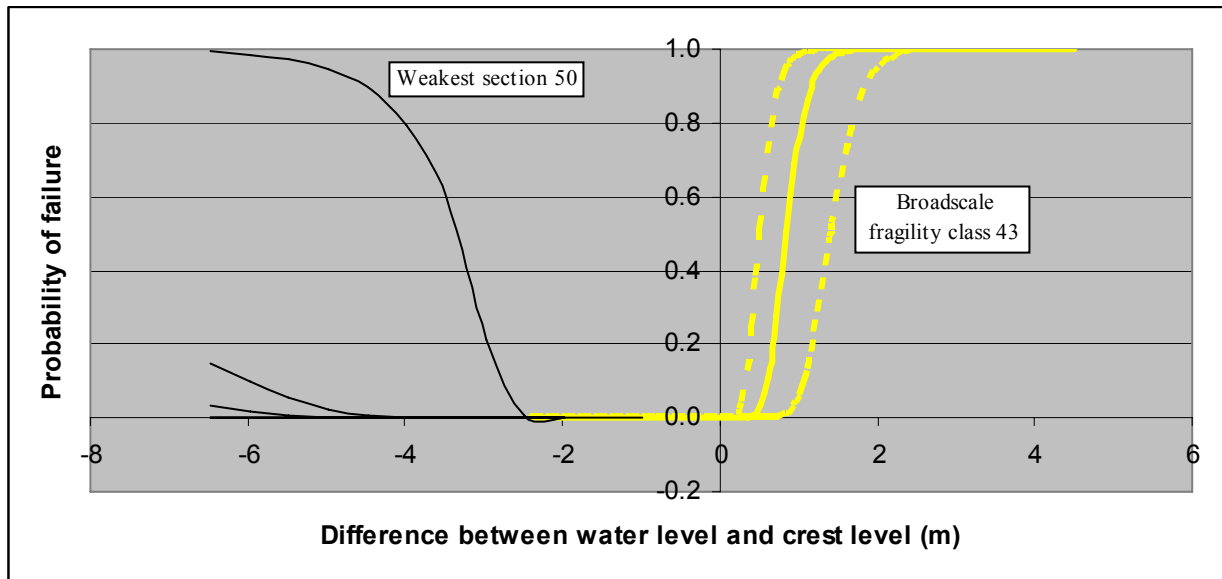


Figure 6.23 *Broadscale fragility, class 43, compared to the fragility of Dartford Creek to Gravesend sheet pile walls. The broadscale fragility with upper and lower bounds are highlighted. The fragility of the weakest section, 50, is indicated, but is not considered to be realistic.*

7. Conclusions and further steps

7.1 Conclusions

The conclusions are broken down into the components of the reliability analysis that were discussed in the chapters, i.e.: structure types and data sources, fault tree and failure mechanisms, individual cross section and system reliability calculation methods, results of the reliability analysis.

Structure types and data sources

The main conclusions are:

- Earth embankments, concrete walls and anchored sheet pile walls are the focus of this report. However, the Dartford Creek to Gravesend frontage consists of a large variety of structure types, each requiring a specific failure mechanism, fault tree and probabilistic analysis.
- The function of the structure type is not primarily flood defence in all cases, like that of the anchored sheet pile wall. The incorporation in the flood risk assessment requires additional attention to cover the full possible range of economic damages. The probability of failure does not equal the probability of breach in such cases.
- The data applied in this report can be improved in many areas. Firstly, the geometry of the flood defences is not based on the latest survey taken this year. Secondly, the borehole data are poorly geo-referenced, the interpolation of soil layers covers too large distances and the soil properties are generalised. Thirdly, the approach to wave conditions is simplified. The influence of the latter is not clear for two reasons: 1) the wave climate is fairly moderate in the estuary; 2) the effects of waves are not sufficiently incorporated in the process-based models, such as wave impact on concrete walls, or toe scouring of sheet pile wall structures.

Fault tree and failure mechanisms

The main conclusions are:

- The list of failure mechanisms taken into account in this reliability analysis is not comprehensive. However, they do represent the failures that historically occurred along the Dartford Creek to Gravesend flood defence line.
- The concrete wall structure is part of larger earth embankment in most cases. The interaction between the concrete wall and the earth embankment structure has not been given further attention. Failure therefore relates to the function of the concrete wall, and does not necessarily imply a full breach.
- A number of failure mechanisms that are known to be relevant for anchored sheet pile walls have not been considered in this study: tidal or wave induced toe scouring (currently a poorly understood process), overtopping water jets eroding the ground behind the sheet pile wall (currently a poorly understood process) and sliding of the sheet pile wall due to rotational slip encapsulating the anchor (computationally intensive).
- For those failure mechanisms that were taken into account, a rising water level has a stabilising effect on the sheet pile wall. Therefore extreme low water levels need to be considered for the probability of failure as well.

Individual cross section and system reliability calculation methods

The main conclusions are:

- Alpha-values provide valuable insight in the contribution of the random variables to the total probability of failure. During the course of the calculations crude Monte Carlo calculations proved to provide poor alpha-value results. The FORM method was therefore used to derive alpha-values.

- The relative standard deviation of the Monte Carlo calculations informs whether to increase the number of simulations to acquire more accurate probability approximations.
- System reliability methods were evaluated. The main conclusions from this evaluation were:
 - Incorporating spatial autocorrelation in the reliability analysis involves making choices about: the type of autocorrelation function (requires field data or consensus in literature), the type of multivariate distribution function (flexible or inflexible for calculations versus more representative of field data), the calculation method (balancing between computationally slow or fast and precise or imprecise).
 - The difference between the joint reliability of independent or autocorrelated cross sections is large. A disadvantage is that sufficient field data to derive autocorrelation functions is often absent. However, an assumption about independency is equally expert judgement based as a well-argued assumption about autocorrelation functions.
 - According to the previous bullet point dependency has an influence on the joint probability. It is reasonable to expect it will therefore have an effect on the flood risk assessment. As field data are often absent any assumption about (in) dependency is synthetic. In support of dependency: it is known from literature that e.g. soil properties are spatially autocorrelated. It is therefore advisable to take the effect into account.
 - The drawback for detailed flood risk assessments then is that taking the length effect into account requires a fine discretisation and therefore many flood spreading simulations. The feasibility of such a method is currently questionable. Interpolations in the damage / inundation database might be a possible solution.
 - In broadscale flood risk assessment the choice of defence line discretisation is coarse and justifies the independency assumption of the the defence sections. However, these defence sections are currently represented by a fragility curve for one cross section. Those fragility curves should therefore be increased as they in fact capture a serial system of cross sections within the defence section. How much the fragility should be increased depends on the desired dependency and was not further investigated in this research.

Results of the reliability analysis

The main conclusions are:

- In this report the interpretation of the probabilities of failure differs among earth embankments, concrete walls and anchored sheet pile walls. This difference in interpretation is caused by: differences in function (flooding versus ground retaining), failure mechanisms not relating to full breach (concrete wall and anchored sheet pile wall) and the relevance of low water levels for anchored sheet piles.
- The previous point makes the comparison between broadscale fragility, which represents the probability of breach, and the Dartford Creek to Gravesend not straightforward. In return, that can be used to reflect on the limitations of the broadscale fragility. A second problem with comparing broadscale fragility with Dartford Creek to Gravesend fragility is that it aims to represent a structure type on average. However, the stronger sections of a structure type generally protect areas with higher economic consequences, whilst the weaker sections protect areas with lower economic consequences.
- Specific to the results achieved for earth embankments:
 - The dominant failure mechanisms are a combination of uplifting and piping, which corresponds with historical failures in the area. The probability is relatively large for a couple of sections, possibly because hydraulic uplift reduction measures are not properly taken into account.
 - The largest sensitivity of the uplifting and piping mechanisms is to the water level and the density of the impermeable layers. Hydraulic uplift reduction measures prove therefore to be a sensible choice.
 - Broadscale fragility under predicts the Dartford Creek to Gravesend fragility in the higher frequent storms with lower economic consequences, whilst over predicting in the low

frequent storms with high economic consequences. Based on these considerations it is hard to judge about the quality of the broadscale fragility.

- Specific to the results achieved for concrete walls:
 - The dominating failure mechanism is piping underneath the toe of the concrete structure. The rest of the failure mechanisms have a different hierarchy according to the type of concrete wall.
 - Toe levels, the groundwater level and the height of the vertical concrete slab turn out to be the dominating variables.
 - The comparison with broadscale fragility is hard to make because the Dartford Creek to Gravesend fragility does not represent full breach for all failure mechanisms.
- Specific to the results achieved for sheet pile walls:
 - The dominating failure mechanism is breaking of the anchor followed by rotational failure of the sheet pile wall.
 - The groundwater level, the coefficients of the horizontal grain stress and the toe level are dominating variables.
 - The comparison with broadscale fragility is hard to make because: 1) the Dartford Creek to Gravesend fragility does not represent breach; 2) failure mechanisms such as toe scouring, erosion due to water jets or overall rotational failure are not taken into account.

7.2 Further steps

Potential further steps include:

- Further investigation into importance measures highlighting the relevant deterioration processes. Apply these importance measures to the Dartford Creek to Gravesend flood defence system to select the relevant deterioration processes for further analysis.
- Understanding the implications of the length effect within the context of flood system analysis mode.
- Extension of the methods to other structure types
- Discussion of the applicability of application of the fragility curves within Task 24

8. References

- Buijs, F.A., Hall, J.W., Sayers, P.B., (2005a) Exploring sensitivity of flood defence reliability to time-dependent processes, Proc. ICOSSAR, Rome, Italy, June 2005 (in press)
- Buijs, F.A., Hall, J.W., Sayers, P.B., Van Noordwijk, J.M., (2005b), Time-dependent reliability analysis of flood defences using gamma processes, proc. ICOSSAR 2005, (in press), Rome, Italy, June 2005
- Chun-Ching Li, Der Kiuregian, A. (1993) Optimal discretization of random fields, Journal of engineering mechanics, Vol. 119, no.6, June 1993
- CUR190 (1997) Chances in civil engineering, part 1: Probabilistic design in theory. CUR Gouda
- Gilbert, S. & Horner, R. (1984) The Thames Barrier (London: Thomas Telford)
- Hohenbichler, M., Rackwitz, R. (1983) First order concepts in system reliability. Structural Safety, 1, 1983, pp. 177-188
- HR Wallingford (1999) Assessment of the wind and waves for the Thames Tidal Walls (West) Strategy Study Area. Wallingford
- HR Wallingford (2004a), Risk Assessment for Flood and Coastal Defence for Strategic Planning, R&D Technical Report W5b-030/TR, A Summary, Defra / Environment agency
- HR Wallingford (2004b), Joint Probability issues within estuaries – a numerical case study for the tidal Thames, HR Wallingford Report TR 143
- Lassing, B.L., Vrouwenvelder, A.C.W.M., Waarts, P.H. (2003), Reliability analysis of flood defence systems in the Netherlands, proc. Conf. ESREL 2003 (2): 1005-1013, Maastricht, The Netherlands, June 15-18
- Pagina: 76
- Terzaghi, K., and Peck, R.B., (1967) Soil Mechanics in Engineering Practice. John Wiley & Sons, New York
- Vrijling, J.K. (2001), Probabilistic design of water defence systems in The Netherlands, Reliab. Eng. Syst. Safe. 74(3): pp. 337-344
- Vrouwenvelder, A.C.W.M., et al. (1999) Theoretical manual PC-Ring, part C: Calculation methods. TNO
- Vrouwenvelder, A.C.W.M., et al. (2001) Theoretical manual PC-Ring, part A: Failure mechanism descriptions. TNO

APPENDICES

Appendix A: Inventory Dartford Creek to Gravesend borehole data archive

Box labelled Length 3 & 4

- Folder labelled 'Length 3/4 stage 3 Works, Site Investigations' containing D.Powell Design Report on Length 3/4 with the following contents (have made paper copies):
 1. Introduction – site location, expected flood level and design approach, description of stage 1.
 2. Soil Investigation – site investigation, laboratory investigation, calibration for soil types 1 and 2 (clay and peat), summary of soil parameters (types 1 and 2 for total 7 types), soil parameters used in design, pore water pressures.
 3. Design procedure and loading criteria – soil parameters, consolidation, short term and long term case (soil parameters, consolidation, loading, riverward and landward stability).
 4. Design limitations and proposals – length 4 short term and long term case, length 3 idem
 5. Consolidation and gravel uplift pressures

Appendices:

1. Gravel uplift pressure
 2. Description of field vane test and the quick undrained triaxial test
 3. Correlation of Field vane test vs quick undrained triaxial test results
 4. Soils classification
 5. Example of site investigation data – discussion
 6. Discussion of soil parameters
 7. Effective stress test results
 8. Site investigation data – length 4
 9. Borehole logs length 4 (not georeferenced!)
 10. Borehole logs length 3 (not georeferenced!)
 11. Site investigation data – length 3
 12. Calculation of consolidation
 13. Comparison of field vane tests
- Folder 'Thames barrier / Thames Tidal walls. Borehole logs, drilled 1970 / '71 lengths 3-11 → georeferenced, soil layer descriptions and depths.
 - Folder 'Lab test results 1982 (Melbourne Lab) from samples retrieved under L3/4 pore water pressure interception contract 3/1/PWP' → mainly length 3, bit length 4. Bit a mixture of information: more borehole soil layer descriptions given depths and consolidation calculations, some particle size distributions (gravel), samples and moisture content (made copies)
 - Folder 'Thames Tidal Flood Defences – Length 3/4 Drillers Logs 1971 – 1977' on site drillers records
 - Folder 'Thames Tidal Flood Defences – Length 4 Drillers Logs February 1976 – January 1979' on site drillers records
 - Folder 'Thames Tidal Flood Defences Length 3 Drillers Logs December 1975 – January 1979 on site drillers records
 - Folder 'Air piezometer information' piezometer readings for several times during a tidal cycle
 - Folder '4/2.7/EI' location along length 4 borehole logs consolidation curves, oedometer readings
 - Folder 'Length3/4 SI, 1981' borehole logs and lab investigations
 - Report 'Investigation of uplift pressures in the gravel layer, lengths 3 & 4' (Golder Associates, for Southern Water Authority, Sept 1978). Analytical predictions and piezometer measurements, plots indicating the effect of pressure relieving pipes (drains) with several diameters (made copies).
 - Folder '4/2.7/E', borehole logs and lab test results
 - Folder '4/9.0/EI' and '4/7.5/EI' containing one or two borehole logs

Problem with all of the information: no clear maps and referencing

Box Labelled Length 5

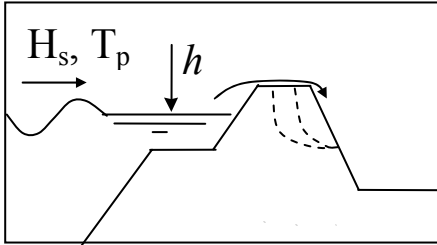
- ‘Thames Tidal Flood Defences Private Frontages, Test pits and soil investigation laboratory test results, Rosherville embayment’ soil classification (very rough) and detailed soil particle size distributions.
- ‘Thames Barrier and Flood Prevention Private Frontages, test pits and soil investigation’ Specification for tendering, so no technical information
- Folder ‘Soil Mechanics investigation’ mixture of locations and qualities: Littlebrook, Stone, Swanscombe, Horrid Hill, Stoke, Long Reach, Twinney, Leysdown, Egypt Bay & St. Mary’s Bay. Quality and type of information varies per location, produced in ‘50s: some settlement / time plots, some borehole records, compression tests
- Report ‘T.T.F.D. Length 5, Site Investigation 1980’ Soil classification and some lab tests: Atterberg limits, water content, bulk density, results of triaxial tests. Clear location references.
- Folder ‘Gravesend 5/12 – 5/13 report’ another copy of the report mentioned under the previous bullet. This folder contains the original report.
- Two copies of Report ‘Factual Report for the Southern Water Authority Gravesend Site Boreholes 5/13/4; 5/13/7; 5/13/2A, May 1980’. For seven samples the results for effective stress triaxial tests are described.
- Folder ‘Site investigation at Gravesend TTFD Lengths 5/12 and 5/13. Mainly borehole logs, soil classifications.
- Folder ‘Northfleet, Britannia Metals, 2No. B/H for confirmation of chalk, August /Sept ‘82’.
- Folder ‘Royal Terrace Pier 5/12013 Aug 82 Sept 82’ description of permeability tests of grout curtain at Royal Terrace Pier.
- Folder ‘Private Frontages 5/12 + 13 Foundations Report. For Royal Pier Road. Gravesend.

Appendix B: Limit state equations of the failure mechanisms

B.1 Earth embankments

Erosion of cover of inner slope by wave overtopping or overflow

Sketch of failure mechanism:



Reliability equation:

Water discharges due to overtopping or overflow respectively hit or scour the inside slope of the embankment. Due to this loading of the inside slope the grass gets damaged. After the grass has been damaged, the embankment body is exposed to the overtopping/overflow water. In the end, if this erosion process continues long enough, the embankment breaches. The duration of this erosion process depends on the duration of the storm.

Limit state equation for wave overtopping:

$$Z = m_c q_c - m_a q_a$$

Wherein q_c is the critical overtopping discharge [m^2/s], m_c is the model uncertainty of the critical discharge model [-], q_a is the calculated discharge [m^2/s] and m_a is the model uncertainty associated with the actual discharge.

Limit state equation for overflow:

$$Z = h_{\text{crest}} + \Delta h_c - h$$

In which h_{crest} [MOD] is the crest level of the embankment, Δh_c [m] expresses the critical height for which almost damage of the grass occurs and h is the actual occurring water level [MOD].

Loading equations:

The q_a is calculated with Owen's wave overtopping model. A separate sheet is incorporated for that after this template.

The loading in case of overflow is caused by the difference in water level

Resistance (strength) equations:

The critical discharge in the wave overtopping limit state equation, q_c , is calculated with the following equation:

$$q_c = \left[\frac{3.8 \cdot c_g^{2/3}}{(6 \cdot 10^5)^{2/3} \cdot \left[1 + 0.8 \cdot \log_{10}(P_r \cdot t_s \cdot \frac{c_g \cdot d_w}{c_g \cdot d_w + 0.4 \cdot c_{RK} \cdot L_{K,inside}}) \right]} \right]^{5/2} \cdot \frac{k^{1/4}}{125 \cdot (\tan \alpha_i)^{3/4}}$$

<p>and crest level.</p>	<p>Δh_c [m] in the overflow limit state equation expresses the critical height for which almost damage of the grass occurs and is calculated with the following equation:</p> $\Delta h_c = \sqrt[3]{\frac{2.78 \cdot q_c^2}{g}}$ <p>In which g is the gravitational constant and q_c the critical discharge as calculated above.</p>
<p>Parameter definitions:</p> <p>c_g = coefficient that represents the erosion endurance of the grass. The values of c_g can range from 10^6 ms in case of good quality to $3.3 \cdot 10^5$ ms in case of bad quality. [m·s]</p> <p>P_t = percentage of the time that overtopping/flowing over occurs. In case of flowing over P_t is 1 and in case of overtopping P_t takes the pulsatory character of overtopping in account [-]</p> <p>t_s = duration of the storm [hours]</p> <p>d_w = the depth of the grass roots. Values of d_w range between 0.05m and 0.07m, factors influencing the magnitude of this factor are: maintenance, location (sea or river embankments) and the type of vegetation. [m]</p> <p>c_{RK} = coefficient with regard to the erosion endurance of the clay cover layer. The values for c_{RK} range from $7 \cdot 10^3$ m·s (bad quality clay) to $54 \cdot 10^3$ m·s (good quality clay). In case of sand $c_{RK} = 0$. [m·s]</p> <p>$L_{k,inside}$ = width of the inside clay cover layer, that can be considered as the total width of the embankment. [m]</p> <p>k = roughness factor according to Strickler of the inside slope. [s⁶/m²]</p> <p>α_i = angle of the inside slope. [degrees]</p>	
<p>Sources of failure mechanism equations / methods:</p> <p>Vrouwenvelder et al. (2001)</p>	
<p>Sources of uncertainties in failure equations / input parameters:</p> <p>Vrouwenvelder et al. (2001)</p>	

Smooth, Impermeable, Simply sloped / Composite Seawall (Owen, 1980)

Simply sloped Seawall

Normal wave attack

Determine the mean overtopping discharge rate per metre run of seawall, Q ($m^3/sec/m$)

$$Q = Q_* T_m g H_s$$

where

Q_* - dimensionless discharge

$$Q_* = A \exp(-BR_*)$$

A, B - empirical coefficients dependent upon the cross-section of the seawall [6]

R_* - dimensionless freeboard (height of the crest of the wall above still water level)

$$R_* = R_c / \left(T_m (g H_s)^{0.5} \right), \\ 0.05 < R_* < 0.30$$

R_c - freeboard (height of the crest of the wall above still water level) (m)

H_s - significant wave height at the toe of the structure (m)

g - acceleration due to gravity (m/sec^2)

T_m - mean wave period at the toe of the structure (sec)

Angled wave attack

$$Q_{angled\ wave\ attack} = Q_r Q$$

where

Q_r - ratio of discharge under angled wave attack to that under normal attack

$$Q_r = 1 - 0.000152\beta^2, 0^0 < \beta \leq 60^0$$

If $\beta > 60^0$ results for $\beta = 60^0$ should be applied

Q - mean overtopping discharge rate per metre run of seawall under normal wave attack ($m^3/sec/m$)

Composite Seawall

In shallow water, $h < 0.55 H_s$, an imaginary simple slope is constructed between the toe and crest of the structure.

Smooth, Impermeable, Bermed Seawall or Composite Seawall

Normal wave attack

Similar to "Smooth, Impermeable, Simply sloped Sea Wall"

Angled wave attack

$$Q_{angled\ wave\ attack} = Q_r Q$$

where

Q_r - ratio of discharge under angled wave attack to that under normal attack

$$Q_r = 1.99 - 1.93 \left\{ 1 - \left[(\beta - 60) / 69.8 \right]^2 \right\} \\ 0^0 < \beta \leq 60^0$$

If $\beta > 60^0$ results for $\beta = 60^0$ should be applied

Q - mean overtopping discharge rate per metre run of seawall under normal wave attack ($m^3/sec/m$)

Composite Seawall

In shallow water, $h < 0.55 H_s$, an imaginary simple slope is constructed between the toe and crest of the structure.

Rough and Armoured Seawall

Normal wave attack

Determine the mean overtopping discharge rate per metre run of seawall, Q ($m^3/sec/m$)

$$Q = Q_* T_m g H_s$$

where

Q_* - dimensionless discharge

$$Q_* = A \exp(-BR_*/r)$$

A, B - empirical coefficients dependent upon the cross-section of the sea wall [6]

R_* - dimensionless freeboard (height of the crest of the wall above still water level)

$$R_* = R_c / \left(T_m (g H_s)^{0.5} \right), \\ 0.05 < R_* < 0.30$$

R_c - freeboard (height of the crest of the wall above still water level) (m)

r - roughness coefficient [6]

If the structure includes berm on smooth, impermeable slope, method applied to "Smooth, Impermeable, Bermed Sea Wall" will be used.

If the structure includes a permeable crest berm, a reduction factor, C_r , will be taken into account.

$$Q_{perm\ berm} = Q \times C_r$$

$$C_r = 3.06 \exp(-1.5 C_w / H_s)$$

where

C_w - crest berm width (m)

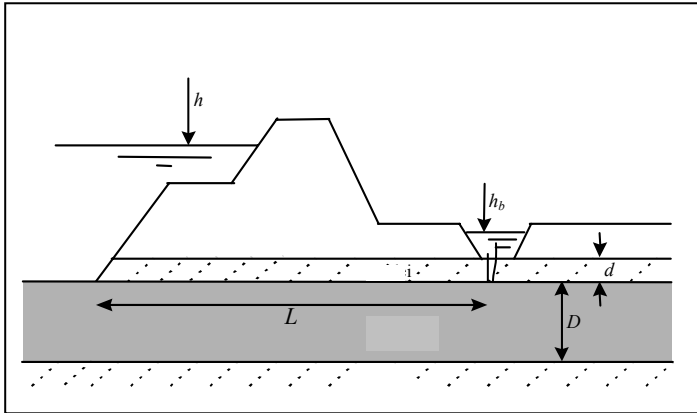
$$C_r = 1 \text{ when } C_w / H_s < 0.75$$

Angled wave attack

Same methods as for "Smooth, Impermeable, Simply sloped Sea Wall" and "Smooth, Impermeable, Bermed Sea Wall".

Uplifting of impermeable layers behind earth embankment

Sketch of failure mechanism:



Reliability equation:

Uplifting occurs if the difference between the local water level h , and the water level "inside", h_b is larger than the critical water level h_c . This is expressed in the reliability function as:

$$Z = m_o h_c - m_h (h - h_b)$$

In which m_o [-] takes the model uncertainty of the model which determines h_c [m] in account and m_h the level of damping [-]. The critical water level expresses the limit water level for which almost uplifting occurs. This water level is based on the properties of the impervious layer.

Loading equations:

The loading is represented by the difference in water level on the river, h [mOD] and the water level in the floodplain h_b [mOD].

Resistance (strength) equations:

$$h_c = \frac{\gamma_{wet} - \gamma_w}{\gamma_w} d$$

In which γ_{wet} [kN/m³] is the saturated volumetric weight of the impermeable soil layers, γ_w [kN/m³] is the volumetric weight of the water and d [m] is the thickness of the impermeable layers.

Parameter definitions:

Are given above

Sources of failure mechanism equations / methods:

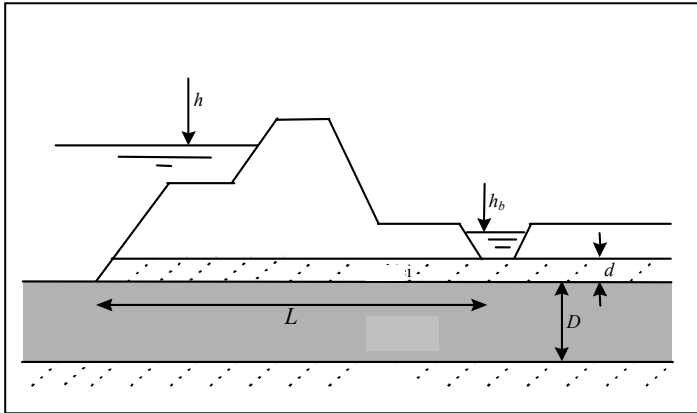
Vrouwenvelder et al. (2001)

Sources of uncertainties in failure equations / input parameters:

Vrouwenvelder et al. (2001)

Piping in water conductive layer underneath the earth embankment

Sketch of failure mechanism:



Reliability equation:

The embankment fails as a consequence of piping if the difference between the local water level h and the inside water level h_b , exceeds the critical water level h_p .

$$Z = m_p h_p - (h - h_b)$$

In which m_p is the model uncertainty of the model with which h_p is described. The critical water level h_p is described by Sellmeijer's model of piping

Loading equations:

The loading is represented by the difference in water level on the river, h [mOD] and the water level in the floodplain h_b [mOD].

Resistance (strength) equations:

$$h_p = \alpha c L \left(\frac{\gamma_k}{\gamma_w} - 1 \right) (0.68 - 0.1 \ln c) \tan \theta$$

Parameter definitions:

L - seepage length [m]

γ_k -volumetric weight of the clay [kN/m³]

γ_w -volumetric weight of the water [kN/m³]

θ -friction angle of the sand with regard to movement [°]

α -factor reflecting the effect of a finite thickness of the water conducting layer, for expression see below

c -describes the characteristics of the sand in the erosion enduring water conducting sand layer, for expression see below

$$\alpha = \left(\frac{D}{L} \right)^{\frac{0.28}{((D/L)^{2.8} - 1)}}$$

D - thickness water conductive sand layer [m]

η - the drag force factor (constant of White) [-]

d_{70} - representative of the large fraction of grains in the sand of the water conducting layer [m]

κ - the intrinsic permeability [m²]

Sources of failure mechanism equations / methods:

Vrouwenvelder et al. (2001)

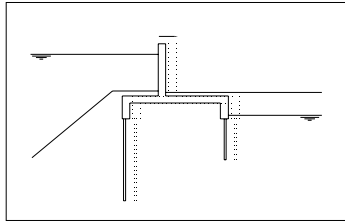
Sources of uncertainties in failure equations / input parameters:

Vrouwenvelder et al. (2001)

B.2 Concrete wall

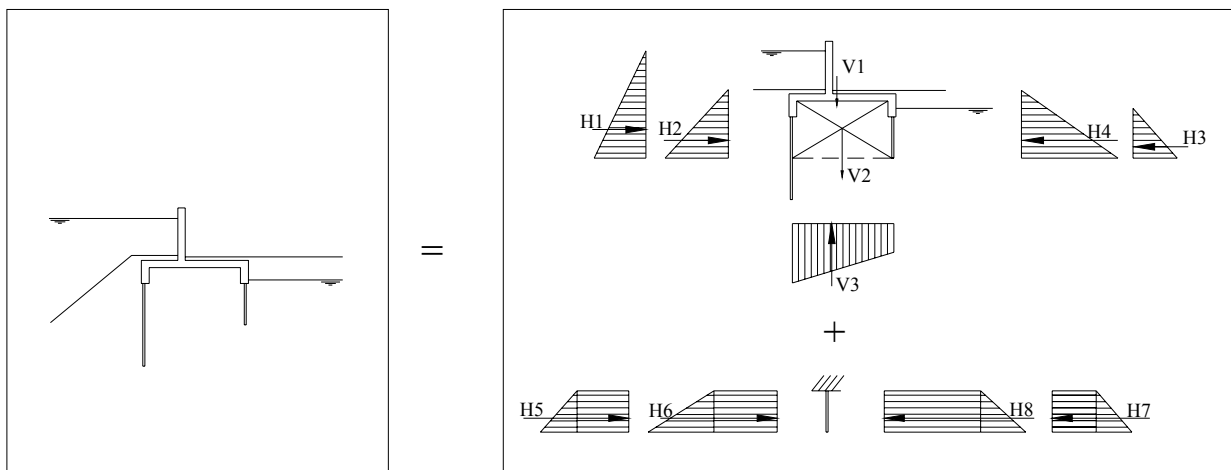
Sliding of concrete wall

Sketch of failure mechanism:



Limit state function:

When the water level reaches the concrete wall, a horizontal hydraulic force is exerted against the wall. This force can initiate sliding of the concrete structure. Resisting forces are the weight of the structure and the pressures of the ground keeping the structure into place.



$$z = m_{C;S;R} \cdot \tan(\delta) \cdot \Sigma V - m_{C;S;S} \cdot \Sigma H$$

where:

$\tan(\delta)$, ΣV , ΣH are the friction coefficient, the resulting vertical force and the resulting horizontal hydraulic loading force [kN per stretching meter]

$m_{C;S;R}$ and $m_{C;S;S}$ are model factors for the horizontal resistance and loading force [-]

The forces on the concrete wall are modelled as illustrated below.

Loading equations:

The resulting horizontal force is built up as follows:

Resistance (strength) equations:

V_1 is the weight of the concrete structure in kN per stretching meter - depends on the geometry of the wall.

<p>Main structure (concrete wall & mobilised soil):</p> $H1 = 0.5 \cdot \gamma_w (h - L_3)^2$ $H2 = 0.5 \cdot K_a \cdot (\gamma_s - \gamma_w) (h_1 - L_3)^2$ $H3 = 0.5 \cdot \gamma_w (gw - L_3)^2$ $H4 = 0.5 \cdot K_p \cdot (\gamma_s - \gamma_w) (h_3 - L_3)^2$ <p>Sheet pile cut-off:</p> $H5 = \gamma_w (h - L_3) (L_3 - L_1) +$ $0.5 \cdot \gamma_w (L_3 - L_1)^2$ $H6 = K_p \cdot (\gamma_s - \gamma_w) (h_1 - L_3) (L_3 - L_1) +$ $0.5 \cdot K_p \cdot (\gamma_s - \gamma_w) (L_3 - L_1)^2$ $H7 = \gamma_w (gw - L_3) (L_3 - L_1) +$ $0.5 \cdot \gamma_w (L_3 - L_1)^2$ $H8 = K_a \cdot (\gamma_s - \gamma_w) (h_3 - L_3) (L_3 - L_1) +$ $0.5 \cdot K_a \cdot (\gamma_s - \gamma_w) (L_3 - L_1)^2$	<p>V_2 is the vertical weight of the mobilised soil in kN per stretching meter:</p> $V_2 = \gamma_s h_s \cdot B$ <p>V_3 is the upward hydraulic force:</p> $V_3 = \gamma_w \cdot (gw - L_3) \cdot B +$ $0.5 \cdot \gamma_w \cdot (L_3 - L_1) \cdot B$
<p>Parameter definitions:</p> <p>h = the river water level [mOD]</p> <p>gw = the river water level [mOD]</p> <p>γ_s = the volumetric weight of the saturated soil [kN / m³]</p> <p>γ_w = the volumetric weight of water [kN / m³]</p> <p>L_1 = the level of the longest sheet pile cut-off [mOD]</p> <p>L_3 = the level of the shortest sheet pile cut-off [mOD]</p> <p>h_1 = the level of the crest in front of the concrete wall on the river side [mOD]</p> <p>h_3 = the level of the crest in front of the concrete wall on the land side [mOD]</p> <p>K_a = the coefficient for active horizontal grain force [-]</p> <p>K_p = the coefficient for passive horizontal grain force [-]</p> <p>B = the width of the concrete structure between extensions [m]</p> <p>h_s = the height of the mobilised soil [m]</p>	

Sources of failure mechanism equations / methods:

Standard stability check of hydraulic structures

Sources of uncertainties in failure equations / input parameters:

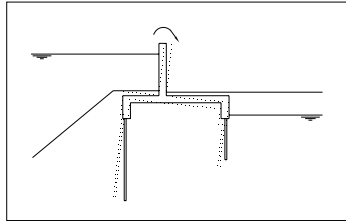
Baecher & Christian (2003);

CUR 190 (1997);

Vrouwenvelder et al. (2001);

Overturning of concrete wall

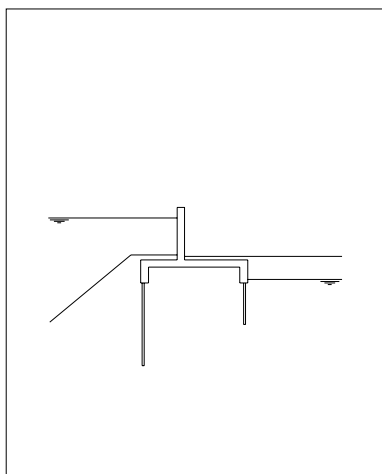
Sketch of failure mechanism:



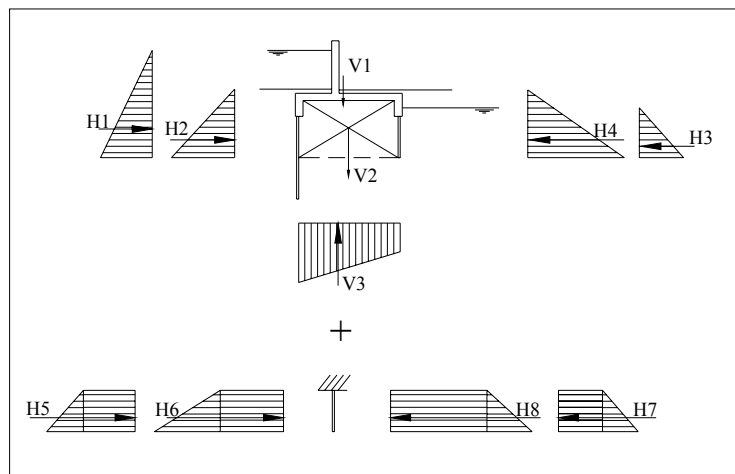
Limit state function:

When the water level reaches the concrete wall, a horizontal hydraulic force is exerted against the wall. This force can overturn the concrete structure. Resisting forces are the weight of the structure and the pressures of the ground keeping the structure into place. Overturning is assumed to occur when tensile stress occurs in the foundational plane. This assumption leads to the following limit state function:

$$z = m_{c;o;R} \cdot 1/6 \cdot B_c - m_{c;o;S} \cdot \Sigma M / \Sigma V$$



=



where:

B_c , ΣM , ΣV are the width of the base of the concrete structure [m], the resulting moment [kNm / m] and the resulting vertical force acting on the concrete wall structure [kN / m]

$m_{c;o;R}$ and $m_{c;o;S}$ are model factors for the strength and loading models [-]

The forces on the concrete wall are modelled as illustrated below.

Loading equations:

The resulting moment is taken around the centre of the base of the mobilised soil and is built up as follows:

Resistance (strength) equations:

V_1 is the weight of the concrete structure in kN per stretching meter - depends on the geometry of the wall.

<p>Main structure (concrete wall & mobilised soil):</p> $M1 = 0.5 \cdot \gamma_w (h - L_3)^2 \cdot 1/3(h - L_3)$ $M2 = 0.5 \cdot K_a \cdot (\gamma_s - \gamma_w)(h_1 - L_3)^2 \cdot 1/3(h_1 - L_3)$ $M3 = 0.5 \cdot \gamma_w (gw - L_3)^2 \cdot 1/3(gw - L_3)$ $M4 = 0.5 \cdot K_p \cdot (\gamma_s - \gamma_w)(h_3 - L_3)^2 \cdot 1/3(h_3 - L_3)$ <p>Sheet pile cut-off:</p> $M5 = \gamma_w (h - L_3)(L_3 - L_1) \cdot 1/2(L_3 - L_1) + 0.5 \cdot \gamma_w (L_3 - L_1)^2 \cdot 2/3(L_3 - L_1)$ $M6 = K_p \cdot (\gamma_s - \gamma_w)(h_1 - L_3)(L_3 - L_1) \cdot 1/2(L_3 - L_1) + 0.5 \cdot K_p \cdot (\gamma_s - \gamma_w)(L_3 - L_1)^2 \cdot 2/3(L_3 - L_1)$ $M7 = \gamma_w (gw - L_3)(L_3 - L_1) \cdot 1/2(L_3 - L_1) + 0.5 \cdot \gamma_w (L_3 - L_1)^2 \cdot 2/3(L_3 - L_1)$ $M8 = K_a \cdot (\gamma_s - \gamma_w)(h_3 - L_3)(L_3 - L_1) \cdot 1/2(L_3 - L_1) + 0.5 \cdot K_a \cdot (\gamma_s - \gamma_w)(L_3 - L_1)^2 \cdot 2/3(L_3 - L_1)$ <p>Moments due to vertical forces:</p> $Mv1 = b_{gr} \cdot V1$ $Mv2 = 0$ $Mv3 = 0.5 \cdot \gamma_w \cdot (L_3 - L_1) \cdot B \cdot (1/2B - 1/3B)$ <p>Resulting moment</p> $\Sigma M = M1 + M2 - M3 - M4 - M5 - M6 + M8 + M9 - Mv1 + Mv3$	<p>V_2 is the vertical weight of the mobilised soil in kN per stretching meter:</p> $V_2 = \gamma_s h_s \cdot B$ <p>V_3 is the upward hydraulic force:</p> $V_3 = \gamma_w \cdot (gw - L_3) \cdot B + 0.5 \cdot \gamma_w \cdot (L_3 - L_1) \cdot B$
<p>Parameter definitions:</p> <p>h = the river water level [mOD]</p> <p>gw = the river water level [mOD]</p> <p>γ_s = the volumetric weight of the saturated soil [kN / m³]</p>	

γ_w = the volumetric weight of water [kN / m³]

L_1 = the level of the longest sheet pile cut-off [mOD]

L_3 = the level of the shortest sheet pile cut-off [mOD]

h_1 = the level of the crest in front of the concrete wall on the river side [mOD]

h_3 = the level of the crest in front of the concrete wall on the land side [mOD]

K_a = the coefficient for active horizontal grain force [-]

K_p = the coefficient for passive horizontal grain force [-]

B = the width of the concrete structure between extensions [m]

b_{gr} = the distance between the centre of gravity of the concrete structure and the centre of the mobilised soil [m]

h_s = the height of the mobilised soil [m]

Sources of failure mechanism equations / methods:

Standard stability check of hydraulic structures

Sources of uncertainties in failure equations / input parameters:

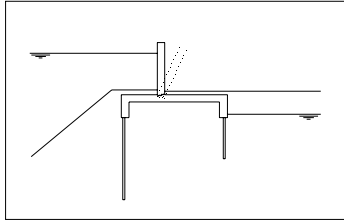
Baecher & Christian (2003);

CUR 190 (1997);

Vrouwenvelder et al. (2001);

Failure of vertical slab of concrete wall due to bending moments

Sketch of failure mechanism:



Limit state function:

The horizontal hydraulic force exerted by the river water level and the ground resting against the riverside of the concrete wall cause bending moments in the vertical slab of the wall. Failure of the vertical slab occurs when there is insufficient reinforcement to take on the tensile stress due to the bending moment:

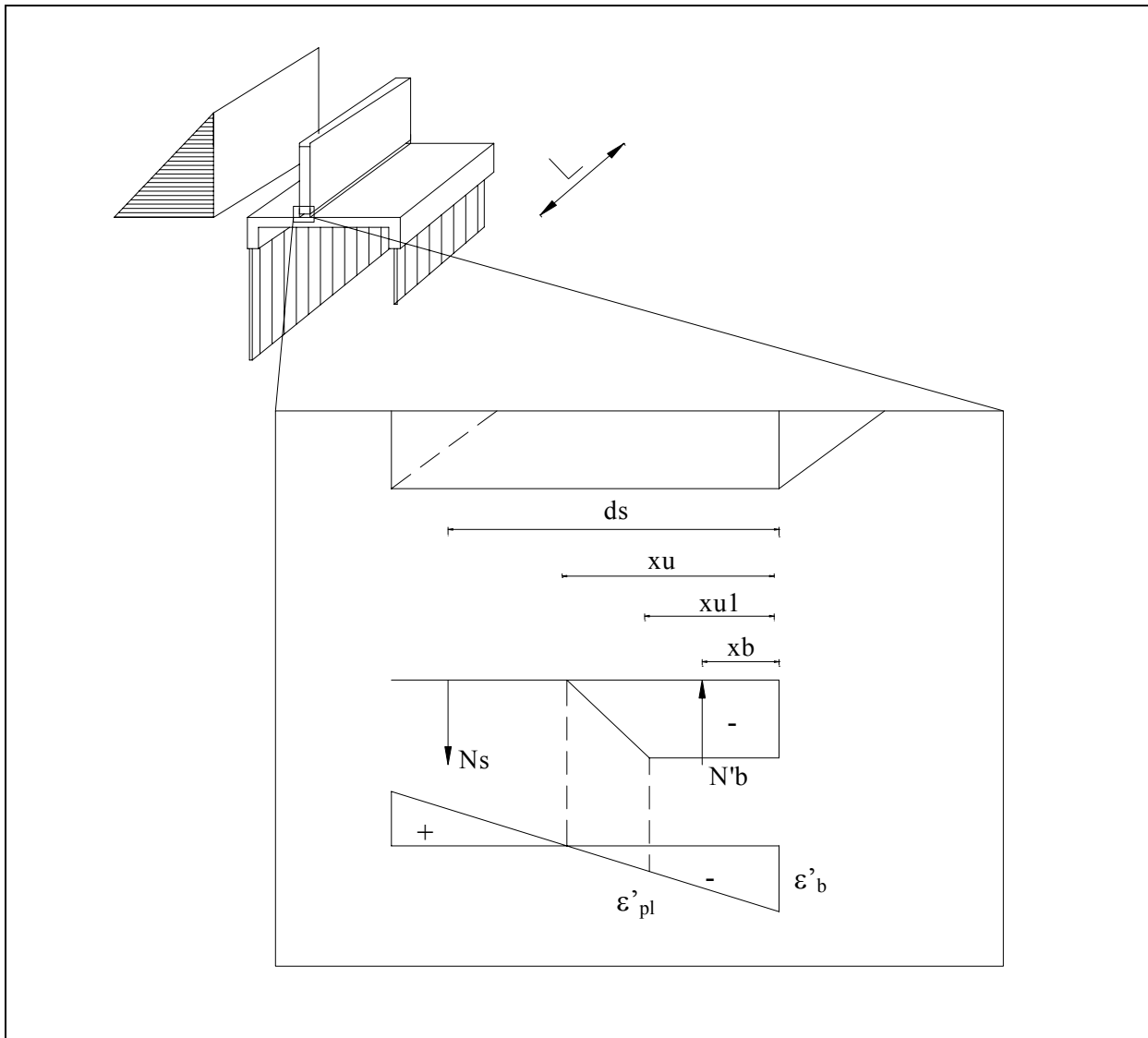
$$z = m_{c;b;R} \cdot M_u - m_{c;b;S} \cdot M_d$$

where:

M_u and M_d are respectively the maximum moment the cross section can take on, based on the maximum tensile stress in the reinforcement, and the actually occurring moment exerted by the hydraulic and geotechnical loading [kNm]

$m_{c;b;R}$ and $m_{c;b;S}$ are model factors for the strength and loading models [-]

The forces in the concrete cross section are modelled as illustrated below.



Loading equations:

The moments are taken around the base of the vertical concrete slab:

$$M1 = 0.5 \cdot \gamma_w (h - (hc-d4))^2 \cdot 1/3 (h - (hc-d4))$$

$$M2 = 0.5 \cdot K_a \cdot (\gamma_s - \gamma_w) (h_1 - (hc-d4))^2 \cdot 1/3 (h_1 - (hc-d4))$$

$$M3 = 0.5 \cdot K_p \cdot (\gamma_s - \gamma_w) (h_3 - (hc-d4))^2 \cdot 1/3 (h_3 - (hc-d4))$$

Resulting moment

$$\Sigma M = M1 + M2 - M3$$

Resistance (strength) equations:

$$N_s = A_s f_s$$

$$x_u = \frac{N_s}{\frac{1}{2} \left(1 + \frac{\epsilon'_b - \epsilon'_{pl}}{\epsilon'_b} \right) L \cdot f'_b}$$

$$x_{u1} = \frac{\epsilon'_b - \epsilon'_{pl}}{\epsilon'_b} x_u$$

$$x_b = \frac{\frac{1}{2} x_{u1}^2 f'_b + \frac{1}{2} (x_u - x_{u1}) \left(\frac{1}{3} (x_u - x_{u1}) + x_{u1} \right) f'_b}{x_{u1} f'_b + \frac{1}{2} (x_u - x_{u1}) f'_b}$$

$$M_u = N_s \cdot (d_s - x_b)$$

Parameter definitions:

h = the river water level [mOD]

h_c = the crest level of the concrete wall [mOD]

h_1 = the ground level on the riverside of the concrete wall [mOD]

h_3 = the ground level on the landside of the concrete wall [mOD]

d_4 = the height of the vertical slab of the concrete wall [m]

γ_w = the volumetric weight of water [kN / m³]

γ_s = the volumetric weight of saturated soil [kN / m³]

N_s = the total tensile force in the steel reinforcement [kN]

A_s = the total area of steel reinforcement in the concrete cross section [m²]

f_s = yield strength of reinforcement steel [kN/m²]

x_u = the pressure zone in the concrete [m]

x_{ui} = the plastic pressure zone in the concrete [m]

x_b = the distance of the resulting pressure in the concrete from the edge [m]

ϵ'_{bu} = the ultimate strain of the concrete [-]

ϵ'_{pl} = the plasticity strain of the concrete [-]

f'_b = the cubic pressure strength of the concrete [kN/m²]

L = length of the concrete slab [m]

K_a = the coefficient for active horizontal grain force [-]

Sources of failure mechanism equations / methods:

According to general standards on concrete design (British and Dutch)

Sources of uncertainties in failure equations / input parameters:

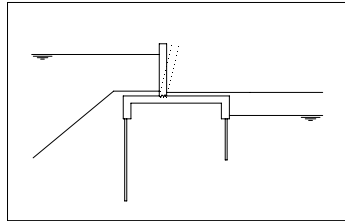
Baecher & Christian (2003);

CUR 190 (1997);

Vrouwenvelder et al. (2001);

Failure of vertical slab of concrete wall due to shear stress

Sketch of failure mechanism:



Limit state function:

The horizontal hydraulic force exerted by the river water level and the ground resting against the riverside of the concrete wall cause shear stress at the base section of the vertical slab. Failure of the vertical slab occurs if the concrete cross section has insufficient width or shear strength to take on the horizontal force. The approach below applies to concrete slabs without reinforcement for shear stress.

$$Z = m_{c;sh;R} \cdot T_u - m_{c;sh;S} \cdot T_d$$

where:

T_u and T_d are respectively the maximum shear stress the cross section can withstand and the actually occurring shear stress exerted by the hydraulic and geotechnical loading [N/mm²]

$m_{c;sh;R}$ and $m_{c;sh;S}$ are model factors for the strength and loading models [-]

The forces in the concrete cross section are modelled as illustrated below.

Loading equations:

The shear forces are determined in the base of the vertical concrete slab:

$$H1 = 0.5 \cdot \gamma_w (h - (hc-d4))^2$$

$$H2 = 0.5 \cdot K_a \cdot (\gamma_s - \gamma_w) (h_1 - (hc-d4))^2$$

$$H3 = 0.5 \cdot K_p \cdot (\gamma_s - \gamma_w) (h_3 - (hc-d4))^2$$

Resulting shear force

$$\Sigma H = H1 + H2 - H3$$

Resistance (strength) equations:

$$\tau_u = \tau_1 \leq \tau_2$$

$$\tau_1 = 0.4 f_b k_\lambda k_h \sqrt[3]{\omega_0}$$

$$k_\lambda = 1.0$$

$$k_h = 1.6 - d_2 \geq 1.0$$

$$\omega_0 = \frac{100 A_s}{L d_2} \leq 2.0$$

$$\tau_2 = 0.2 f'_b k_n k_\theta$$

$$k_n = 1.0$$

$$k_\theta = 1.0$$

Parameter definitions:

h = the river water level [mOD]

h_c = the crest level of the concrete wall [mOD]

h_1 = the ground level on the riverside of the concrete wall [mOD]

h_3 = the ground level on the landside of the concrete wall [mOD]

d_4 = the height of the vertical slab of the concrete wall [m]

d_2 = the width of the vertical slab [m]

γ_w = the volumetric weight of water [kN / m³]

γ_s = the volumetric weight of saturated soil [kN / m³]

f'_b = the cubic pressure strength of the concrete [kN/m²]

f_b = the cubic tensile strength of the concrete [kN/m²]

ω_0 = reinforcement percentage [-]

τ_1 = the maximum shear stress the cross section can take on, if no shear stress reinforcement is present [kN/m²]

$k_{\lambda}, k_h, k_r, k_{\theta}$ = coefficients

L = length of the concrete slab [m]

K_a = the coefficient for active horizontal grain force [-]

Sources of failure mechanism equations / methods:

According to general standards on concrete design (British and Dutch)

Sources of uncertainties in failure equations / input parameters:

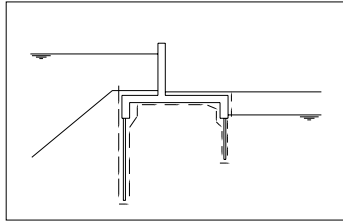
Baecher & Christian (2003);

CUR 190 (1997);

Vrouwenvelder et al. (2001);

Piping directly underneath sheet pile cut-off

Sketch of failure mechanism:



Limit state function:

Failure due to piping directly underneath the sheet pile cut-off is taken into account if the water level exceeds the ground water level in the earth bank behind the wall. This ensures a positive water head over the concrete structure, which drives the piping process. One of the requirements is that the water level persists long enough for the piping process to initiate.

$$z = m_{c;p;R} \cdot \Delta h_c - \Delta h_a$$

where:

Δh_c and Δh_a are respectively the critical head difference associated with piping underneath the sheet pile cut-off and the actual head difference occurring over the concrete structure [m]

$m_{c;p;R}$ is a model factor for the strength model [-]

The forces in the concrete cross section are modelled as illustrated below.

Loading equations:

The head over the concrete structure:

$$\Delta h_a = h - gw$$

Resistance (strength) equations:

The critical head associated with the piping process:

$$\Delta h_c = (L_v + 1/3 L_h) / c_t$$

Parameter definitions:

h = the river water level [mOD]

gw = the groundwater level behind the concrete structure [mOD]

L_v = the vertical seepage length [m]

L_h = the horizontal seepage length [m]

c_t = the creep ratio [-]

Sources of failure mechanism equations / methods:

Terzaghi (1967)

Sources of uncertainties in failure equations / input parameters:

Baecher & Christian (2003);

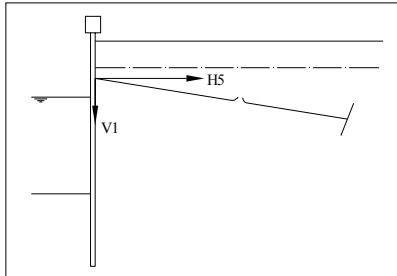
CUR 190 (1997);

Vrouwenvelder et al. (2001);

B.3 Anchored sheet pile wall

Insufficient strength of the tie rod

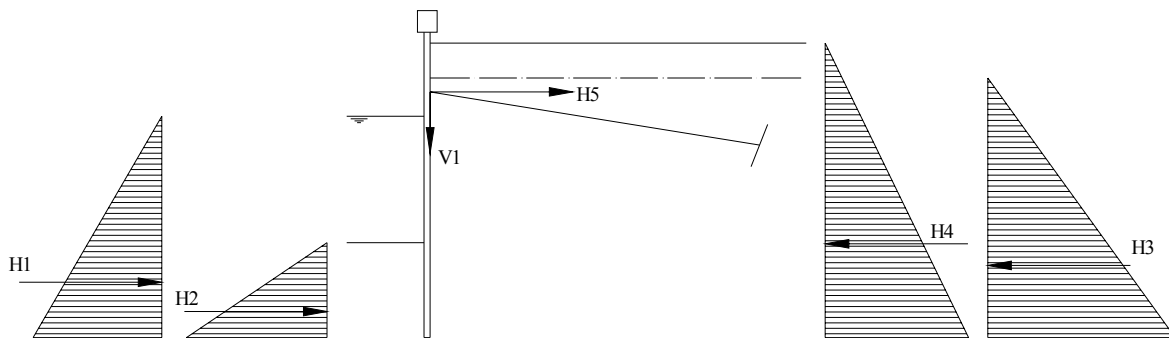
Sketch of failure mechanism:



Limit state function:

The tie rod supports the sheet pile wall in taking on the forces. Failure of the tie rod occurs if the stress occurring in the tie rod exceeds the tensile strength of the steel.

$$z = m_{spa;ab;R} F_u - m_{spa;ab;S} \cdot F_{tot}$$



where:

F_u and F_{tot} are respectively the tensile force capacity of the tie rod as derived from the steel yield stress and the total occurring force in the anchor due to the forces acting on the sheet pile wall [kN /m]

$m_{spa;ab;R}$ and $m_{spa;ab;S}$ are model factors for the horizontal resistance and loading force [-]

The forces on the sheet pile wall are modelled as illustrated below.

Loading equations:

The horizontal force on the sheet pile wall consists of the following contributors:

$$H1 = 0.5 \cdot \gamma_w (h - L_1)^2$$

$$H2 = 0.5 \cdot K_p \cdot (\gamma_s - \gamma_w) (h_1 - L_1)^2 *$$

Resistance (strength) equations:

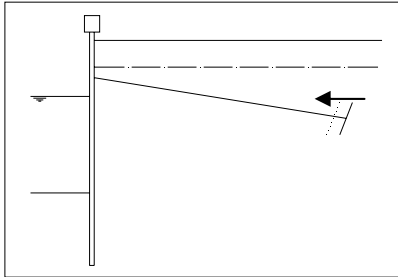
The maximum force the tie rod can take on is a function of the total area of the tie rods and the yield stress of the tie rod steel.

$$F_u = A_s \cdot f_s$$

$H3 = 0.5 \cdot \gamma_w (gw - L_1)^2$ $H4 = 0.5 \cdot K_a \cdot (\gamma_s - \gamma_w) (h_3 - L_1)^2 *$ <p>The tie rod makes up for the difference between the horizontal forces mentioned above:</p> $H5 = (H4 + H3 - (H1 + H2))$ $F_{tot} = H5 \cdot w_a / \cos(\alpha)$ <p>*built up by the different soil layers</p>	
<p>Parameter definitions:</p> <p>h = the river water level [mOD]</p> <p>gw = the river water level [mOD]</p> <p>γ_s = the volumetric weight of the saturated soil [kN / m³]</p> <p>γ_w = the volumetric weight of water [kN / m³]</p> <p>L_1 = the toe level of the sheet pile wall [mOD]</p> <p>h_1 = the level of the crest in front of the sheet pile wall on the river side [mOD]</p> <p>h_3 = the level of the crest in front of the sheet pile wall on the land side [mOD]</p> <p>K_a = the coefficient for active horizontal grain force [-]</p> <p>K_p = the coefficient for passive horizontal grain force [-]</p> <p>w_a = the distance between two tie rods [m]</p> <p>A_s = the total area of the tie rod [m²]</p> <p>f_s = the yield stress of the steel [kN/m²]</p> <p>α = the angle of inclination of the tie rod [°]</p>	
<p>Sources of failure mechanism equations / methods:</p> <p>Standard stability check of hydraulic structures</p>	
<p>Sources of uncertainties in failure equations / input parameters:</p> <p>Baecher & Christian (2003);</p> <p>CUR 190 (1997);</p> <p>Vrouwenvelder et al. (2001);</p>	

Insufficient shear strength of the soil near the anchor head

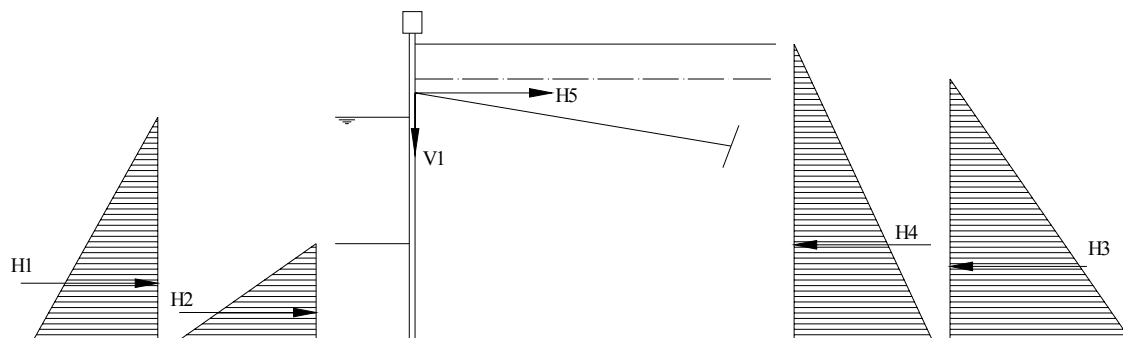
Sketch of failure mechanism:



Limit state function:

The anchor head transfers the force from the tie rod to the soil. Failure occurs if the stress exerted by the anchor head exceeds the shear strength of the soil.

$$Z = m_{spa;as;R} F_r - m_{spa;as;S} \cdot H_5$$



where:

F_r and H_5 are respectively the force capacity of the soil around the anchor head and the total occurring horizontal force in the anchor due to the forces acting on the sheet pile wall [kN /m]

$m_{spa;as;R}$ and $m_{spa;as;S}$ are model factors for the horizontal resistance and loading force [-]

The forces on the sheet pile wall are modelled as illustrated below.

Loading equations:

The horizontal force on the sheet pile wall consists of the following contributors:

$$H1 = 0.5 \cdot \gamma_w (h - L_1)^2$$

Resistance (strength) equations:

The maximum force the tie rod can withstand based on the strength of the soil is defined as follows:

$H2 = 0.5.K_p .(\gamma_s - \gamma_w)(h_1 - L_1)^2 *$ $H3 = 0.5 .\gamma_w(gw - L_1)^2$ $H4 = 0.5.K_a .(\gamma_s - \gamma_w)(h_3 - L_1)^2 *$ <p>The tie rod makes up for the difference between the horizontal forces mentioned above:</p> $H5 = (H4 + H3 - (H1 + H2)) .w_a$ $F_{tot} = H5$ <p>*built up by the different soil layers</p>	$F_r = 0.5(\alpha + \beta - 1)h_a d_a^2 \gamma_d \left(\frac{1 + \sin(\varphi)}{1 - \sin(\varphi)} - \frac{1 - \sin(\varphi)}{1 + \sin(\varphi)} \right) - q h_a d_a (\alpha + \beta - 1) \frac{1 - \sin(\varphi)}{1 + \sin(\varphi)}$ $\alpha = b_a / h_a$
<p>Parameter definitions:</p> <p>h = the river water level [mOD]</p> <p>gw = the river water level [mOD]</p> <p>γ_s = the volumetric weight of the saturated soil [kN / m³]</p> <p>γ_w = the volumetric weight of water [kN / m³]</p> <p>L_1 = the toe level of the sheet pile wall [mOD]</p> <p>h_1 = the level of the crest in front of the sheet pile wall on the river side [mOD]</p> <p>h_3 = the level of the crest in front of the sheet pile wall on the land side [mOD]</p> <p>K_a = the coefficient for active horizontal grain force [-]</p> <p>K_p = the coefficient for passive horizontal grain force [-]</p> <p>w_a = the distance between two tie rods [m]</p> <p>h_a = the height of the anchor head [m]</p> <p>b_a = the width of the anchor head [m]</p> <p>d_a = the depth of the bottom of the anchor head [m]</p> <p>γ_d = the volumetric weight of the soil [kN / m³]</p> <p>$\alpha = b_a / h_a$ [-]</p> <p>β = factor according to Buchholz [-]</p> <p>q = surcharge load behind the anchored sheet pile wall [kN / m²]</p> <p>φ = the angle of internal friction of the soil [°]</p>	

Sources of failure mechanism equations / methods:

Lecture notes hydraulic structures TUDelft

Sources of uncertainties in failure equations / input parameters:

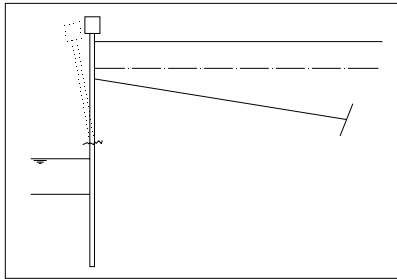
Baecher & Christian (2003);

CUR 190 (1997);

Vrouwenvelder et al. (2001);

Breaking of sheet pile wall due to bending moments

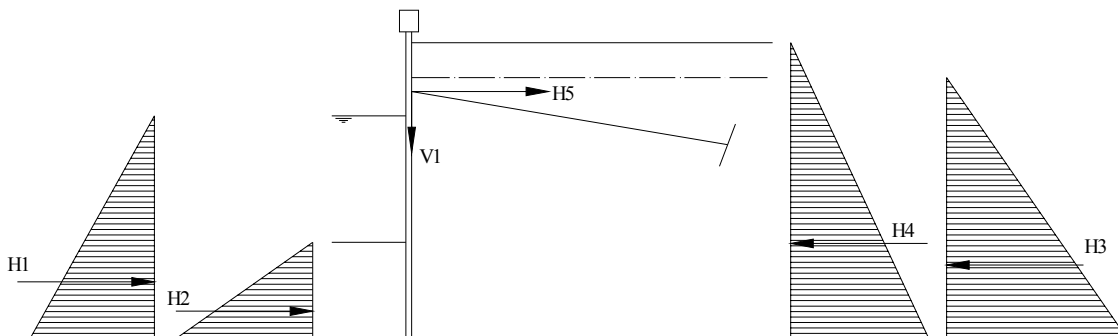
Sketch of failure mechanism:



Limit state function:

Failure occurs if the capacity of the sheet pile cross section is exceeded by the actually occurring bending moments. From the maximum occurring bending moment in the anchored sheet pile a maximum tensile stress in the sheet pile wall can be derived, using the moment of inertia and the height of the section. That maximum occurring tensile stress is compared against the yield stress of the sheet pile steel.

$$Z = m_{spa;b;R} f_s - m_{spa;b;S} \cdot \sigma_b$$



where:

f_s and σ_b are respectively the yield stress of the steel cross section and the maximum tensile stress occurring in the sheet pile cross section [kN /m²]

$m_{spa;b;R}$ and $m_{spa;b;S}$ are model factors for the strength and loading models [-]

The forces on the sheet pile wall are modelled as illustrated below.

Loading equations:

The maximum tensile stress in the sheet pile cross section is:

$$\sigma_b = M_{max} \cdot z / I_z$$

The maximum and minimum moments are

Resistance (strength) equations:

The yield stress f_s of the steel sheet pile cross section determines the limit of the tensile stress.

found where the shear force in the cross section is 0. M_{max} is the highest of those maxima and minima. The shear force in the cross section at a level x can be found with the following equations:

$$H1 = 0.5 \cdot \gamma_w (h - x)^2$$

$$H2 = 0.5 \cdot K_p \cdot (\gamma_s - \gamma_w) (h_1 - x)^2 \quad *$$

$$H3 = 0.5 \cdot \gamma_w (gw - x)^2$$

$$H4 = 0.5 \cdot K_a \cdot (\gamma_s - \gamma_w) (h_3 - x)^2 \quad *$$

The maximum moment can be found by combining with the arm of the force

$$M1 = 0.5 \cdot \gamma_w (h - x)^2 \cdot \frac{1}{3}(h - x)$$

$$M2 = 0.5 \cdot K_p \cdot (\gamma_s - \gamma_w) (h_1 - x)^2 \cdot \frac{1}{3}(h_1 - x) \quad *$$

$$M3 = 0.5 \cdot \gamma_w (gw - x)^2 \cdot \frac{1}{3}(gw - x)$$

$$M4 = 0.5 \cdot K_a \cdot (\gamma_s - \gamma_w) (h_3 - x)^2 \cdot \frac{1}{3}(h_3 - x) \quad *$$

*built up by the different soil layers

Parameter definitions:

h = the river water level [mOD]

gw = the river water level [mOD]

γ_s = the volumetric weight of the saturated soil [kN / m³]

γ_w = the volumetric weight of water [kN / m³]

x = the level of the cross section associated with the maximum moment [mOD]

h_1 = the level of the crest in front of the sheet pile wall on the river side [mOD]

h_3 = the level of the crest in front of the sheet pile wall on the land side [mOD]

K_a = the coefficient for active horizontal grain force [-]

K_p = the coefficient for passive horizontal grain force [-]

z = the distance between the centre of gravity and the outer edge of the sheet pile profile [m]

I_z = the moment of inertia of the sheet pile cross section [m⁴/m]

M_{max} = the maximum bending moment in the sheet pile wall

Sources of failure mechanism equations / methods:

Sheet pile handbook

Sources of uncertainties in failure equations / input parameters:

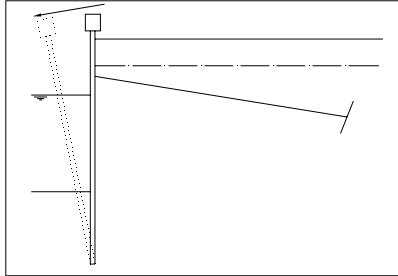
Baecher & Christian (2003);

CUR 190 (1997);

Vrouwenvelder et al. (2001);

Rotation of sheet pile wall after tie rod failure

Sketch of failure mechanism:



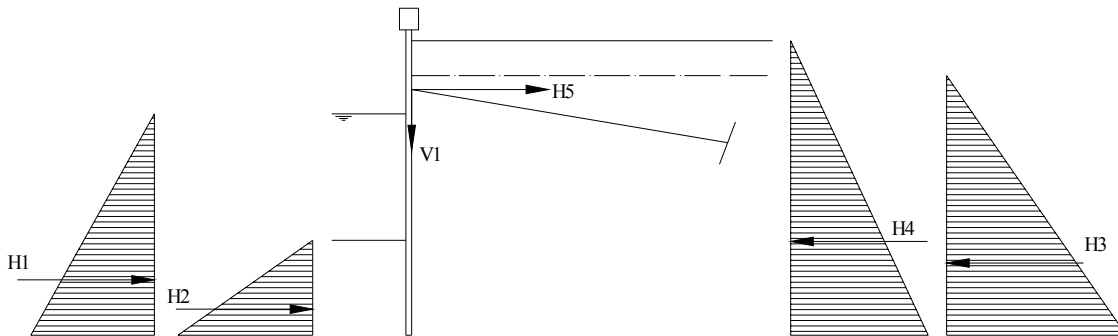
Limit state function:

Collapse of the sheet pile wall after failure of the tie rod depends on the moment equilibrium around the toe of the sheet pile, described by:

$$z = m_{spa;m;R} M_r - m_{spa;m;S} \cdot M_l$$

where:

M_r and M_l are respectively the moment exerted by the forces on the river side and the



forces on the land side of the sheet pile wall [kNm]

$m_{spa;m;R}$ and $m_{spa;m;S}$ are model factors for the strength and loading models [-]

The forces on the sheet pile wall are modelled as illustrated below.

Loading equations:

The resulting loading moment is taken around the toe of the sheet pile wall and is built up as follows:

$$M3 = 0.5 \cdot \gamma_w (gw - L_1)^2 \cdot 1/3 (gw - L_1)$$

$$M4 = 0.5 \cdot K_a \cdot (\gamma_s - \gamma_w) (h_3 - L_1)^2 \cdot 1/3 (h_3 - L_1)^*$$

Resistance (strength) equations:

The resulting resisting moment is taken around the toe of the sheet pile wall and is built up as follows:

$$M1 = 0.5 \cdot \gamma_w (h - L_1)^2 \cdot 1/3 (h - L_1)$$

$$M2 = 0.5 \cdot K_p \cdot (\gamma_s - \gamma_w) (h_1 - L_1)^2 \cdot 1/3 (h_1 - L_1)^*$$

$M_l = M3+M4$ *built up by the different soil layers	$M_r = M1+M2$ *built up by the different soil layers
Parameter definitions: h = the river water level [mOD] gw = the river water level [mOD] γ_s = the volumetric weight of the saturated soil [kN / m ³] γ_w = the volumetric weight of water [kN / m ³] h_1 = the level of the crest in front of the sheet pile wall on the river side [mOD] h_3 = the level of the crest in front of the sheet pile wall on the land side [mOD] K_a = the coefficient for active horizontal grain force [-] K_p = the coefficient for passive horizontal grain force [-]	
Sources of failure mechanism equations / methods: Standard stability check	
Sources of uncertainties in failure equations / input parameters: Baecher & Christian (2003); CUR 190 (1997); Vrouwenvelder et al. (2001);	

